PREDICTION AND MEASUREMENT OF INTERVERTEBRAL MOVEMENTS OF THE LUMBAR SPINE

A thesis submitted in partial fulfillment of the requirement for the degree of

Doctor of Philosophy

by

Sun Loi Wah

Department of Rehabilitation Sciences

The Hong Kong Polytechnic University

SEP 2005

CERTIFICATE OF ORIGINALITY

I hereby declare that this thesis is my own work and that, to the best of my knowledge and belief, it reproduces no material previously published or written, nor material that has been accepted for the award of any other degree or diploma, except where due acknowledgement has been made in the text.

______________________________ (Signed)

SUN LOI WAH (Name of Student)

ABSTRACT

Measurement of intervertebral movements is essential in the clinical diagnosis and assessment of low back pain and spinal disorders such as instability. It is possible to measure gross movements of the entire lumbar spine using markers or sensors attached to the skin. But such techniques are not accurate enough to provide information about intervertebral movement as the magnitude of the movement is similar to that of the error due to soft tissue deformation underlying the sensors. Radiographic methods are able to provide accurate data, but this involves identification and superimposition of vertebral images which is a time consuming and technically demanding process. This thesis attempted to address the above limitations by two related studies. The purpose of the first study was to examine the feasibility of an inverse kinematic algorithm in predicting intervertebral movements using information derived from skin-mounted sensors. The second study involved the development of an automatic method of identifying vertebral images in radiographs and computing their movements. This would significantly reduce data processing time and increase the attraction of the radiographic method as a clinical tool for measuring intervertebral movements.

In the first study, an inverse kinematic model was employed to determine the optimum intervertebral joint configuration for a given forward-bending posture of the human spine. An optimization equation with physiological constraints was employed to determine the intervertebral joint configuration. Experimental validation

was performed using lateral radiographs of the lumbosacral spines of twenty-two subjects (9 men and 13 women, 40 ± 14 years old). The model was found to be valid for predicting the intervertebral rotations of the lumbar spine segments but not intervertebral translations. The differences between the measured and predicted values of intervertebral rotations were generally small (less than 1.6 degrees). Pearson product-moment correlations were found to be high, ranging from 0.83 to 0.97, for prediction of intervertebral rotation, but poor for intervertebral translation (R = 0.08 to 0.67). The inverse kinematic model can be clinically useful for predicting intervertebral rotation when X-ray or invasive measurements are undesirable. It is also useful in biomechanical modeling, which requires accurate kinematic information as model input data.

Knowledge of the intervertebral translations of the spine is essential in the clinical assessment of some clinical disorders such as instability, spondylolysis or spondylolisthesis. Unfortunately, such assessment could not reliably performed using the inverse kinematic method but only by radiographic measurement. In the second part of this study, the precision and accuracy of a new automatic method to determine intervertebral movements were examined. Active contour was employed for segmentation of vertebral body image, providing a rapid and accurate measurement of vertebral shape using Fourier descriptors. A Genetic Algorithm was then utilized to determine the displacements of the vertebral bodies. Lateral radiographs of the lumbosacral spines of twenty-two healthy male volunteers (21 ± 1 years old) were taken in full flexion and extension. The vertebral body image was fitted with a quadrangle and its corners to be digitised. This allowed the intervertebral movement to be determined manually. The mean differences in the angles determined by the manual and automatic method were less than 1.4 degrees;

whereas the mean differences in posterior-anterior and superior-inferior translations less than 1.2 mm and 0.8 mm respectively. The correlation of vertebral body outline as determined by the automatic method in the flexion and extension films was high, with R values ranging from 0.994 to 0.997. This indicates that no image distortion or out-of-plane movements occur. The root mean square error of data among five repeated measurements were less than 0.15 degrees, 0.014 mm and 0.012 mm for sagittal rotation, postero-anterior and supero-inferior translations respectively. The use of active contour in automatic measurement of intervertebral movement was not only accurate but also convenient as the whole process only required 2 to 3 minutes compared to about 20 minutes for the manual digitisation method. The above results show that the technique could be reliably employed to quantify intervertebral translations as well as rotations using flexion-extension radiographs.

It is concluded that the inverse kinematic model would be clinically useful when only information about intervertebral rotation is required. However, the automatic method of segmentation and tracing of vertebral images should be employed when knowledge of intervertebral translations is required and when highly accurate measurements are desired. Future studies should explore the feasibilities of using the above methods in patients with spinal pathologies. The radiographic method should be extended to videofluoroscopic images so that dynamic information about intervertebral movements could be obtained.

PUBLICATIONS

Sun LW, Lee RYW, Lu W and Luk DK (2004) Modelling and simulation of the intervertebral movements of the lumbar spine using an inverse kinematic algorithm. Medical & Biological Engineering & Computing. **42**(6):740-6.

Sun LW, Lu W, Luk DK and Lee RYW (2005) Automatic measurement of intervertebral movements of the lumbar spine using radiographic images. Journal of Biomechanical Engineering. (To Be Submitted)

Yang ZY, Sun LW, Griffith JF, Leung PC, Pope M and Lee RYW (2005) Error analysis of skin surface measurement method for motion analysis of lumbar spine. Spine. (To Be Submitted)

INTERNATIONAL CONFERENCE PAPER

Sun LW and Lee RYW (2005) Automatic Measurement of Intervertebral Movements Using Radiographic Images. In: Proceedings of 27th Annual Conference of the IEEE Engineering in Medicine and Biology Society, Shanghai, p220.

Yang ZY, Griffith JF, Leung PC, Pope M, Sun LW, Lee RYW (2005) The Accuracy of Surface Measurement for Motion Analysis of Osteoporotic Thoracolumbar Spine. In: Proceedings of 27th Annual Conference of the IEEE Engineering in Medicine and Biology Society, Shanghai, p278.

Sun LW and Lee RYW (2005) Automatic measurement of lumbar spinal kinematics from lateral radiographs. In: Proceedings of XXth Congress of the International Society of Biomechanics and 29th Annual Meeting of the American Society of Biomechanics, Cleveland, Ohio, USA, p908.

Yang ZY, Sun LW, Griffith JF, Leung PC and Lee RYW (2005) The accuracy of surface measurement for osteoporotic spine motion analysis. In: Proceedings of XXth Congress of the International Society of Biomechanics and 29th Annual Meeting of the American Society of Biomechanics, Cleveland, Ohio, USA, p793.

Sun LW and Lee RYW (2004) Development of a new motion analysis system using gyroscopic sensors. In: Proceedings of the XVth Congress of the International Society of Electrophysiology and Kinesiology, Boston, p251.

Sun LW and Lee RYW (2004) Validity of an inverse kinematic model in determining the intervertebral movements of the lumbar spine. In: Proceedings of the XVth Congress of the International Society of Electrophysiology and Kinesiology, Boston, p251.

Sun LW and Lee RYW (2003) Prediction of the Intervertebral Movements of the Lumbar Spine using an Inverse Kinematic Model. In: Proceedings of Mechanics in Medicine and Biology, Taiwan, p53.

ACKNOWLEDGEMENTS

I would like to acknowledge the help given by all those in the Department of Rehabilitation Sciences and thank them for their friendship and support. Above all I would like to thank my principal supervisor, Raymond Lee. He directed me in my research pursuit, gave me valuable advice and widened the scope of my knowledge in various research disciplines throughout my doctoral studies. Without the guidance that Raymond provided, I would not have finished this thesis. The manner in which he freely gave of his wisdom and for brightening the sometimes lonely path of a doctoral degree, I am particularly thankful. I feel honoured to have had a supervisor who is an excellent researcher and also as a dear friend. Thank you, Raymond.

I am pleased to acknowledge the financial support of the Hong Kong Polytechnic University Internal Competitive Research Grant A-PD88.

Finally, and without doubt, most importantly to my parents and my family, whose love and support has kept me sane throughout this project, I give thanks. I love you all.

Loi-Wah SUN

TABLE OF CONTENTS

LIST OF FIGURES

CHAPTER 1

CHAPTER 2

CHAPTER 3

CHAPTER 4

CHAPTER 5

CHAPTER 6

CHAPTER 7

LIST OF TABLES

CHAPTER 2

CHAPTER 3

CHAPTER 4

CHAPTER 6

CHAPTER I INTRODUCTION

1.1 STATEMENT OF THE PROBLEM

1.1.1 Low Back Pain Problem

Low back pain (LBP) is a widespread problem, and measurement of intervertebral movements of the lumbar spine motion plays an essential role in the assessment and diagnosis of low back pain (DVORAK, J, PANJABI, MM et al. 1991). LBP is a medical problem with important social and economic consequences. It affects 39 percent of the population in Hong Kong at some time during their lives (LAU, EMC, EGGER, P et al. 1995). It is the second leading cause of work absenteeism (DEYO, RA and BASS, JE 1989). The lifetime prevalence of low back pain has been estimated to be 60 to 80 percent, and the one year prevalence is 15 to 20 percent (ANDERSSON, GBJ 1991). Among the working age population, approximately half report symptoms of back pain during a one-year period (VALLFORS, B 1985; STERNBACH, RA 1986). Approximately 5 to 10 percent of low back patients experience chronic problems (LAHAD, A, MALTER, AD et al. 1994), but these individuals account for nearly 60 percent of health care expenditures for low back pain. Back pain has resulted in substantial financial costs to the health service, and in Britain, this amounts to approximately HK$8,400 million per annum (ROSEN, M, BREEN, A et al. 1994).

1.1.2 Spinal Instability

Spinal instability is frequently mentioned, rarely defined and remains a controversial concept from different way in engineering and clinical medicine. We agree that “instability” is a biomechanical term. The definitions of spinal instability describe when an applied force produces displacement of part of a motion segment exceeding that found in a normal spine (POPE, MH and PANJABI, M 1985). White et al. (WHITE, AA and PANJABI, MM 1990) reported normal segmental motion in the lumbar spine. There are three engineering definitions of instability.

(i) Describe the behavior of a system at its end-point (terminal instability). It defined as a condition of a spine in which application of a small load causes an inordinately large displacement (BOGDUK, N and TWOMEY, LT 1991).

(ii) Invokes an increased neutral zone (PANJABI, MM, GOEL, V et al. 1992). The neutral zone is that part of the range of physiological intervertebral motion, measured from the neutral position, within which the spinal motion is produced with a minimal internal resistance. The stress-strain curve of a lumbar segment exhibits instability in terms of an increased neutral zone compared to a normal curve.

(iii) Invokes a decreased equilibrium. Figures 1 a to d show the continuum of stability. The deepest bowl (Fig. 1a) is most stable, and the hump (Fig. 1d) is least stable. The ball in the bowls seeks the energy well or position of minimum potential energy. Flattening the bowl or decreasing the steepness of the sides decreases stability (MCGILL, S 2002).

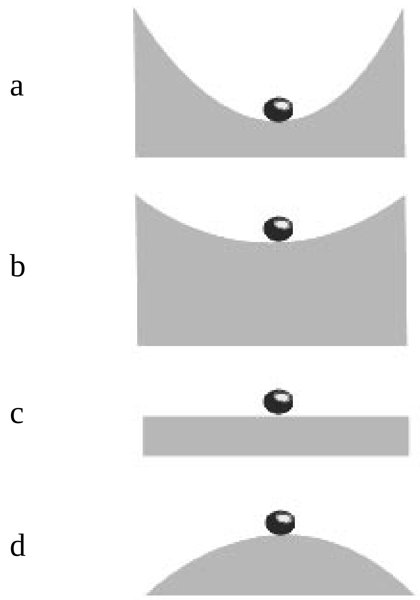

Fig. 1 The continuum of stability (adapted from McGill 2002).

Another two distinct clinical definition of instability are described as follow:

(i) Describe when an applied force produces displacement of part of a motion segment exceeding that found in a normal spine (POPE, MH and PANJABI, M 1985).

(ii) Invokes abnormal range of motion (PANJABI, M, CHANG, D et al. 1992b). It defined in terms of the altered ratios between translation and rotation on movements. In our study, the instability focuses on the abnormal range of motion as the spines flexes and extends.

Instability of the human spine is a significant cause of LBP. Instability is characterized by movement in the motion segment beyond normal constraints (FRYMOYER, JW 1988; JOSEPHSON, M, HAGBERG, M et al. 1996; MARENA, C, GERVINO, D et al. 1997; HARREBY, MS, NYGAARD, B et al. 2001). The diagnosis of intervertebral instability is based on radiological findings of abnormal vertebral motion (PITKANEN, M, MANNINEN, H et al. 1997): (a) Forward translation of one vertebrae over the other – anterior sliding instability; (b) Back translation – posterior sliding instability; (c) Excessive angular movement of a motion segment/rotation – angular instability; (d) Abnormal axial rotation in which the posterior margin of the vertebral body has a focal double contour during bending. Thus it is clinically important to develop an accurate method of assessing intervertebral motions of the spine, which plays a major role in the diagnosis of spinal disorders and assessment of treatment and progress.

1.1.3 The Gold Standard for Measurement of Intervertebral Movement

Evaluation of the range and patterns of movement is a key concern for a clinician. An important component of lumbar spine kinematics is that of sagittal plane rotation and translations (WHITE, AA and PANJABI, MM 1978). Radiography have long been the gold standard for determination and analysis of the lumbar spinal kinematics (ANDERSON, JA and SWEETMAN, BJ 1975) and planar and serial biplanar radiography have provided data documenting static end range motion of the spine in three planes (PEARCY, M, PORTEK, I et al. 1984; PEARCY, MJ 1985).

Clinically, gross motion is often measured by a goniometer (BOONE, DC and AZEN, SP 1979). Most of the clinical techniques measure gross movements of the entire lumbar spine using measurement devices attached to the skin, such as the fingertips-to-floor, skin distraction and inclinometers methods (SCHOBER, P 1937; LOEBL, WY 1967; SAUR, PM, ENSINK, FB et al. 1996; NG, JK, KIPPERS, V et al. 2001). This techniques have been showed to be unreliable (BURNETT, AF, BARRETT, CJ et al. 1998) and they provide one-dimensional information only, but the lumbar spine exhibits complex three-dimensional motions. Surface measurements using markers or sensing devices are subjected to large error due to the deformation of underlying soft tissues disguising the true vertebral movement (PEARCY, MJ and HINDLE, RJ 1989). Ruler, markers or Inclinometer are simple to measure gross movements clinically but the measurement result is not accurate because of the error due to skin movement. Techniques are sufficient for clinical measurement but are not accurate for scientific study. They are only accurate and reliable for determining the total gross movement of a region of the spine but not accurate enough for discriminating the contribution of the movement of individual intervertebral joints (PEARCY, MJ and HINDLE, RJ 1989; LEE, RYW 2001). Surface measurements of intervertebral movements may only be achieved by fixing markers or sensing devices rigidly to the spinous processes with pins or screws (KAIGLE, AM, POPE, MH et al. 1992; KANAYAMA, M, ABUMI, K et al. 1996), but this is an invasive surgical procedure which may have the risk of infection and cause pain.

Various techniques have been previously employed to measure the three-dimensional movements of the lumbar spine. Electro-Optical devices (PEARCY, M, GILL, JM et al. 1987) and electromagnetic tracking systems (PEARCY, MJ and HINDLE, RJ 1989; BURNETT, AF, BARRETT, CJ et al. 1998; VAN HERP, G, ROWE, P et al. 2000; LEE, RYW 2001) appear to be able to provide accurate data, but they are generally less than ideal. Electro-Optical systems are rather complex, expensive and time consuming to be unsuitable for routine clinical use. Electromagnetic devices, which are highly accurate and inexpensive, have been shown to be a promising technique for clinical evaluation of the intervertebral movements. However, they can be adversely affected by the presence of metals, and correction for metallic distortion is very time consuming and complicated. Electromagnetic tracking system is suitable for measuring spinal movements in a clinical environment that affected less by the presence of metal.

Radiographic techniques are able to give accurate measurements of the intervertebral movements in three dimensions, but it has the inherent health risk of repeated x-ray exposure. Since the measurements are based on static images of the spine, they are unable to provide information about the kinematic patterns of movements but only the end points of motion. Nevertheless, x-ray technique may be considered as the most appropriate clinical method of measurement of intervertebral movements. Previous error studies (LEE, RYW and EVANS, J 1997) showed that the mean measuring error involved in determining sagittal rotation and translations were 1.0° and 0.6 mm. Technique was high reliable in measuring intervertebral movements. While radiography is advantaged in being able to look under the skin and directly measure the position of the bony structures in relation to one another, without its own sources of measurement error. The motion ranges computed from digitization data of radiographs were regarded as the “standard” values. The radiographic measurement techniques have been described in detail in previous studies (LEE, RYW 1995; LEE, RYW and EVANS, J 1997) and Appendix I (A1.4). Stereo radiographic techniques are able to give accurate measurements of intervertebral movements of the spine in 3-dimensional space. The technique involves identification and superimposition of vertebral images which is a time consuming and technically demanding process.

In summary, measurement of the intervertebral movements of the lumbar spine is fraught with difficulties. This is primarily because the spine is rather inaccessible and the nature of its movements is very complex. Motion cannot be easily measured by surface or non-invasive techniques. Various above techniques have restrictions that limit their utility in clinical environments. Accuracy, reliability, safety and cost are the limitations of the existing measurement methods. Therefore, non-invasive and more precise methodology to measure gross motion as well as intervertebral motion should be developed.

1.2 PURPOSE OF STUDY

This thesis attempted to eliminate the limitations described by two related studies. The purpose of the first study is to evaluate the validity of using an inverse kinematic model to determine the intervertebral movements with a given knowledge of the total flexion movement of the lumbar spine and the positions of the spinous processes. Information derived from skin-mounted sensors attached on the back of the subject. The mathematical model was used to predict the intervertebral movements of the lumbar spine. An *in-vivo* experiment study was used to valid the segmental kinematic prediction using inverse kinematic model.

The purpose of the second study was to develop an automatic method of identifying vertebral images in radiographs and computing their segmental movements in both rotational and translation motions. This would significantly reduce data processing time and increase the attraction of the radiographic method as a clinical tool for measuring intervertebral movements. The accuracy of a new automatic method for morphometry of intervertebral movements was examined.

This dissertation presents the results from two studies motivated by the author's specific concerns regarding the determination and analysis of the intervertebral movements of the lumbar spine. An attempt was made to develop clinical guidelines for spinal motion measurements. It was hoped that the indirect skin measurement method and the new radiological method would prove to be useful in clinical as well as research studies.

1.3 ORGANIZATION OF THESIS

Chapter 1 provides a general introduction to the thesis and specifically states the research problems. The purpose of the study is described. The organization of the thesis is outlined.

Chapter 2 reviews the relevant literature regarding techniques used in measurement of spinal kinematics either in clinic or laboratory-based situations. Detailed descriptions of the techniques of radiographic measurement of intervertebral movements *in vivo* and *vitro* are studied. A short summary of the advantages and disadvantages of the existing methods are studied.

Chapter 3 focuses on errors in surface measurements. Experimental validation was conducted to evaluate the validity of using an inverse kinematic model for determining the intervertebral movements of the lumbar spine with given knowledge based on the surface detection method.

Chapter 4 describes an indirect method of determination of intervertebral movements of the lumbar spine: Prediction of intervertebral movements using an inverse kinematic algorithm. Experimental validation is included. This chapter was previously published in Medical & Biological Engineering & Computing, **42**(6):740-6.

Chapter 5 reports pilot studies regarding two segmentation approaches were implemented to extract vertebrae contours.

Chapter 6 describes a direct method to determine intervertebral movements of the lumbar spine: Radiographic measurement of intervertebral movements *in vivo* (direct method). Experimental validation is included.

Chapter 7 provides a summary and synthesis of the key findings presented of the thesis and the general conclusion. Recommendations for future research are made.

CHAPTER 2 MEASUREMENT TECHNIQUES OF SPINAL KINEMATICS

A literature review of the existing techniques for measuring lumbar spine motions is presented. This chapter evaluates the past and current methods of measuring lumbar spine movements. The wide variety of historical measurement techniques may be classified as either clinic or laboratory-based approaches. Clinical methods are generally easier to administer and provide an adequate degree of precision for its intended application. The precise laboratory-based methods are characterized by determining the total movements and require highly specialized personnel and instrumentation. Radiographic techniques have been applied to measure spinal motions. A short summary of the existing methods either in clinic or laboratory-based settings is presented. The advantages and disadvantages of various techniques are also compared. Some methodological issues are addressed to allow therapists or researchers to choose the appropriate methods for their applications.

2.1 CLINIC-BASED MEASUREMENT METHODS

2.1.1 Skin Distraction Method

Traditional measures of the spinal movements are based upon non-invasive surface measurement methods. The skin distraction method is used for measuring forward bending of the trunk (SCHOBER, P 1937; MACRAE, IF and WRIGHT, V 1969). Unfortunately, this technique is unrepresentative of the actual movements of the spine. It only records the end points of motion and provides a linear one-dimensional measure with no information about the rotational movement in the sagittal plane (PEARCY, MJ and HINDLE, RJ 1989).

2.1.2 Inclinometer

Surface measurements are unable to characterize intersegmental geometry. Surface measurements using markers or sensory devices are subject to large errors due to the deformation of the underlying soft tissues disguising the true vertebral shape. When an inclinometer is used to measure joint motion, a high reliability in the lateral bending movement measure ($R > 0.9$) was found (NG, JK, KIPPERS, V et al. 2001). On the contrary, the intrarater reliability was poor for the extension movement ($R = 0.15 \sim 0.42$). An inclinometer cannot measure axial rotation, based on the pendulum principle (SAUR, PM, ENSINK, FB et al. 1996). The inclinometer is a simple device and may be the method of choice in routine clinical practice when sophisticated techniques are not available for three-dimensional analysis.

2.2 LABORATORY-BASED MEASUREMENT METHODS

2.2.1 Mechatronic Device

During the last decade, many new sensors have been developed using the continuously advancing technology. They are generally more compact in size and low in cost (KO, WH 1986). In the aerospace and robotic industries, gyroscopes are widely used to provide information on position and orientation of rigid bodies (WRIGLEY, W, HOLLISTER, WM et al. 1969; SHABANA, AA 1994). Gyroscope is an angular velocity sensor that is based on the measurement of the Coriolis force of a vibrating device (WRIGLEY, W, HOLLISTER, WM et al. 1969). It delivers an output voltage, which is proportional to the rotational velocity. The angular orientation can then be obtained from integration of the gyroscopic signals. The modern solid-state gyroscope uses ceramic vibrating unit (SHINOZUKA, N, OIE, Y et al. 1996; TONG, K and GRANAT, MH 1999).

Tong and Granat (TONG, K and GRANAT, MH 1999) performed a study of using uni-axial gyroscopes to measure knee motions during walking. However, this study was only limited to the measurement of motions in one anatomical plane. Lee (LEE, RY, LAPRADE, J et al. 2003) described a new method of measuring the three-dimensional movements of the lumbar spine in real time. The measurement system consisted of solid-state gyroscopes that were attached to the human trunk. They measured the angular rates of rotations in three dimensions, which were then integrated to obtain the orientation. The sensors contained gravitometers and magnetometers that provided additional information for eliminating any drift of the gyroscopes. The reliability of the data provided by the gyroscopic system was examined in a group of 19 young and healthy subjects. The similarity of the movement–time curves obtained in three repeated measurements was assessed by the coefficient of multiple correlations. The coefficients were found to be high, ranging from 0.972 to 0.991. The reliability of the data was slightly lower for measuring axial rotation. The device did not only quantify the kinematic patterns in the primary plane of movements, but also the accompanying movements in the other planes. Flexion and extension were found to be mainly confined to the sagittal plane, whereas lateral bending and axial rotation always accompanied each other. Angles derived from integration can be distorted by noises.

One limitation of solid-state gyroscope is the zero frequency offset, or bias, when the sensor is stationary. The bias will lead to an angular drift after integration of the gyroscopic signals. Some authors addressed this problem and proposed methods of correcting such error. Pong and Granat (TONG, K and GRANAT, MH 1999) performed high pass filtering of the signals to eliminate the bias. Luinge et al (LUINGE, HJ, VELTINK, PH et al. 1999) proposed predicting the drift error using a Kalman filter and signals from accelerometers, and compensated for the error using feedback. Lee et al. (LEE, RY, LAPRADE, J et al. 2003) employed bandpass filter effectively to minimise the errors. The integration of signals is carried out numerically using the incremental outputs from the gyroscopes, and involves very time consuming and heavy burden of computing on the computer. The gyroscopic system could provide reliable orientation information by applying appropriate compensating algorithm. Lee at al. (SUN, LW and LEE, RYW 2004) showed that the gyroscope can be used to measure orientation information if the gyroscope should be well calibrated before use and its signal is processed appropriately. The bias drift of the gyroscope is independent from its location, but changes continuously with time and temperature.

2.2.2 Electro-Optical

Electro-Optical techniques are also able to give accurate measurements of joint motion in three dimensions. However, they suffer from various disadvantages, which make them unsuitable for routine clinical use. The optical methods are too complex, time consuming and expensive. Electrogoniometers have been used to obtain time-dependent changes in posture when measuring the postures associated with human activities (LEE, RYW and MUNN, J 2000). Due to attachment across the joint, electrogoniometers create a constraint that limits the motion of soft tissues. They therefore possibly modify the natural motion of the joint.

2.2.3 Electromagnetic

An electromagnetic tracking system is an alternative tool in human body kinematic motion studies (PEARCY, MJ and HINDLE, RJ 1989; LEE, RYW and MUNN, J 2000; KARDUNA, AR, MCCLURE, PW et al. 2001; LEE, RYW and WONG, TKT 2002; WONG, TKT and LEE, RYW 2004). The positions and orientations of the sensors relative to the sources are calculated by detecting the signal sent back from the sensors under an electromagnetic field. An electromagnetic tracking device (Fastrak system) is used for measuring rotational motions of the scapula and humerus with respect to the thorax. Three receivers were placed on the T3, the humerus and the scapula (KARDUNA, AR, MCCLURE, PW et al. 2001). In lumbar spine studies, this is very common method to capture spinal motion. Two sensors are attached to the sacrum and the spinous process of L1 in lumbar spine studies. A low-cost, highly accurate and reliable electromagnetic motion tracking system can record kinematic patterns, having a total root-mean-square error of less than 0.2 degrees (PEARCY, MJ and HINDLE, RJ 1989). One of the major disadvantages is the interference of metal. This system can be adversely affected by the presence of metals, and correction for metallic distortion is time consuming and complicated. The method is therefore not suitable for patients with metallic implants.

Lee et al. (LEE, RYW and WONG, TKT 2002; WONG, TKT and LEE, RYW 2004) used the system to study the effects of lower back pain on the relationship between the movements of the lumbar spine and hip. The kinematics of both the lumbar spine and hips was measured. Measurement methods that do not discriminate the movements of the two joints, such as the finger-to-tip method and single inclinometry, could provide misleading information.

2.3 RADIOGRAPHIC TECHNIQUES

There have been numerous studies to investigate lumbar kinematics (ALLBROOK, D 1957; WHITE, AA and PANJABI, MM 1978; STOKES, IA, MEDLICOTT, PA et al. 1980; YAMAMOTO, I, PANJABI, MM et al. 1989; BELL, GD 1990; YOSHIOKA, T, TSUJI, H et al. 1990; DVORAK, J, PANJABI, MM et al. 1991; PANJABI, M, CHANG, D et al. 1992b; FROBIN, W, BRINCKMANN, P et al. 1997; LEE, RYW and EVANS, J 1997; TAKAYANAGI, K, TAKAHASHI, K et al. 2001; ZHENG, Y, NIXON, MS et al. 2003; ZHENG, Y, NIXON, MS et al. 2004). These studies can be divided into two categories: *in vitro* studies and *in vivo* studies. An advantage of *in vitro* studies is a direct measurement of the spinal column. There is a possibility that the motions created *in vitro* studies are different from actual physiologic conditions because most of the muscles and the ligaments are removed from the specimens. *In vivo* studies have the advantage of obtaining kinematic information under physiologic conditions. Radiography has commonly been used to investigate spinal motion *in vivo* studies, and to study segmental lumbar spine instability. Kinematic measurements of the spine shed light on specific relationships between spinal mechanics and disabilities. Many such relationships have seemed plausible to clinicians, but very few have been proved. Research on intervertebral motion *in vivo* should be an essential prerequisite to knowledge about the mechanical disorders of the spine.

2.3.1 Plane X-ray Superimposition Studies

In Vitro and *in vivo* radiography have been used in the measurement of lumbar spine motion with some success (WHITE, AA and PANJABI, MM 1978; PEARCY, M, PORTEK, I et al. 1984; DVORAK, J, PANJABI, MM et al. 1991; PANJABI, M, CHANG, D et al. 1992b; FROBIN, W, BRINCKMANN, P et al. 1997; WILKE, HJ, ROHLMANN, A et al. 2003). A series of experiments were performed on cadeveric spines (*in vitro*) (CUNNINGHAM, BW, GORDON, JD et al. 2003) and human subjects (*in vivo*) radiographically. These biomechanical studies have greatly enhanced the understanding of the kinematics of the lumbar spine and the mechanics of clinical assessment techniques. In-plane superimposition studies, tracing the image with the subject in different positions were superimposed. A bony segment was fitted over another tracing or X-ray film and the displacements of adjacent segments were measured. The technique has been studied in previous studies (PEARCY, M, PORTEK, I et al. 1984; LEE, RYW 1990). However, the method was not valid with respect to out-of-plane images such as biplanar radiographs (TIBREWAL, SB, PEARCY, MJ et al. 1985). Biplanar radiography also is unable to provide information about the kinematic patterns of movement, only measuring the extremes of movement. Nevertheless, it has been used in clinical assessment.

2.3.2 Assumptions

The measurement of kinematics from planar radiographs involves two assumptions. First, it is assumed that motions are restricted to the plane of study. Coupled movements, movements that occur in an unintended or unexpected direction during the executation of a desired motion, can occur (BOGDUK, N and TWOMEY, LT 1991). The work of Pearcy (PEARCY, MJ and HINDLE, RJ 1989) reported the three-dimensional patterns of movements in the lumbar spine. Voluntary flexion and extension on the sagittal plane are accompanied by very little rotation and translations on the coronal and axial planes (PEARCY, MJ 1985). As Pearcy (PEARCY, M 1986) has pointed out, although there is not any significant out-of-plane movement for flexion and extension, the same are not true for lateral bending and axial rotation.

Second, an intact vertebral body is assumed to be a rigid body for the purposes of kinematic analysis. The shape of a typical lumbar vertebral body, projected onto the sagittal plane, approximates a quadrilateral as shown in Fig. 2.1. Lines were drawn tangentially to the superior, inferior, anterior and posterior margins. The intersections of these lines define four unique reference points (DVORAK, J, PANJABI, MM et al. 1991; PANJABI, MM, GOEL, V et al. 1992). There are two advantages in using a tangential box of this kind to define reference points.

First, if the lines are placed carefully, variation is minimized because there can only be one true tangent drawn across two convex protrusions. Second, the effects of poor edge definition due to image noise are minimized because the enclosing box has an averaging effect.

In spinal motion analysis, different parameters are used to describe the kinematics (MUGGLETON, JM and ALLEN, R 1997). Segmental ranges of vertebral rotations and translations have been found to be useful for the assessment of instability (VAN DEN BOGERT, AJ, SMITH, GD et al. 1994; FROBIN, W, BRINCKMANN, P et al. 1997).

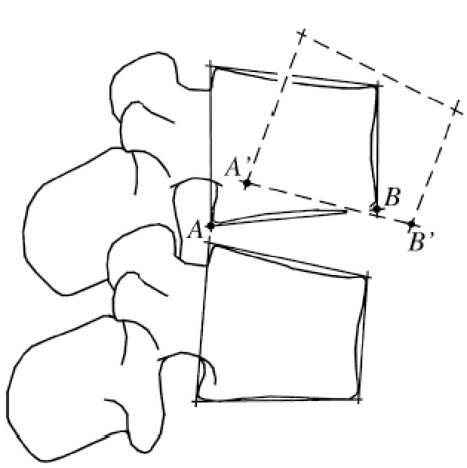

Fig. 2.1 Relative displacement of the upper vertebra in an image (adapted from Harvey 1998).

2.3.3 Measurement of Vertebral Rotation

The shape of a lumbar vertebral body when projected on the sagittal plane approximates a quadrilateral. If lines were drawn tangentially to the superior, inferior, anterior and posterior margins, their intersections define four unique reference points, which is so called quadrangle. Its defining the final position of the lower vertebra have been overlaid on to those of the initial position. The relative displacement of the upper vertebral image and location of the instantaneous axis of rotation IAR may then be found from the initial positions of the two reference points, *A* and *B*, on the upper vertebral body, and their final positions, *A*' and *B*', as described in Panjabi et al. (PANJABI, M, CHANG, D et al. 1992b).

Flexion–extension involves rotation and displacement of all of the lumbar vertebrae. In order to measure the kinematics in the sagittal plane at a particular intervertebral joint, the final position of the lower vertebra (represented by its enclosed box) was superimposed on to its initial position (also represented by an enclosed box). Then the relative vertebral positions before and after displacement may clearly be seen by the positions of the upper vertebral boxes (Fig. 2.1). The points *A* and *B* (inferior reference points of the upper vertebra) moved from their original locations to *A*' and *B*', respectively. The calculation of kinematic parameters based on this motion was described in detail in Harvey et al. (HARVEY, SB and HUKINS, DWL 1998).

2.3.3.1 Alternative Method of Analysis

Figure 2.2 shows the superposition of the initial and final lower vertebra using the enclosed box as described in the previous section. The upper vertebra is also represented by its enclosed box. The upper vertebral box may be divided into two triangles, each having its own independent centroid, A and B as shown in Fig. 2.2. Relative intervertebral displacement may then be represented by the movement of *A* to *A*' and *B* to *B*', retaining the rigid body assumption. These centroids may be used as alternative reference points in kinematic calculations.

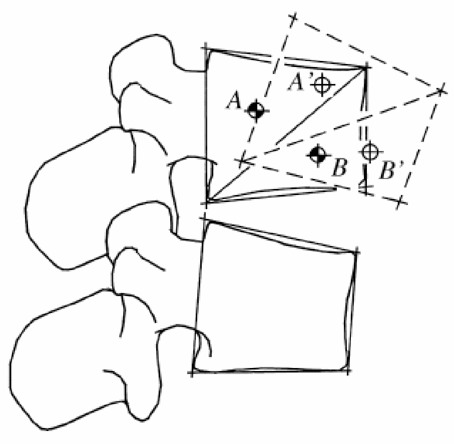

Fig. 2.2 Relative displacement of the upper vertebral centroids in an image (adapted from Harvey 1998).

2.3.4 Measurement of Vertebral Translation

Methods for measuring sagittal plane displacement from lateral views of the lumbar spine have been described in previous studies (PEARCY, M, PORTEK, I et al. 1984; STOKES, IA, BEVINS, TM et al. 1987; DVORAK, J, PANJABI, MM et al. 1991). Of particular interest to those studying the spine has been the alignment of vertebrae in the sagittal plane, or the amount of translation of one vertebra relative to the adjacent ones.

Measurement protocols were based on auxiliary lines fitted to the upper or lower vertebral endplates or to the anterior or posterior cortex of the vertebrae. Displacement was assessed from the intersection of the auxiliary lines. In Fig. 2.3, displacement D1 is determined as the distance of the projection of the dorsal corner of the cranial vertebra from the respective dorsal corner of the caudal vertebra, measured along the tangent to the endplate of the caudal vertebrae (solid lines). This protocol, however, is not symmetric with respect to the two vertebrae. If a tangent is drawn to the endplate of the cranial vertebra and the rule is followed accordingly (dotted lines), a displacement at D2 results. Furthermore, if both vertebrae are imagined to rotate simultaneously, but in opposite directions about their appertaining centre points, CP, so that no net dorsoventral translation occurs, D1 and D2 change nevertheless. These findings suggest that the current definition of "displacement" may not be optimally chosen (FROBIN, W, BRINCKMANN, P et al. 1996).

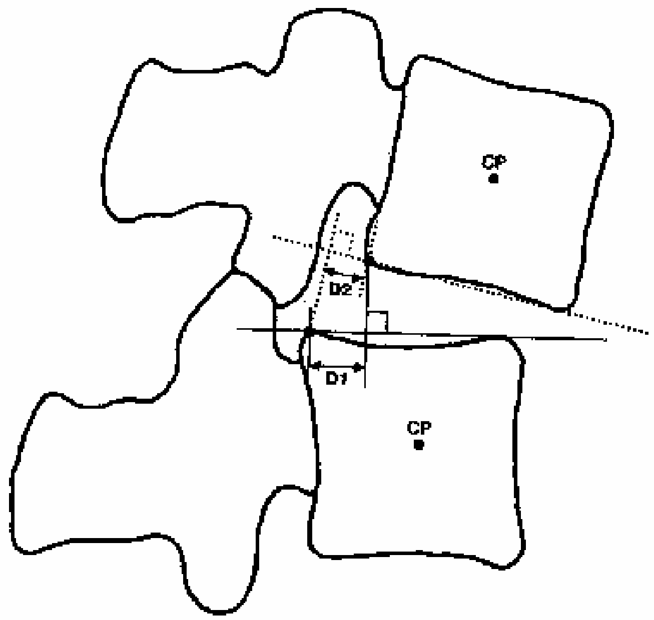

Fig. 2.3 Example of a protocol to measure sagittal plane displacement from a lateral radiograph of the lumber spine (adapted from Bernhardt et al. 1992).

Some previous studies on displacement report estimates of the measurement errors. For sagittal plane translational motion, Wall et al. (WALL, MS and OPPENHEIM, WL 1995) reported errors in the measurement of displacement in the L5/S1 joint between 3 % and 11 % of vertebral depth depending on the actual magnitude of the displacement and the obliquity of the x-ray beam. Studies using biplanar radiography report measurement errors between 1.5 and 3 mm for translational motion (STOKES, IA, MEDLICOTT, PA et al. 1980; PEARCY, M, PORTEK, I et al. 1984).

To summarize, analysis of current methods suggests that measuring sagittal plane displacement might profit (i) from a better geometric definition of sagittal plane displacement; (ii) from reducing subjective influences in the measurement procedure; and (iii) from making adequate allowances for distortion of the radiographic image. Past studies (STOKES, IA, MEDLICOTT, PA et al. 1980; PEARCY, M, PORTEK, I et al. 1984) reported a wide range of measurement errors in sagittal plane displacement.

Lines joining vertebral body corners are constructed in Fig. 2.4. Dorsal and ventral mid-points (D and C) are identified on each vertebra. Centre points (C) are defined as mid-way between V and D. The bisectrix of the midplane lines is constructed, and perpendiculars from the mid-points (C) are drawn. Translation, *d*, is defined as the distance between the intersections of the perpendiculars on the bisectrix. *d* is normalized by the mean width of the upper vertebra. Frobin et al. (FROBIN, W, BRINCKMANN, P et al. 1996) concluded that sagittal plane translation should be measured along the disc bisector (Fig. 2.4). However, the translation measured in a direction fixed with respect to one vertebra is extremely sensitive to the actual sagittal angulation between the two vertebrae.

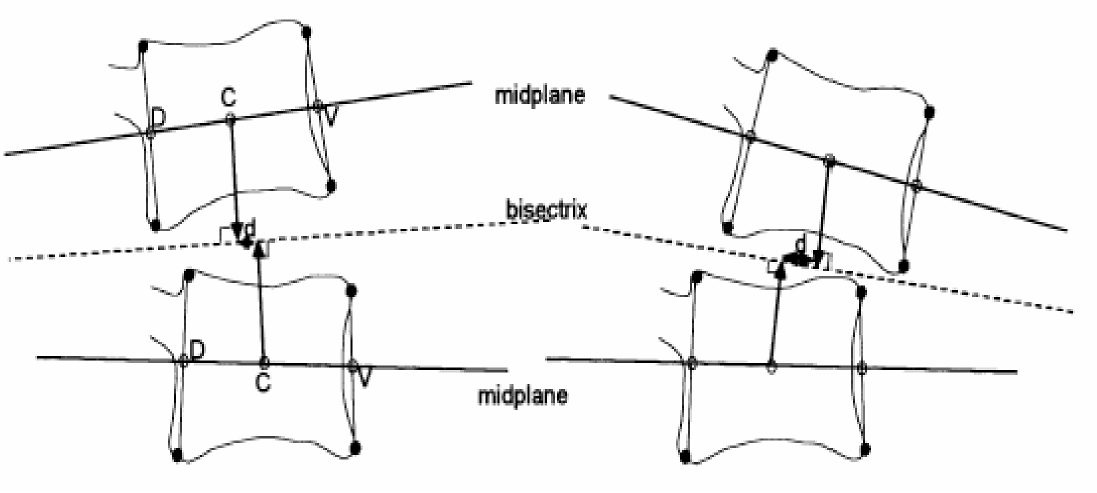

Fig. 2.4 Translation measurement protocol with a moving reference (adapted from Frobin et al. 1996).

2.3.4.1 George's Line

George's line is a radiological construction that has been used for almost a century by clinicians to infer improper alignment of the spine. It is the posterior vertebral alignment line, and, in the intact spine, it forms a smooth curve. The posterior body surfaces can be connected with this line, which traverses across the intervertebral disc, the key landmarks being the superior and inferior posterior body corners. It is the disruption of this line that has traditionally prompted radiologists to infer some kind of instability due to ligamentous laxity, fracture, dislocation, or degenerative joint disease. It is considered that the alignment should be maintained in both flexion and extension and consequently at all stages in between. There are a number of implications from maintaining George's line that can give us vital insights into the relationships between commonly used spinal measurement parameters.

2.3.5 Determination of the Instantaneous Axis of Rotation (IAR)

Many kinematic studies were conducted to determine the normal range of motion (WHITE, AA and PANJABI, MM 1978; PEARCY, M, PORTEK, I et al. 1984; YAMAMOTO, I, PANJABI, MM et al. 1989; DVORAK, J, PANJABI, MM et al. 1991; PANJABI, MM, GOEL, V et al. 1992). In addition to measuring the normal range of motion, instantaneous axis of rotation (IAR) (Fig.2.5) for assessment of lumbar segmental motion was studied (PEARCY, MJ and BOGDUK, N 1988; WHITE, AA and PANJABI, MM 1990; AMEVO, B, WORTH, D et al. 1991).

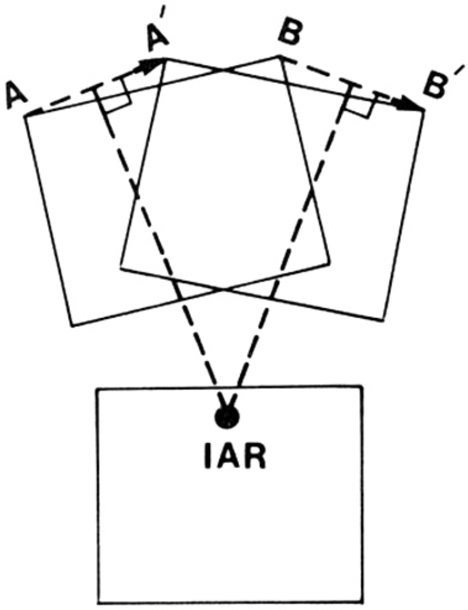

Fig.2.5 Calculation of the IAR as the point of intersection of the perpendicular bisectors of the vectors for the motion of two points on a rigid body (adapted from Pearcy 1998).

Instantaneous centre of rotation (IAR) is often used to quantify intervertebral joint movement on a plane (PANJABI, MM 1979; DIMNET, J 1980; PANJABI, MM, BOEL, VK et al. 1982). IAR is determined by the point of intersection of the perpendicular bisectors of the displacement vectors for the motion of two points on a rigid body (WHITE, AA and PANJABI, MM 1978) as shown in the Fig. 2.5.

Unfortunately, IAR is very sensitive to error. Small errors in measuring the landmark coordinates could lead to relatively large errors in locating the IAR (DIMNET, J 1980). Pearcy and Bogduk (PEARCY, MJ and BOGDUK, N 1988) examined the within- and between-observer errors in locating the centre of rotation on lateral radiographs while flexion and extension motion. It reported there was generally high uncertainty in locating the centres of rotation. Between-observer errors were always greater than within-observer errors. Moreover, the magnitude of errors varied among different movements. The errors for the movement from full extension to flexion were generally smaller than those for the smaller magnitude movements of flexion or extension alone. The authors believed that only the centres of rotation for the movement from full extension to full flexion could be determined reliably. Panjabi et al (PANJABI, MM 1979; PANJABI, MM, BOEL, VK et al. 1982) reported that the error was found to be unacceptably large if the magnitude of rotation was less than 5^{o}; and if the markers A and B were located at distances of less than 30mm from the centre of rotation. And also if the markers subtended an angle of 90^{o} to each other, the error was minimal. Panjabi et al. (WHITE, AA and PANJABI, MM 1978) found that the errors at the L1/2 and L5/S1 segments were found to be unacceptable greater than the other levels during the movement from extension to flexion. The concept of instantaneous centre of rotation proves to be useful only when the magnitude of movement is large. The intervertebral movements of the lumbar spine would be expected to be small (less than 5^{o}). Hence, the determination of the centre of rotation in this case would be potentially erroneous and might not be meaningful in my study.

2.4 INVERSE KINEMATICS

Inverse kinematics is a method used in robotic engineering for determining joint configurations given a desired position and orientation of the end-effector of the robot in achieving a certain goal (CRAIG, JJ 1989; MCCARTHY, JM 1990; ALLARD, P, STOKES, IAF et al. 1995; ZATSIORSKY, VM 1998).

2.4.1 Theory of Inverse Kinematics

In an engineering approach, a human body or its parts are modeled as a structure that consists of a series of rigid links connected at joints. The number of degrees of freedom of an articulated system is the number of joint angles necessary to specify the state of the structure. Forward kinematics involves a transformation from joint angles to coordinates (CRAIG, JJ 1989; MCCARTHY, JM 1990). If all the joint angles are specified, the coordinates of the end of a limb, called the end-effector (such as the hands and feet), can be easily computed (forward kinematics). Inverse kinematics is given a desired end point or position for an articulated structure to determine the joint angles. What usually interests us, is finding the joint angles from the end-effector's coordinates. Goal-directed movement, such as moving a hand to open a door or placing a foot at a specified location on the ground, requires the computation of inverse kinematics, which solves for the set of joint angles from the end-effector's location and orientation.

Mathematically, the transformation from kinematic coordinates space to internal joints space is the classic inverse kinematics problem. McCarthy (MCCARTHY, JM 1990) stated that if we define the coordinates of a manipulator as the n-dimensional vector of joint angles $\theta \in R^n$, and the position and orientation of the manipulator's end-effector as the m-dimensional vector $\mathbf{x} \in R^{m}$, the forward kinematic function can generally be written as:

$$\mathbf{x} = f(\theta) \qquad (1)$$

while what we need is the inverse relationship:

$$\theta = f^{-1}(\mathbf{x}) \qquad (2)$$

For redundant manipulators, i.e., $n > m$, solutions to Eq. (2) are usually non-unique and even for $n = m$ multiple solutions can exist. Therefore, inverse kinematics algorithms need to address how to determine a particular solution to Eq. (2) in face of multiple solutions. The detail information was shown on Appendix I. However, redundant Degree of Freedoms (DoFs) are not necessarily disadvantageous as they can be used to optimise additional constraints, e.g., manipulability constraints, etc. Thus it is useful to solve the inverse problem (2) by imposing an optimization criterion:

$$g = g(\theta) \qquad (3)$$

where g is usually a cost function that has a unique global optimum.

An iterative approach utilizes the Jacobian matrix for solving inverse kinematics problems in my study. For sufficiently small changes, the change in angle and change in position are linearly related by the Jacobian matrix $\mathbf{J}$:

$$\mathbf{dx} = \mathbf{J}(\theta)\, \mathbf{d}\theta \qquad (4)$$

This equation can be solved for $\mathbf{d}\theta$ by taking the inverse of $\mathbf{J}$ if it is squared i.e. $n = m$, and non-singular. The Jacobian matrix $\mathbf{J}$ is the defined as follows:

$$\mathbf{J} = (\mathbf{dx/\,d}\theta_1 \ \ \mathbf{dx/\,d}\theta_2 \ldots \mathbf{dx/\,d}\theta_N) \qquad (5)$$

The column vectors $\mathbf{dx/\,d}\theta_i$ are the partial derivatives of the end point with respect to the ith joint angle of θ_i. Thus, we can rewrite (4) as

$$\dot{\theta} = J^{-1}\dot{\theta} \qquad (6)$$

This is only valid when J is non-singular. With articulated system, however, J is quite often irregularly shaped, and has no inverse. A Moore-Penrose pseudoinverse $\mathbf{J}^+$ is a good approximation, and will work for matrices of any shape. The properties of pseudoinverse of a matrix $\mathbf{J}$ are the unique matrix (Appendix I).

For a redundant manipulator n is greater than m, which necessitates the use of additional constraints, e.g., the optimization criterion g in Eq. (3), to obtain a unique inverse. A pseudo-inverse provides solution by minimizing g in the null space of $\mathbf{J}$:

$$\dot{\theta} = \mathrm{J}^+ \cdot \dot{x} + \left(I - J^+ \cdot J\right)\left(-k\frac{\partial g}{\partial \theta}\right)^T \qquad (7)$$

Forward kinematics is simple and straightforward, because a set of joint angles specifies exactly one position. Inverse kinematics, however, is difficult. Most real systems are underconstrained, so for a given goal position, there could be infinite solutions (i.e. many different joint configurations could lead to the same endpoint). A problem arises from the fact that inverse transformations are often ill-posed. The field of robotics has developed many inverse kinematics systems, which due to their constraints, have closed-form solutions.

2.4.2 Prediction of Human Body Joint Motion Using Inverse Kinematics

The inverse kinematic method has been successfully used to model the movements of various body joints (SOMMER, HJ, 3RD and MILLER, NR 1980; FUJIE, H, MABUCHI, K et al. 1993; JUNG, ES, CHOE, J et al. 1994; ZHANG, X and CHAFFIN, DB 1996; ZATSIORSKY, VM 1998; WANG, X 1999). Sommer (SOMMER, HJ, 3RD and MILLER, NR 1980) described a spatial inverse kinematic model to predict an in-vivo wrist joint under typical physiological loading conditions. The method employs a nonlinear least squares algorithm to minimize the aggregate deviation between postulated model motion and experimentally measured anatomical wrist motion.

A 6-axis articulated manipulator with 6 degrees of freedom (DOF) of motion was constructed (FUJIE, H, MABUCHI, K et al. 1993). It modified to control and measure both the force and position of synovial joints for the study of joint kinematics. It performed an anterior-posterior (A-P) translation test on a human cadaveric knee under simulate physiological loading conditions. It showed that system simulated complex loading conditions and measured the resulting joint kinematics.

Jung et al. (1994) (JUNG, ES, CHOE, J et al. 1994) employed a psychophysical cost function (potential function) to define a cost value for each joint movement angle and developed a regression model to predict the perceived discomfort with respect to the joint movement. Zhang (ZHANG, X and CHAFFIN, DB 1996) developed a new optimization-based differential inverse kinematics approach for modeling three-dimensional dynamic seated postures.

Wang (WANG, X 1999) also utilized a seven-Degree Of Freedom (DOF) arm model using an inverse kinematics algorithm to predict arm reach postures. How motions of each joint involved in arm movements can be used to control the end-effector (hand) position and orientation was examined. The algorithm was used both in rule-based form and by optimization through appropriate choice of weight coefficients. Since an end-effector motion-oriented method was used to describe joint movements, observed behaviours of arm movements implemented in the algorithm. It was shown that the inverse kinematics problem due to the kinematic redundancy in joint space is ill-posed only at the control of hand orientation but not at the control of hand position. The method of Wang et al. (WANG, X 1999) has the advantage that it handled the non-linearity of joint limits. No matrix inverse calculation was needed, thus avoiding the stability and convergence problems often occurring near a singularity of the Jacobian. Unfortunately, due to the complexity and unpredictable nature of spinal motions, previous research has not been able to establish any behavioural rules of intervertebral movements. It is therefore not possible to employ the behaviour-based approach of Wang et al. (WANG, X 1999) in my study.

2.4.3 Problem of Inverse Kinematic Model: Application to the Lumbar Spine.

Usually the kinematics function of the human body is highly nonlinear, rapidly becoming more and more complex as the number of links increases. The inverse kinematic method has never been applied to model the movements of the spine. This is probably because the spine has unlimited numbers of degrees of freedom, and finding an optimal solution to the inverse kinematic problem would be extremely difficult. The inversion of the function becomes very difficult to perform analytically. For instance, forward bending movement of the spine can be accomplished with an infinite number of combination of configurations of the various intervertebral joints.

However, a solution may be feasible and restricted to a limited range of solutions if appropriate constraints could be imposed on the kinematic modeling. For instance, the positions of the most posterior parts of the spinous processes may be determined by surface measurements. Such information may be used to reduce the number of solutions. For instance, additional information may be obtained from the surface curvature of the back to help determine the movements of the intervertebral joints (STOKES, IA, BEVINS, TM et al. 1987). Most importantly, model only finds an approximate solution to optimizing the motion of the spine due to a cost function (constraints) that cause a slight amount of interference between simulated results and actual movements of the spine in real. This interference can cause an amount of unwanted movements in unconstrained joints on the spine. The potential functions are very essential to determine the best solution under an optimisation approach. The constraints should be imposed based on the physiological range of movements of the human spine. It also employs to minimise the magnitude of the intervertebral movements. The modeling and appropriateness of the potential functions of the lumbar spine for the inverse kinematic model were described on Chapter 4. It is believed that robotics technologies should be modified to control and measure both the orientation and position of human spinal joints for the study of joint kinematics.

2.5 CINERADIOGRAPHY

Many authors addressed the determination of the normal range of motion (WHITE, AA and PANJABI, MM 1978; PEARCY, M, PORTEK, I et al. 1984; YAMAMOTO, I, PANJABI, MM et al. 1989; DVORAK, J, PANJABI, MM et al. 1991). In addition to measuring the normal range of motion, Ogston et al. (OGSTON, NG, KING, GJ et al. 1986) used instantaneous axis of rotation (IAR) for assessment of lumbar segmental motion. Weiler et al. (WEILER, PJ, KING, GJ et al. 1990) used the ratio of translation to rotation as an instability factor. Ito et al. (ITO, M, TADANO, S et al. 1993) calculated strain distribution of intervertebral discs to visualize motion patterns of each lumbar segment. Most of the kinematic studies, however, were two-dimensional analyses using lateral functional radiograph films. Pearcy et al. (PEARCY, M, PORTEK, I et al. 1984; PEARCY, MJ 1985) measured three-dimensional lumbar motion *in vivo* by biplanar radiography. However, this technique is not widely used by spine surgeons because of its technical difficulties. There are few studies to investigate continuous motion characteristics using cineradiography (FIELDING, JW 1957; KANAYAMA, M, ABUMI, K et al. 1996).

In 1994, Simonis et al. (SIMONIS, C, ALLEN, R et al. 1994) developed robust algorithms for the computation of vertebral kinematics from digitized videofluoroscopic images and manual marking protocols using rigid templates (SIMONIS, C, ALLEN, R et al. 1994). It was assumed that the vertebra is a rigid body with no deformation under motion. The protocol reduced the manual effort required in marking the images. A parallel technique for calculating planar kinematic parameters has been developed, but the marking of vertebrae continues to dominate the procedure.

Kanayama et al. (KANAYAMA, M, ABUMI, K et al. 1996) measured continuous vertebral displacement of normal lumbar segments in the sagittal plane from the neutral position to maximum flexion. They concluded that each lumbar segment started stepwise from the upper to the lower level with phase lags and that there was a constant relation between horizontal displacement and angular motion of each lumbar vertebra. However, differences in motion characteristics of the lumbar spine between forward flexion and backward flexion were not investigated in this experiment. Harada et al. (HARADA, M, ABUMI, K et al. 2000) analyzed continuous motion of the normal lumbar spine in the sagittal plane and clarified differences of motion characteristics between forward and backward flexion using cineradiography.

Due to the high radiation dosage, only a limited number of static images can be obtained using plain X-rays, usually in the neutral position and at the extreme positions of mobility. Consequently, it is not possible to determine the intermediate states or to describe the motion as the spine moves from flexion to extension. Computerized topography (CT) cannot yield movement information since it requires the patient to be as stationary as possible during image acquisition whilst dynamic magnetic resonance imaging (MRI) is not yet sufficiently fast in image acquisition for motion analysis.

To overcome these problems, digitized videofluoroscopy (DVF) was developed (ADAMS, MA, DOLAN, P et al. 1988). DVF incorporates a fluoroscope, an image intensifier and a video camera, which allows two-dimensional dynamic images of the spine to be captured at low radiation exposure. Once captured on videotape, the image sequences then can be digitized into a number of successive frames and the motion patterns analyzed on a computer. However, due to the low radiation exposures, the images of the lumbar spine have poor quality and anatomical landmarks are difficult to identify. Despite the reduced quality compared with a normal plain X-ray, a sequence of such images provides a wealth of information on segmentation motion. One of the difficulties associated with DVF is manually marking of the vertebrae as well as the identification of individual anatomical landmarks. It is a very time-consuming.

2.6 VIDEOFLUOROSCOPY

2.6.1 Landmark Locating

In spinal motion studies, it is essential to locate the landmarks that can be used to determine the positions of the vertebral bodies. This type of location was originally achieved manually and consisted of locating, typically, the corners of the vertebrae as anatomical landmarks. However, it is difficult to place markers exactly on the vertebral corners and, furthermore, repeatability cannot be assured. Panjabi et al. (PANJABI, M, CHANG, D et al. 1992b) discussed errors that can arise when manually marking X-ray images of the spine. The errors in vertebral rotation and translation were determined (PEARCY, M, PORTEK, I et al. 1984; LEE, RYW 1995). The landmark locating for radiographic measurement method has been described in detail in previous studies (PEARCY, M, PORTEK, I et al. 1984; LEE, RYW 1995; LEE, RYW and EVANS, J 1997). They reported that a measurement accuracy of 1.0^{o} and 0.6 mm could be achieved for the rotational and translational movements, respectively. It has been shown to be extremely difficult to measure very small movements (less than 1 degree of rotation).

2.7 DIGITAL RADIOGRAPHY STUDIES

Several alternative methods were proposed for the evaluation of lumbar spine instability, including biplanar X-ray photogrammetry (TAKAYANAGI, K, TAKAHASHI, K et al. 2001) or the determination of the instantaneous axis of rotation (WHITE, AA and PANJABI, MM 1978; PEARCY, M, PORTEK, I et al. 1984; PEARCY, MJ and BOGDUK, N 1988; YAMAMOTO, I, PANJABI, MM et al. 1989; DVORAK, J, PANJABI, MM et al. 1991). It remains a controversial issue. Within the last few years, there have been reports of *in vivo* dynamic motion studies using cineradiography or videofluoroscopy (HARADA, M, ABUMI, K et al. 2000; TAKAYANAGI, K, TAKAHASHI, K et al. 2001). Although plain functional radiographs may reveal static states at two points of maximum flexion and extension positions, they do not provide information on detailed motion during flexion and extension. Zheng (ZHENG, Y, NIXON, S et al. 2001) used dynamic-motion analysis to try to evaluate the pattern of lumbar motion during flexion in patients with degenerative spondylolisthesis or lumbar spine instability and compared the results with those of asymptomatic volunteers. Selvik et al. (SELVIK, G 1989; SELVIK, G 1990; STURESSON, B, UDEN, A et al. 2000) have great success with an integrated approach to the assessment and treatment of the Lumbopelvic-hip region using roentgen stereophotogrammetry. They described how to determine the best evidence when identifying sacroiliac joint (SIJ) dysfunction.

2.7.1 Image Processing for Shape Detection

Monteith and Page et al. (PAGE, WH, MONTEITH, W et al. 1993) developed a method for automatic tracking of digitized fluoroscopic images after the first frame was manually identified. The match criterion used was based on minimizing the sum of the absolute window surrounding each vertebral body corner. The corners were tracked independently, and no attempt was made to restore rigidity at the end of the process. However, the repeatability of marking of the corners was not good. The differences were small when the results were compared with a vertebrae's absolute motion, but, when compared with a vertebrae's motion relative to the sub-adjacent vertebrae, the differences were considerably larger.

Bifulco et al. (BIFULCO, P, CESARELLI, M et al. 1995) attempted to provide a more robust framework for the automatic recognition of vertebrae by performing template matching, using cross-correlation as a similarity measure. Their approach was to define a vertebra template manually, then computed the approximate translation of the centroid of the template by cross-correlating the template with identically shaped regions in the next frame. The maximum reading was found when the centroid of the template approximately overlays its corresponding location in the subsequent image. Repeatedly rotating and resampling the template is time-consuming. Following the work of Bifulco (BIFULCO, P, CESARELLI, M et al. 1995), Muggleton started her work in 1997 (MUGGLETON, JM and ALLEN, R 1997). She used an annular template matching method, which was defined by outer and inner templates comprising the whole vertebral body. It utilized the fact that vertebrae move as rigid bodies so corresponding points on each vertebra may be identified throughout the sequences. To compute in-plane rotations, a polar implementation of the cross-correlation technique was employed. A tracking algorithm minimized the computational effort required. In-plane rotations may be calculated to an accuracy of at least 1 degrees. Repeated analysis revealed standard deviations of less than 0.5 degrees for intervertebral rotations and less than 0.25 mm for translation. She also considered the vertebral translation in the sagittal plane application of George's line (MUGGLETON, JM and ALLEN, R 1997).

Allen and his colleagues (SIMONIS, C, ALLEN, R et al. 1994; COOPER, R, CARDAN, C et al. 2001) investigated the problem of automated marking of anatomical landmarks. They investigated fluoroscopic motion sequences combined with an MRI image. A cross-correlation-based method of feature extraction was developed as a basis for automating the calculation of intervertebral kinematics. CT images were acquired from the lumbar spine at 1mm increment (The Visible Human Project). A three-dimensional model of the lumbar spine was designed from real data. The model was used for the validation of the landmark locating and tracking algorithms to gain better understanding of the movement of the spine and displaying the vertebral kinematics. Simonis (ADAMS, MA, DOLAN, P et al. 1988) used a template-matching method to improve the repeatability, in which a template comprising the whole vertebral body was defined. Muggleton and Allen (MUGGLETON, JM and ALLEN, R 1997) obtained some improvement by using an annular template, which was defined by outer and inner templates. Zheng followed their work and used only the part between these two templates to find the shape of the spine. The Hough Transform (HT) was used to locate the lumbar spinal segments automatically (ZHENG, Y, NIXON, S et al. 2000a; ZHENG, Y, NIXON, S et al. 2000b; ZHENG, Y, NIXON, S et al. 2000c). The HT is a powerful tool in computer vision.

2.7.2 Segmentation: The Hough Transform

The theory of the Hough Transform (HT) is quite simple. In line extraction, points in the image are transformed into lines in a slope-intercept space. Lines in the slope-intercept space corresponding to collinear points will intersect at a point. This point defines the slope and intercept of the line through the collinear points. Quantizing the slope-intercept space into cells and counting the number of lines crossing each cell reduces the search for collinear points in the images to determine the maximum cell in the slope-intercept space. Sklansky (SKLANSKY, J 1978) showed that it provides a result equivalent to that derived by template matching but with less computational effort.

Zheng et al. (SKLANSKY, J 1978; ZHENG, Y, NIXON, S et al. 2000a; ZHENG, Y, NIXON, S et al. 2000b) applied the Generalized Hough Transform (GHT), which uses a continuous formulation to provide improved performance in scaling and measurement of rotation. They were able to successfully extract lumbar segments from fluoroscopic images of the spine. The target shape was described by a set of Fourier descriptors, which locate it in an accumulator space from which the object parameters of translation (both in the x- and y- direction), rotation and scale can be determined. The new Hough Transform approach was applied to the moving vertebrae. They included optimization via a genetic algorithm, because without it the extraction of moving multiple vertebrae is computationally daunting. The major advantages for using optimized concurrent HT to locate five lumbar vertebrae are that the relationships between objects are considered and the false extraction is excluded. Only the relative positions between the vertebrae were considered, but the technique provides temporal information in a motion sequence. In the follow-up work in 2002 (ZHENG, Y, NIXON, S et al. 2000c), a spatial-temporal HT was designed. The new approach was particularly attractive for coping with medical image sequences of poor quality.

In the study of Zheng and Allen (ZHENG, Y, NIXON, MS et al. 2003; ZHENG, Y, NIXON, MS et al. 2004) a solid model of the human lumbar spine was employed for visualization of spine motion. In kinematic studies, the parameters obtained are abstracted from the instantaneous axis of rotation and intervertebral angle. It often cannot provide clinicians with very intuitive data. In some clinical studies, traditionally two-dimensional images in the sagittal or coronal planes are taken, and the clinician forms a three-dimensional impression by mentally transforming these images. Mathematical visualization of the lumbar spine in three-dimensions can allow clinicians to observe the lumbar spine from different viewpoints and angles. Visualization and animation could be an effective way to present kinematics data to clinicians and could be helpful in clinical teaching or for presenting diagnostic information to patients.

2.7.3 Segmentation: The Active Shape Model

Other computer vision techniques have also been employed in vertebral image extraction (SMYTH, PP, TAYLOR, J et al. 1999). The Active Shape Modeling (ASM) segmentation is that described by Cootes and Taylor (COOTES, TF, HILL, A et al. 1994) of the University of Manchester. ASM has been most successful in segmenting irregular, noisy images, and deformable template methods. Cootes et al. (COOTES, TF, HILL, A et al. 1994; HILL, A, COOTES, TF et al. 1994) described a technique to use Active Shape Models for building compact models of the shape and appearance of human organs in medical images. The model was demonstrated by locating ventricles in a 3D MR image of the brain and tracking the left ventricle of the heart in an echocardiogram sequence. The Active Shape Model (ASM) has also been used for the measurement of vertebral shapes on lateral dual x-ray absorptiometry (DXA) scans of the spine for detecting of osteoporotic fractures (STOKES, IA, MEDLICOTT, PA et al. 1980). The ASM was a robust tool for measuring vertebral shape on normal spine DXA scans.

Researchers associated with Cootes carried out segmentation on images of the lower thoracic and upper lumbar spine (T7 to L4) acquired by dual x-ray absorptiometry (DXA), reported by Smyth (SMYTH, PP, TAYLOR, J et al. 1999). Smyth used a single shape template to model the 10 T7 to L4 vertebrae in a collection of 78 DXA images acquired from females aged 44 to 80. To get a measure of the accuracy of the ASM segmentation, Smyth (SMYTH, PP, TAYLOR, J et al. 1999) manually marked 73 landmark points on each vertebra in every image in consultation with a radiologist, and compared the converged ASM vertebra boundaries with the manually-marked boundaries. Further, to estimate how reproducibility errors occur when boundary markings manually acquired by multiple human readers. Smyth had four readers independently mark six boundary points on each vertebra in each of the images, and computed variances in point placement across these readers.

Significant results (SMYTH, PP, TAYLOR, J et al. 1999) showed that (i) ASM successfully converged for 94 % of the L3 vertebra with an increasing rate of success up to 99.2 % convergence for T7; (ii) the maximum error observed between the manually marked boundaries and the ASM boundaries was 1.61 pixels, for the L4 vertebra; (iii) for all but two of the vertebra, the ASM/manually-marked error observed was less than the reproducibility error of the four human readers. Gatton (GATTON, ML and PEARCY, MJ 1999) reported that spine x-ray segmentations had been obtained at a useful level by using deformable models in an interactive system for digitized lumbar spine images.

The ASM Toolkit software has a limitation on shape extraction of a template. In order to run the ASM algorithm, the user was required to manually initialize the ASM search by anchoring the template to the image with a manually-placed point, after which the algorithm would deform and move the template to seek to the vertebrae. Manually-derived vertebra landmarks used for template building and converged vertebra boundaries produced by ASM were studied in this thesis.

A problem addressed by ASM algorithm is to reliably determine the location and orientation of the vertebrae on the images. ASM is a local optimization algorithm: it searches for the object location within relatively small neighborhood of the current shape. Firstly, it searches a large section of the image; then as it converges onto an object in that area, it searches at a finer and finer level until the most satisfactory solution is obtained. The ASM work currently used in this study extend the previous approach with a Genetic Algorithm for optimization. Genetic Algorithm (THE MATHWORKS INC 1994) was used to refine the search using highly correlated parts of the vertebrae images. The detail information was described on Chapter 6.

2.7.4 Spinal Visualization and Animation

Visualization utilizes image integration, which enables clinicians to view integrated images and visualize anatomical structures in two-dimensions by combining anatomical, functional and physiological information. Visualization is based on a solid model, which has been described in detail by Cooper et al. (COOPER, R, CARDAN, C et al. 2001). In this current study, two types of data are integrated for visualization. The first is used to construct the surface model and the second is used to specify the animation of the lumbar spine.

The Visible Human Project (VHP) provides complete anatomically detailed, three-dimensional representations of the male and female human body (ZHENG, Y, NIXON, MS et al. 2003; ZHENG, Y, NIXON, MS et al. 2004). CT scan data of the lumbar spine of the young male subject from the VHP is used to construct the vertebral surface models. These surface meshes are used with some geometric scaling, so their source data must be accurate and representative of healthy vertebrae with little or no abnormalities or defects. The wire-frame rendering approach was used due to its simplicity. A family of lines represents the boundaries between structures, and triangular meshes are used for efficiency to represent the complex surfaces. This surface model is completed using illumination and shading. These models can be personalized by geometrical scaling according to the determined vertebral sizes of a subject, at least in two-dimensions, from digital videofluoroscopic images (DVF). Motion parameters are obtained by calculating the parameters extracted by the Hough Transform from a DVF image sequence. Coupled motion was not taken into account since, in sagittal plane bending, coupled axial rotation was reported on the order of 1 degrees (PEARCY, M, PORTEK, I et al. 1984).

The visualization program was written in Visual C++ for the Windows 95/NT platform. The program processes mesh and animation data from files and displays it by appropriate OpenGL routines. OpenGL is very famous for graphics applications. It can be used by calling out some subroutines in the main programs under major operating systems (OS).

2.7.5 Three Dimensional Computer Simulation

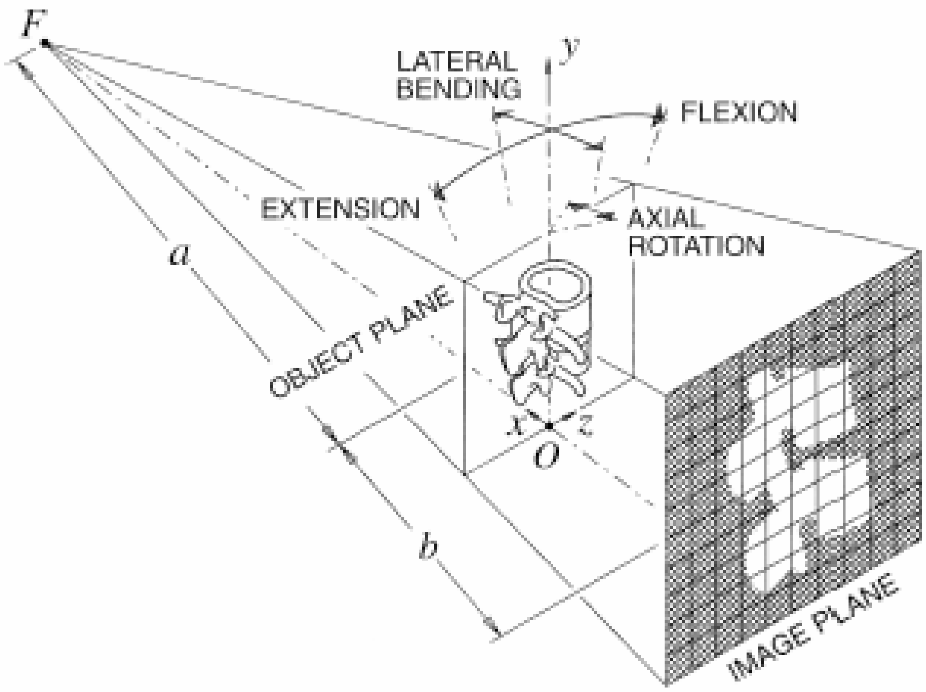

Fig. 2.6 Computer simulation of a radiographic system (adapted from Harvey 1997).

In three-dimensional computer simulation was developed in the previously cited studies (HARVEY, SB and HUKINS, DWL 1997; HARVEY, SB and HUKINS, DWL 1998), two identical three-dimensional lumbar vertebra models were aligned so that their sagittal plane was parallel to the image plane of a cone-beam radiographic imaging system. The simulation involved inducing a relative displacement of the upper vertebra in the sagittal plane concurrently with flexion–extension and either axial rotation or lateral bending of the entire lumbar spine about the global origin, *O*.

This relative displacement consisted of either a translation (shear or compression) or flexion between two adjacent vertebrae. Projecting this result on to the image plane produced the simulated radiographic images. Figure 2.6 shows how the three-dimensional model of the spine was projected to obtain a model image.

Each identical vertebra was assigned reasonable dimensions (GILAD, I and NISSAN, M 1985) and was represented by 140 body points. Their height was 27 mm and they had an elliptical cross-section with major and minor axes of 43 and 34 mm, respectively. The intervertebral disc space was 9 mm. The *x*-axis was defined by the axis of the X-ray cone beam, which was perpendicular to the sagittal plane. The vertebrae were bisected by this plane and aligned so that the axis of the vertebral bodies defined the *y*-axis, as shown in Fig. 2.6. The origin, *O*, of this coordinate system is referred to as the global origin. Vertebrae were able to undergo flexion–extension in the sagittal (*yz*) plane, axial rotation in the transverse (*xz*) plane and lateral bending in the coronal (*xy*) plane about the *x*, *y*, and *z*-axes, respectively.

A simulated cone-beam of X-rays was projected through the vertebrae at various stages of flexion–extension of the whole lumbar spine. The simulation involved inducing a relative displacement of the upper vertebra, in the sagittal plane, relative to the lower vertebra. This displacement consisted of either from 1 to 10 degrees flexion or from 1 to 10 mm shear or compression. To determine their effect on the calculation of relative displacements of adjacent vertebrae, axial rotation or lateral bending of the whole spine was also combined with flexion–extension. The X-ray beam emanated from a focus, *F*, defined by a =1080 mm, where a is the distance from the global origin along the direction of the positive *x*-axis. The object plane was located at x = 0 mm, and the image plane at b = 130 mm, where b is the distance from the global origin along the direction of the negative *x*-axis (HARVEY, SB and HUKINS, DWL 1997). For the relative flexion displacement, the rotational axis was parallel to the x axis and passed through the most posterior and inferior reference point on the upper vertebra. The inferior endplates of the lower and upper vertebrae were located at y =81 and y =117 mm, respectively (HARVEY, SB and HUKINS, DWL 1997). The range of motion of the whole lumbar spine was based on published data (GILAD, I and NISSAN, M 1985). Flexion–extension was from –15 degrees (extension) to 51 degrees (flexion), axial rotation from –5 degrees to 5 degrees and lateral bending from –18 degrees to 18 degrees about the global origin, i.e., a lateral bend of 18 degrees or an axial rotation of 5 degrees was combined with flexion–extension. The effect of a placement error was simulated by the introduction of a random 0.5 mm variation to the locations of the reference points. This value was chosen to be of the order of the simulated input variation in previous studies (0.1 mm (PANJABI, MM 1979) and 0.5 mm (PEARCY, M, PORTEK, I et al. 1984)).

The three-dimensional movements of the lumbar spine on computer simulation were constructed and analysed. The relative flexion between a pair of adjacent vertebrae was maintained while the pair was subjected to flexion–extension about the global origin, and either axial rotation or lateral bending as described previously. In this way, a set of simulated images was generated for each position of the spine for a range of relative movements between adjacent vertebrae. These images were displayed on a computer monitor. The relative motions of the adjacent vertebrae were then measured from these simulated images. The difference between actual and measured intervertebral movements was used as a measure of error. For the parameters shear, compression and angle of flexion, the maximum difference was used, while for ICR and centroid locations the root mean square (RMS) variation in difference was used (HARVEY, SB and HUKINS, DWL 1997).

2.8 SUMMARY

This chapter provides a review of the various methods of measurements of spinal motions. A comparison of the existing techniques is summarized in Table 2.1. Radiographic methods and, to a lesser extent, segmental vertebral body tracking are the appropriate methods identified as capable of precisely measuring intersegmental positions. X-ray techniques are considered the more accurate clinical method as it is not affected by soft issue variation across subjects. Electromagnetic tracking systems have been used to quantity spinal motion in the three axes and can achieve highly precise measures of vertebral bodies in space. Alternatively, skin surface instrumentation techniques are still commonly applied clinically because they are simple and easy methods. Various techniques have restrictions that limit their utility in clinical environments. Accuracy, reliability, safety and cost are as the limitations of the existing measurement methods. Clinicians should be aware of these issues if an appropriate measurement technique is to be chosen and the clinical data are to be interpreted appropriately. It is concluded that there is a need to develop further the current measurement techniques. These developments include improving the amount of information that could be gathered from surface measurement and increasing the feasibility of the radiographic method as a clinical tool.

Table 2.1 Comparison between existed techniques.

	Surface	Radiographic	Electro-optical	Electro-magnetic	Mechatronic
Advantage	·Non Invasive ·Simple ·Easy to use ·Low cost ·Light weight	·High Accuracy ·Determine intervertebral motion ·High reliability	·Non invasive	·Non Invasive ·High accuracy ·Simple ·Easy to use	·Non Invasive ·High accuracy ·Low cost
Disadvantage	·Less Accuracy ·Less reliability ·Soft tissue variation ·One plane only	·Invasive (Health risk: x-ray)	·Less reliability ·Loss information	·Less reliability ·Soft tissue variation ·Metal interference	·Subject to device limitations ·Soft tissue variation

Widespread clinical use of the measurement methods is not likely if it is invasive, risky and imposes high cost to the health care system. Considerable studies have been conducted to investigate and validate the wide variety of lumbar measurement tools. Several tools are perceived to have problems that limit their utility in clinical environments. Reliability, reproducibility, safety and cost are often cited as limitations to the existing measurement methods. According to Cunningham, "...a nonroentgenographic method of measuring postural curves would be an excellent clinical and research tool if the method was inexpensive, expedient, reliable, and valid" (CUNNINGHAM, BW, GORDON, JD et al. 2003). This thesis examines the possibility of increasing the amount of information that can be derived from surface techniques without the use of radiation. This involves the use of inverse kinematic modelling for movement prediction. And if x-ray measurements have to be employed, this study examines how its clinical feasibility can be enhanced by an automated method. In conclusion, there is a need to develop further the current measurement techniques.

CHAPTER 3 ERROR ANALYSIS OF SURFACE MEASUREMENTS

3.1 INTRODUCTION

Several non-invasive surface methods have been described in the previous literature for measuring spinal geometry and kinematics. These include the use of skin markers (STOKES, IA, BEVINS, TM et al. 1987; BRYANT, JT, REID, JG et al. 1989; SICARD, C and GAGNON, M 1993; LEE, YH, CHIOU, WK et al. 1995; CHEN, YL and LEE, YH 1997), electromagnetic devices (PEARCY, MJ and HINDLE, RJ 1989; MCGILL, SM and KIPPERS, V 1994; NELSON, JM, WALMSLEY, RP et al. 1995), flexible tape measurement (ANDERSON, JA and SWEETMAN, BJ 1975; STOKES, IA, BEVINS, TM et al. 1987) and ultrasonic digitizer (LETTS, M, QUANBURY, A et al. 1988). In comparison with imaged-based methods (MRI, X-ray, etc.), the benefits of surface methods are that they are inexpensive and efficient, and do not have the risk of ionising radiation. However, surface measurements only provided information about the deformation of the skin surface overlying the spine. There is currently no information whether surface measurements can accurately reflect movements of the underlying bone. For instance, skin-mounted sensors have been employed to measure the gross motions of the lumbar spine (PEARCY, MJ and HINDLE, RJ 1989; BURNETT, AF, BARRETT, CJ et al. 1998). Such measurements are subject to errors due to relative movements between the soft tissues and the vertebrae. The size of such errors has not been evaluated experimentally. The potential of surface measurement should be further explored to provide information rather than just gross motions of the whole lumbar spine. For instance, Gatton and Pearcy (GATTON, ML and PEARCY, MJ 1999) were able to use a series of skin-mounted sensors to study the sequence of motions of the vertebral segments. It is unclear if surface measurements could be used to study intervertebral joint movements.

3.2 AIM OF STUDY

The aim of this study was to examine the error involved in the measurement of sagittal movements of the lumbar spine using skin-mounted electromagnetic motion sensors. Spinal movements measured by these sensors were compared with those recorded by radiographs simultaneously. The validity of surface measurements in determining both the gross motions and the intervertebral motions of the spine was studied.

3.3 SUBJECTS AND METHODS

3.3.1 Subjects

Twenty-two healthy male volunteers were recruited from the Duchess of Kent Children's Hospital, Hong Kong. Subject age, height and weight are given in Table 3.1. Lateral radiographs of their lumbosacral spines were taken in full flexion and extension while standing. Subjects who showed any signs of fracture or dislocation, spinal instability, spondylolisthesis, narrowed disc spaces, osteophytes, transitional lumbosacral vertebrae or any structural disorders of the lumbar spine, or those who had previous history of spinal surgery were excluded. The study was approved by the Ethics Committee of Department of Rehabilitation Sciences, The Hong Kong Polytechnic University. Subjects were informed about the experimental procedure and any potential risks prior to the attainment of a written consent form (Appendix II).

3.3.2 Instrumentation

3.3.2.1 Radiographic equipment

The radiographic equipment employed (Fig. 3.1) was Fuji RX medical X-ray film (Fuji Photo Film Co., Tokyo, Japan). The x-ray beam was tightly coned to the lumbosacral spine and protective radiographic shields were worn by all subjects. The study was limited to a small sample of male subjects only as the reproductive organs could not be effectively protected in females.

Each subject experienced only three standard lateral exposures (each exposure was taken at about 90 kV and 40 mAs at a focus-film distance of 1.00 m, equivalent to a skin entry dose of approximately 1x10-3 Gy each).

Fig. 3.1 The radiography equipment

Table 3.1 The subject's information.

Subject's initial	Age, years	Weight, kg	Height, m	BMI, kgm^{-2}
NBH	20	74.5	1.727	24.98
CWT	21	64	1.7	22.15
FTF	20	64.6	1.698	22.41
NYH	22	63.04	1.802	19.41
CKW	22	70	1.76	22.60
LKW	22	67.3	1.75	21.98
CSC	21	66	1.74	21.80
LYN	22	75.9	1.78	23.96
LWM	22	67	1.74	22.13
YCK	22	67.2	1.75	21.94
CYL	23	66	1.7	22.84
NWK	21	72	1.75	23.51
TYC	20	67.4	1.76	21.76
WKH	20	70	1.76	22.60
YYH	20	71	1.76	22.92
CKP	22	60	1.73	20.05
KWC	22	64.5	1.74	21.30
CWC	24	69.1	1.85	20.19
KYK	19	60	1.71	20.52
WHT	19	65	1.77	20.75
PHM	22	74.5	1.73	24.89
WWC	21	74	1.77	23.62
Mean	21	67.9	1.75	22.2
Standard Deviation	1	4.5	0.03	1.45

3.3.2.2 Electromagnetic tracking system (Fastrak System)

The Fastrak system (Fastrak, Polhemus, 40 Hercules Dr, Colchester, Vermont, USA) was used in this study as the motion-sensing device. The system consists of a source of pulsed electromagnetic waves and four sensors of signals. The source was placed in fixed positions close to the subject. The sensors were attached to the skin overlying spinous processes.

Before measuring the motions from Fastrak system, the validity of the system was performed. Two machines were employed in this study (Fig. 3.2). They were synchronized in data collection using a pulse signal from an external box.

The procedure of constructing of a Fastrak system with 8 sensors was showed as follow:

1) Stylus was attached on the sensor 1 of system I;
2) Four markers locations on the fixed plate were collected by one second. They are spacing 100 mm between each other;
3) Eight sensors (both System I and II) were aligned a line, shown as "x" on Fig. 3.2. Then, the directional cosine matrix of local coordinate frame on system I was constructed.;
4) Repeat the above 1 to 3 steps by system II.
5) By matrix computation, a Fastrak system with 8 sensors was developed. The system is only valid if the measuring error of the two corresponding markers were less than 0.1mm for 8 times repeated measures.

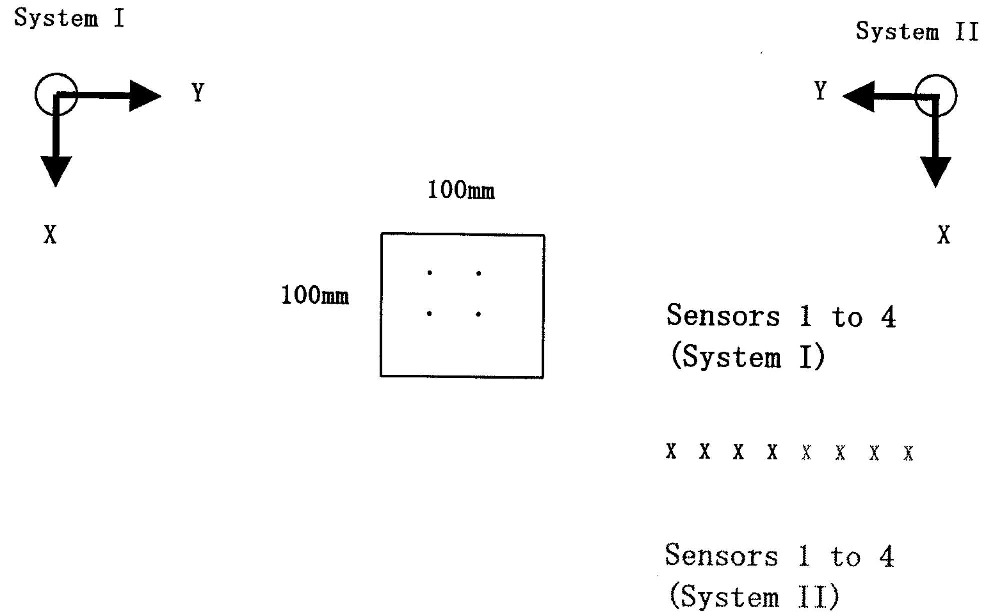

Fig. 3.2 Synchronized two machines to be a Fastrak system with 8 sensors.

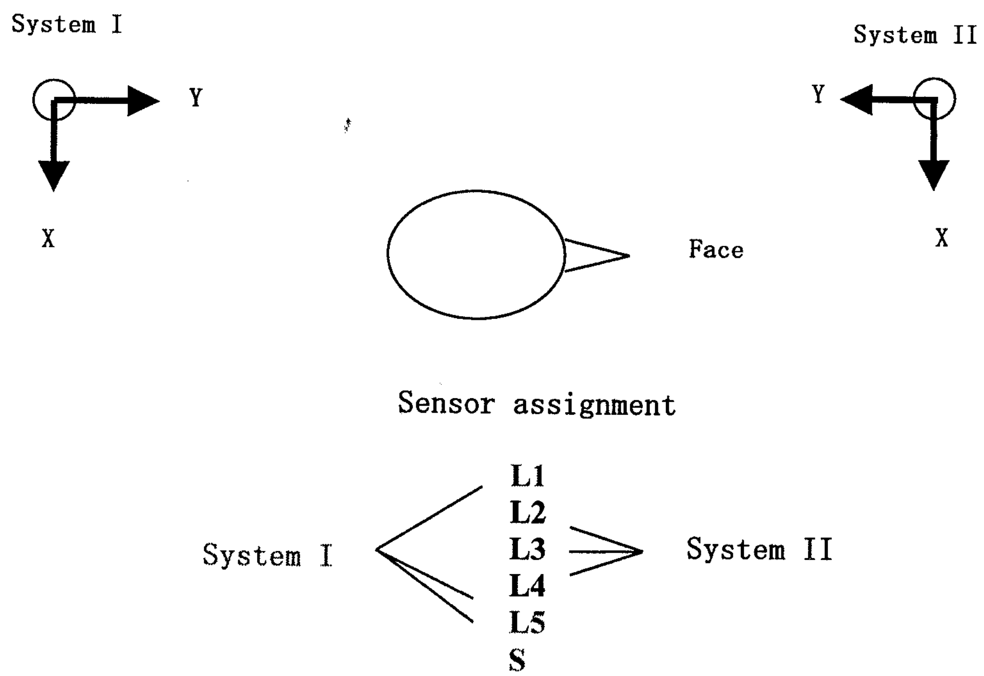

Fig. 3.3 Fastrak system for spinal motions measurement.

The subject exposed his back to which six sensors (three Polhemus RX2 and three RX1C) were attached (L1 to S1) using double-sided adhesive tape. The distance between L1 and S2 was small and it would be impossible to fit six standard RX2 sensors (size 0.9" L x 1.1" W x 0.6" H, 0.32 oz.) between them. Thus two types of sensors were used. The smaller RX1C sensors (size 0.89" L x 0.50" W x 0.45" H, 0.13 oz) were also employed. The three RX2 sensors were placed on the spinous processes of L1, L5 and S1 and the three RX1C sensors were placed on L2, L3 and L4. They are shown in Fig. 3.3. A Fastrak system with a maximum up of 8 sensors developed in this study.

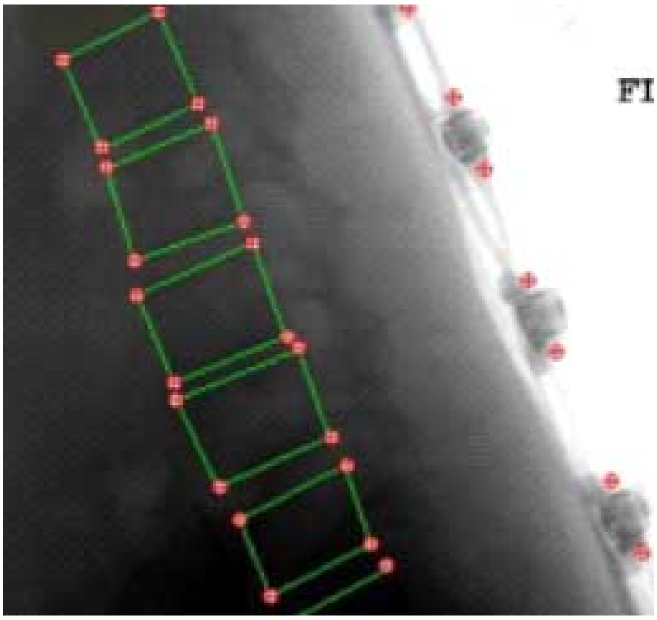

Fig. 3.4a Four-point quadrangles and skin mounted sensors with radio-opaque markers on the lumbosacral spine.

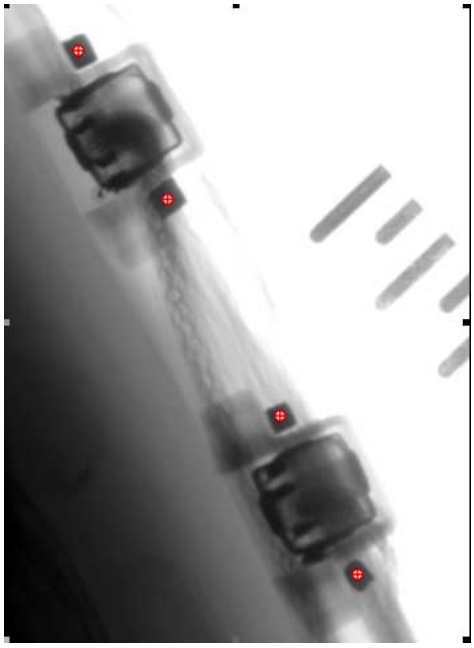

Fig. 3.4b The sensors of the Fastrak system with radio-opaque markers attached on the back.

Two radio-opaque lead markers were fixed on each sensor so that its position could be accurately detected on the radiographs. To ensure that the sensors stayed attached during the movement, straps were applied around the subject's trunk to apply slight positive pressure. Data were sampled at 30 Hz per sensor and acquired by a personal computer. The above arrangement had been used by previous studies and found to be reliable and accurate (LEE, RYW 1995; GATTON, ML and PEARCY, MJ 1999).

3.4 EXPERIMENTAL ALUATION

Subjects were asked to stand upright with the pelvis rigidly fixed to a frame with the left side of the body facing the film. Sagittal images of the lumbar spine (L1-Sacrum) were acquired in three postures: neutral, flexion and extension of the trunk using a conventional radiograph system (Figs. 3.5 (a), (b) and (c)). Three x-ray films were taken in the sequence of subject that stand upright, with his left side of body facing the film; Afterward, subject bent forward and then extend backward. Examiner commented that images are unclear. The clarity of the x-ray image will affect the accuracy of the study. It depends on the resolution of the image size and the brightness and contrast of the intensity. In the study, image represents by 3068 to 4336 pixels and has 13M size of tiff format for each image. They are sufficient for clinical diagnosis as well scientific study.

After taking X-ray, movement measurements by Fastrak system were performed on forward and backward bending. Data was collected with one second when subject stand upright (Neutral) and legs separated with shoulder width. Ten seconds movement measurements were performed to measure neutral to flexion, and flexion to extension, back to neutral movement respectively. Such movement measurements were repeated three times. A minute warm-up exercises done in all of the six different directions - forward, backward, side bending, axial rotation to the left and right before data collection.

A special radiographic ruler (with 5 mm apart) was attached to the subject's back in the sagittal plane to allow for scaling of the X-rays to account for the magnification factor (Fig. 3.4 (b)).

Fig. 3.5a Subject was examined on flexion position.

Fig. 3.5b Subject was examined in standing position.

Fig. 3.5c Example of an active extension examination. The pelvis was rigidly fixed by a Jix-Fixture.

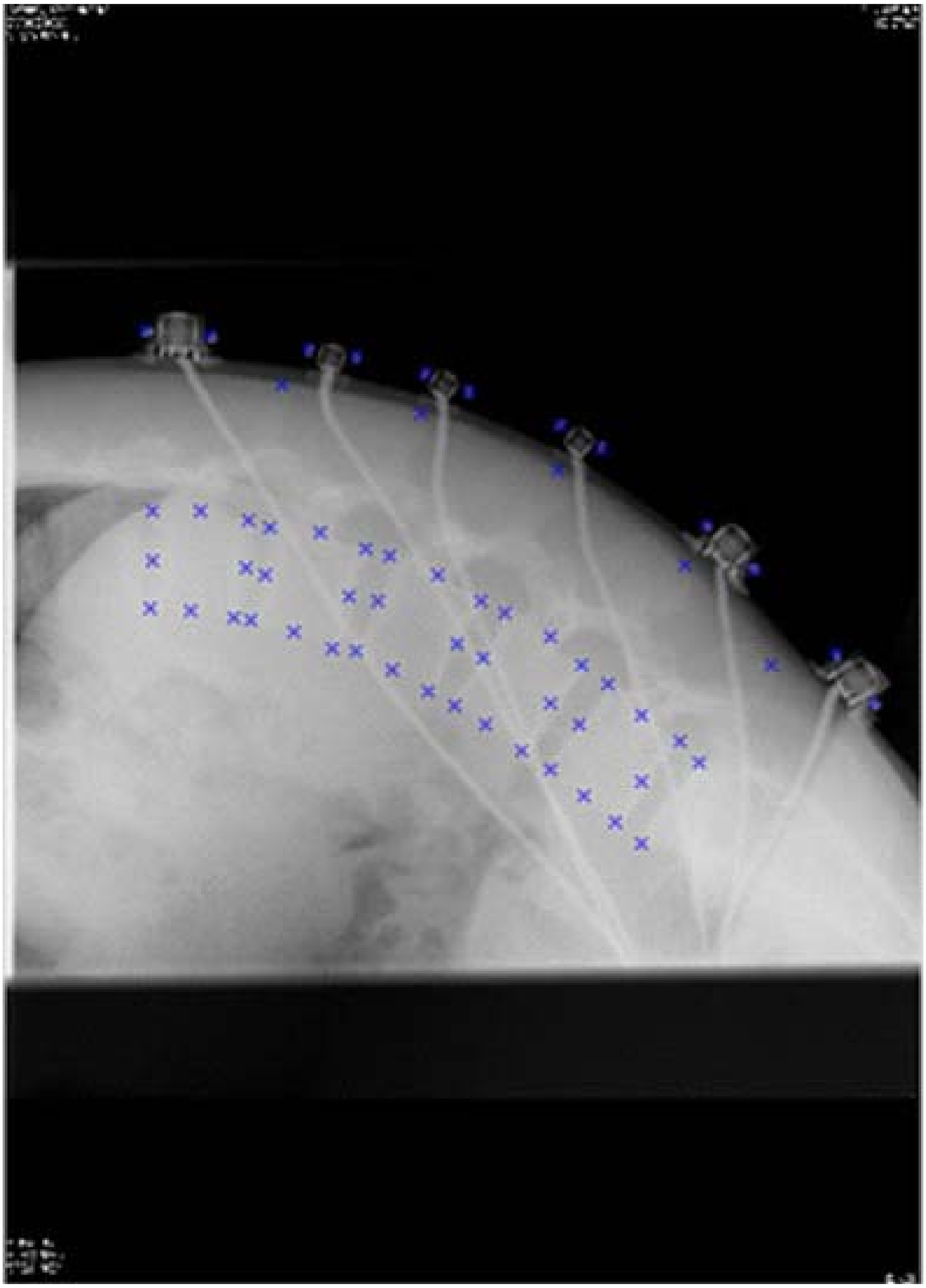

Fig. 3.6a Digitization of the lateral flexion radiographs of the lumbosacral spine.

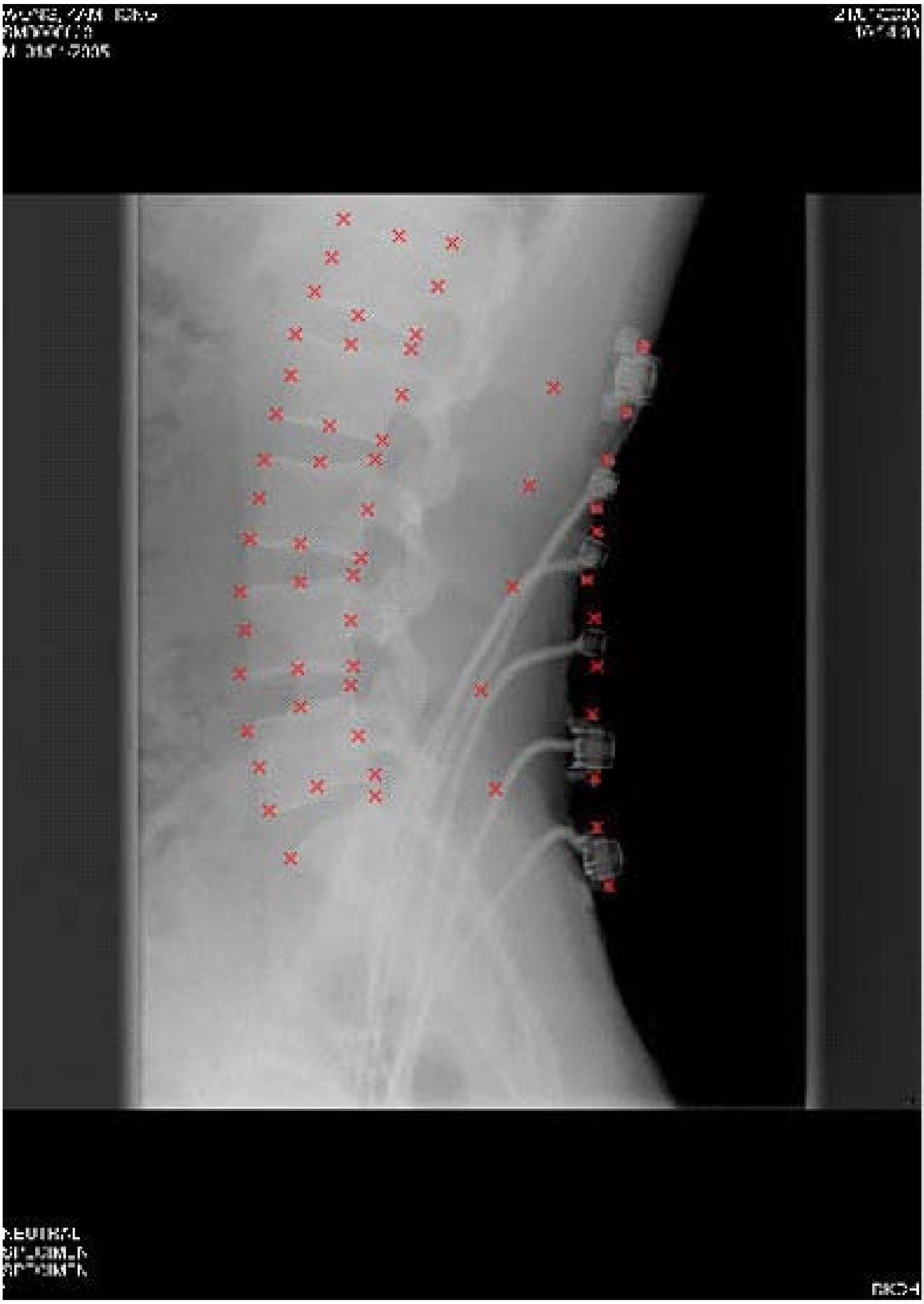

Fig. 3.6b Digitization of the lateral standing radiographs of the lumbosacral spine.

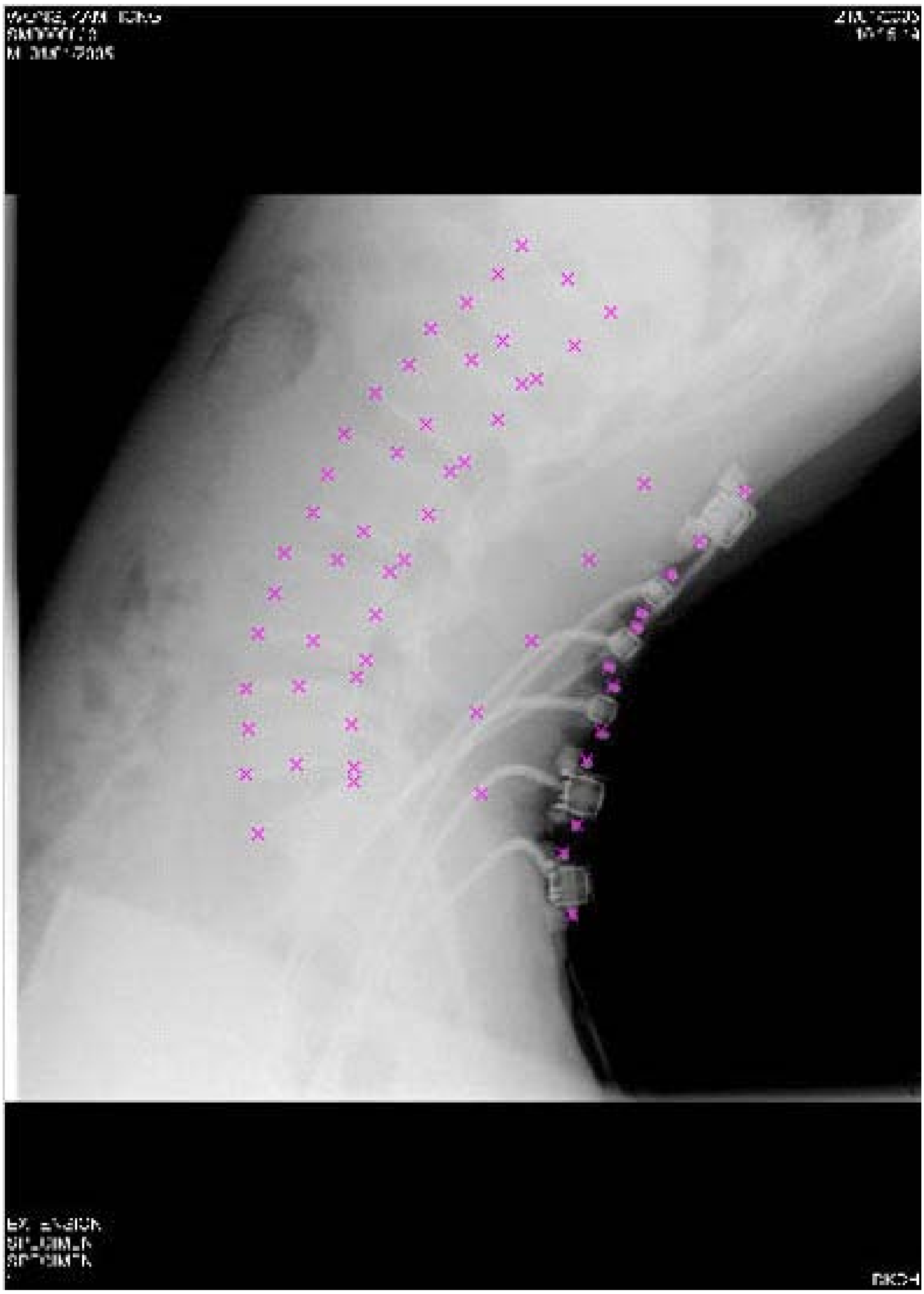

Fig. 3.6c Digitization of the lateral extension radiographs of the lumbosacral spine.

The vertebral body were marked on the three radiographs using the method presented by Frobin (FROBIN, W, BRINCKMANN, P et al. 1996; FROBIN, W, BRINCKMANN, P et al. 1997) Tangent was constructed to the two most prominent points of each margin on the vertebral body image. Quadrangle was created by four tangents. They were fitted with quadrangles in each image, as shown in Fig. B (Appendix I). Intersections of these lines were determined as corners of the vertebral body. The corners of the quadrangle defined four unique reference points for the motion analysis. They were consistent during the data processing. The positions of the posterosuperior and anterosuperior corners of the sacrum, which define a global coordinate system, were also recorded for each image. The technique has been described in detail in previous work (LEE, RYW 1995; LEE, RYW and EVANS, J 1997). They also were presented in Appendix I. The coordinates of the four vertebral body corners (superior and inferior, anterior and posterior) and the midpoints of each side of the vertebral bodies, the tip of the spinous processes, and the two lead markers of the sensors were digitised using computer software. In total, fifty-nine points (11 points per vertebra, plus 2 points for the sacrum) were recorded on each image (Figs. 3.6a to c). All morphological measurements were carried out by the same radiologist to minimise inter-rater variability.

After the radiographic examination, subjects were requested to stand in an area which was free of metals, and perform trunk flexion and extension movement. Data was acquired from the L1 and Sacrum sensor of the Fastrak system so that the gross flexion and extension movement of the spine could be derived from the direction cosine information provided by the machine.

3.5 DATA ANALYSIS

3.5.1 The Reliability Test

The reliability of data acquisition was examined. Digitisation of images on the radiograph was repeated five times. Intra-class correlation (ICC) (3,1) was employed to examine the reliability among the five measurements as presented in Table 3.2. Due to ethical reasons and prevent to expose large doses of radiation on subject, repeated measures of study methods on same subject is prohibited. However, Pearcy and Hindle (PEARCY, MJ and HINDLE, RJ 1989) reported that electromagnetic motion tracking system was accurate and reliable, having a RMS less than 0.2 degrees. Previous reliability studies (LEE, RYW 2001) showed that the intra-class correlation coefficients ranging from 0.93 to 0.99. The radiographic measurements were considered to be sufficiently reliable and accurate.

Table 3.2 Intra-class correlation coefficient (ICC) values of digitisation of image in five repeated measures among 22 subjects

	Mean ICC (3,1)				
	L5/S	L4/5	L3/4	L2/3	L1/2
Angle, deg	0.96	0.96	0.96	0.88	0.92
Posteroanterior translation, mm	0.99	0.99	0.99	0.98	0.95
Superoinfoerior translation, mm	0.99	0.99	0.99	0.98	0.95

3.5.2 Motions Derived from the Radiograph and the Electronic Output of the Fastrak Machine

The sagittal rotations and translation of the intervertebral joints were calculated from the radiographs. Sagittal rotation of the motion segment was determined from the average of change in the inclination of the line vectors joining any two of the vertebral body corners. The rotational angle, θ, between two vertebrae, V_1 and V_2, was calculated using the following equation:

$$\theta = \frac{\sum_{i=1}^{4} ang(E_1^i, E_2^i)}{4} \qquad (1)$$

where E_1^i, E_2^i are the edge vectors defined by the corner points of V_1 and V_2 and the function *ang* is the angle between given vectors. The calculation for each pair of the vertebral body corners was then averaged to provide the best estimate of intervertebral movements. Sagittal translations along the postero-anterior and supero-inferior directions were calculated by the changes in the locations of the centres of the upper vertebral body images with the lower vertebral body superimposed.

Similarly, the two lead markers of the Fastrak sensors were also employed to determine the intervertebral movements. The gross motions of the whole lumbar spine were also calculated from the images of the vertebral bodies of L1 and Sacrum, and also from the images of the L1 and Sacrum Fastrak sensors. As explained above, gross motion of the lumbar spine was also derived directly from the electronic output of the Fastrak machine. The 3x3 direction cosine matrix output (Section A1.5, Appendix I) describes the orientations of the sensors relative to the source. The relative orientation between the L1 and sacral sensors, which described the movements of the whole lumbar spine, were derived from these matrices. The method of computation was based on the mathematical techniques proposed by Lee (LEE, RYW 2001) for the purpose of describing spinal motions.

3.5.3 The Comparability of the Motions Derived from the Vertebral Image, the Sensor Images and Electronic Output of Fastrak Machine

There are three kind of data obtained in the study. Motion derived from the vertebral image was used as standard value for comparison as it represented the "true" movements of individual vertebrae on different segment levels. Motions derived from the vertebral images and the sensor images are directly comparable because they were simultaneously measured. Whilst validation for the intervertebral movement of the spine obtained from plane radiography and skin-mounted electromagnetic sensors in the study, it was to capture a movement as it was being radiographed. Two radio-opaque lead markers on each skin-mounted sensor were attached. They are rigid bodies. The orientation as well as positions of sensors can be accurate determined on the radiographs as it is being exposed to radiation. Therefore, the vertebral image and the sensor images are comparable.

Motions derived from the vertebral images and the electronic output of the Fastrak machine were indirectly comparable because they were obtained in two separate trials. Two measurement systems should not be synchronized at the same time in real clinical practice. Motions derived from the vertebral image and the electronic output of the Fastrak machine were only obtained in two separate trials. However, they are still comparable when two data were matched as best as possible.

3.5.3.1 Curve fitting method

Since the Fastrak machine recorded the movements either in flexion to extension, flexion to neutral or neutral to extension with sampling rate 30 Hz, data measured from the electronic output of the Fastrak machine were a dynamic data in a continuous sequence (Fig. 3.7). However, the motions derived from the vertebral image are static in 3 positions (Flexion, Extension and Neutral). The Curve fitting method was performed to match motion derived from the vertebral image and the electronic output of the Fastrak machine. It was employed to find a best matched frame of Fastrak data to the corresponding digitized sensors on X-ray images of the three postures.

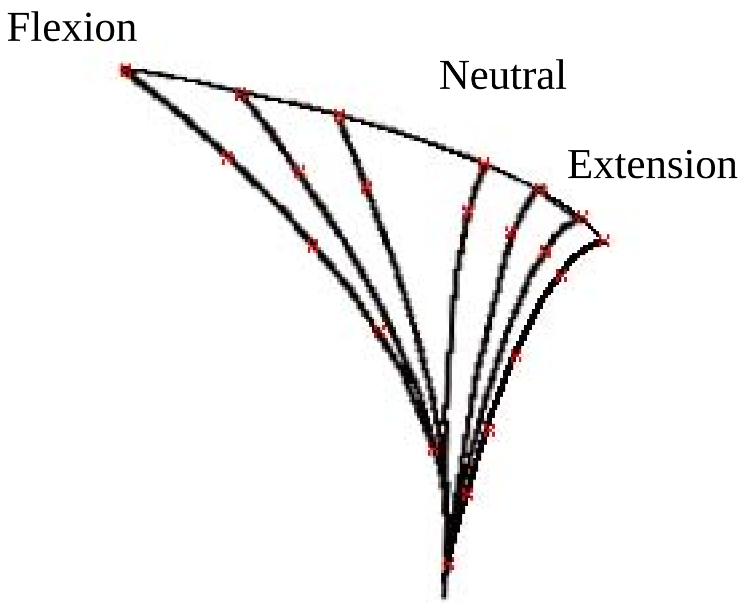

Fig. 3.7 Continuous sequences of data measured by Fastrak machine during performing Flexion and Extension motion.

The procedure of curve fitting method are described as follow:

1. The centres positions of the sensors on 3 x-ray films were fitted a Spline curve (Fig. 3.8). The Cubic equation represented the curve. The curve was then resampled as hundreds of points;

2. For each frame on the continuous sequence, the positions of the sensors derived from Fastrak machine were fitted with another Spline curve (Fig. 3.9);

3. The best matched frame was determined by obtaining the smallest Euclidian residual between two curves;

4. The gross motions were calculated. When the corresponding frames of the three X-ray images were located, the range of motion calculated based on the three frames of Fastrak data were calculated.

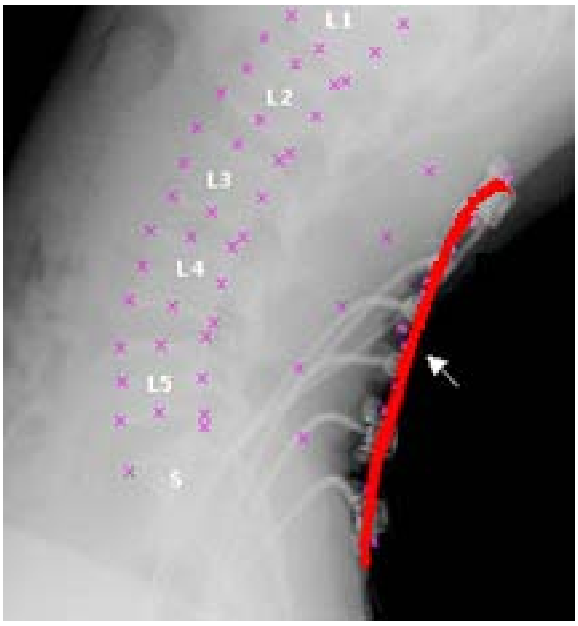

Fig. 3.8 The centres positions of the sensors on radiograph was fitted a Spline curve.

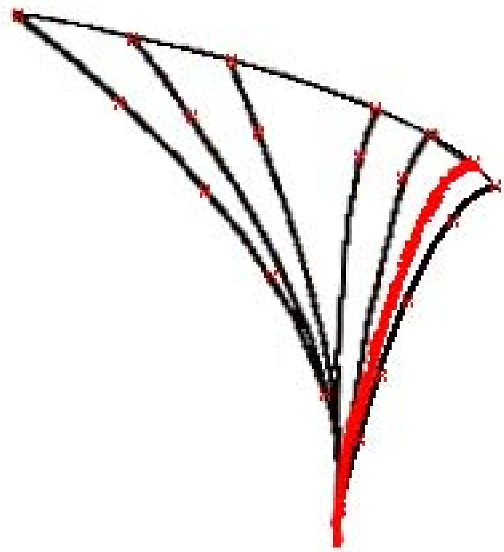

Fig. 3.9 The centres positions of the sensors derived from Fastrak machine was fitted a Spline curve.

3.6 STATISTICAL ANALYSIS

The dependent variables measured in this study included:

1. Gross lumbar spine motions and intervertebral motions determined from the vertebral images;
2. Gross lumbar spine motions and intervertebral motions determined from the sensor images; and
3. Gross lumbar spine motions determined from the electronic output of the Fastrak machine.

The Statistical Package for Social Sciences (Version 11 for Windows) (SPSS Inc., Chicago, Illinois 60606, USA) was employed in this study. Linear regression was used to examine the relationship among the movements derived from the vertebral body image, those derived from the sensor image and those recorded by the Fastrak sensors. Pearson's product correlation coefficient, R was determined to assess the degree of association between various sets of data. R varies from zero (Two sets of data are completely random) to one (Two sets of data are identical). The regression equation described by an equation, which relating the *y* values (derived from the vertebral images) to the *x* values (derived from the sensor images or the output data from the Fastrak machine).

$$y = bx + a \qquad (2)$$

where *b* is the gradient and *a* is the intercept. High value of *b* imposes a steep slope. Intercept *a* value means where the line cuts the y axis. y axis is the data determined from the vertebral image.

Sets of Regression analysis test were performed as follow: Linear regression between gross motions (sagittal rotation of L1 with respect to L1 to Sacrum) derived from vertebral images and sensor images.

Repeat test for full flexion to full extension, full flexion to neutral, neutral to full extension motion. This analysis was performed for range of motion for Flexion and Extension (F/E), Flexion and Neutral (F/N) and Neutral and Extension (N/E). No rational factor of the movement should be determined between full flexion to full extension, full flexion to neutral and neutral to full extension. Each movement was collected correspondingly, described on paragraph 2 on Section 3.4.

3.7 RESULTS

3.7.1 Gross Lumbar Spine Motions and Intervertebral Motions Determined from the Vertebral Images

The gross range of motions of the whole lumbar spine (from L1 to Sacrum) calculated from the vertebral body images are presented in Table 3.3. Intervertebral movements of the lumbar spine from L1 to S1 calculated from the vertebral bone images during the flexion and extension motion are reported on Table 3.4.

Similar magnitudes of motions (either in rotation or translations) were observed at L2/3, L3/4 and L5/S. The angle of rotation was around 14º and the translation motions were 2 mm and 1 mm along the postero-anterior direction and supero-inferior direction respectively. L4/5 had the greatest motion (17.7º, 12.9 mm along postero-anterior direction and 1mm along supero-anterior direction) and L1/2 had the smallest motion (9.7º, 2 mm along postero-anterior direction and 0.1 mm along supero-anterior direction). The large standard deviation of ROM reported due to the large intra-variance of subject. However, similar age, weight, height and BMI of subjects were considered. Warm up exercise done on each subject before examination in order to maintain the normal condition of the flexibility (or Stiffness) of the spine.

Table 3.3 Gross lumbar spine motions (L1-Sacrum) determined from the vertebral images and sensor images among 22 subjects.

Motion		Flexion / Extension		Flexion / Neutral		Neutral / Extension	
		Vertebrae	Sensors	Vertebrae	Sensors	Vertebrae	Sensors
Rotation, deg	Mean	69.1	60.4	56.8	49.4	12.6	11.6
	Std. Deviation	9.1	10.9	9.2	10.2	5.6	9.1
	Minimum	52.8	35.2	41.4	34.8	3.4	-9.5
	Median	69.5	63.0	56.0	49.6	11.1	10.9
	Maximum	82.5	81.2	75.5	76.1	25.8	26.0
Poster-anterior	Mean	11.0	-47.5	8.8	-40.6	2.3	-6.9
Translation, X/mm	Std. Deviation	2.4	12.6	2.5	11.5	1.2	4.9
	Minimum	7.1	-69.6	5.3	-67.4	1.0	-19.1
	Median	10.4	-43.7	8.6	-37.8	1.9	-6.3
	Maximum	16.0	-26.9	15.4	-24.2	5.2	-0.8
Supero-anterior	Mean	2.2	18.2	2.1	12.0	0.2	6.3
Translation, Y/mm	Std. Deviation	3.2	7.2	2.8	6.7	1.4	3.8
	Minimum	-2.7	7.8	-1.3	2.0	-3.1	-1.4
	Median	1.6	17.1	1.2	12.3	-0.1	5.6
	Maximum	13.7	40.3	13.1	36.2	3.7	13.9

Table 3.4 Mean (Standard Deviation, SD) intervertebral motions determined from the vertebral images and sensor images. The mean difference is defined as a difference between data determined from vertebral images and sensor images among 22 subjects.

	Motion segment					
Angle, degree	**L5/S**	**L4/5**	**L3/4**	**L2/3**	**L1/2**	**Total**
Vertebrae, i	13.7 (5.8)	17.7 (4.6)	13.8 (3.5)	14.0 (3.8)	9.7 (4.8)	69.0 (9.1)
Sensors, j	9.4 (9.0)	17.4 (8.1)	10.6 (5.3)	9.6 (6.9)	13.4 (-6.8)	60.4 (10.9)
Difference (i-j)	4.3	0.3	3.2	4.4	-3.7	8.6
Postero-anterior translation, mm	**L5/S**	**L4/5**	**L3/4**	**L2/3**	**L1/2**	**Total**
Vertebrae, i	1.4 (5.8)	12.9 (0.9)	2.5 (0.8)	2.4 (0.6)	2.0 (1.1)	11.1 (2.3)
Sensors, j	6.8 (3.9)	-21.3(17.1)	-28.1(-8.4)	-11.2(6.2)	16.4(10.6)	-47.3(26.1)
Difference (i-j)	-5.5	0.3	3.2	4.4	-3.7	58.5
Supero-inferior translation, mm	**L5/S**	**L4/5**	**L3/4**	**L2/3**	**L1/2**	**Total**
Vertebrae, i	1.0 (0.7)	0.9 (0.7)	0.1 (0.6)	-0.2 (0.5)	0.1 (1.0)	2.2 (3.2)
Sensors, j	4.6 (9.0)	3.7 (8.1)	2.4 (5.3)	2.3 (6.9)	5.1 (-6.8)	18.2 (7.2)
Difference (i-j)	-3.6	-2.8	-2.3	-2.6	-5.0	-16.1

3.7.2 Gross Lumbar Spine Motions and Intervertebral Motions Determined from the Sensors Images

Gross lumbar spine motions and intervertebral motions determined from the sensor images are presented in Tables 3.3 and 3.4. The rotational gross motion (from L1 to Sacrum) determined from sensor images was similar but less than the rotation motion determined from vertebral images, both in three different motions for Flexion and Extension (F/E), Flexion and Neutral (F/N) and Neutral and Extension (N/E). However, the translational gross motions were different and larger than motions determined form vertebral images. The absolute and percentage differences of rotational and translational gross motions of the whole lumbar spine (from L1 to Sacrum) determined from vertebral images and sensor images were presented as Table 3.6.

Regarding the intervertebral movements, the greatest mean motion was seen at L4/5 and L5/S had the least range of motion. The variations in the mean magnitudes of these movements followed a different trend from those values derived from the vertebral images

3.7.3 Gross Lumbar Spine Motions Determined from the Electronic Output of the Fastrak Machine

The mean sagittal rotation, postero-anterior translation and supero-inferior translations of the L1 sensors with respect to the sacrum sensor from full flexion to full extension, full flexion to neutral and neutral to full extension were reported in the Table 3.5. The magnitude of flexion rotation was much larger than that of extension rotation.

Table 3.5 Gross lumbar spine motions (L1-Sacrum) determined from the electronic output of the Fastrak machine among 22 subjects.

	Flexion/Extension		Flexion/Neutral		Neutral/Extension	
	Mean	SD	Mean	SD	Mean	SD
Rotation, deg	66.9	10.7	47.2	10.3	20.0	11.5
Postero-anteriortranslation, mm	31.8	22.5	10.5	20.8	21.4	15.7
Supero-inferiortranslation, mm	28.8	28.3	-6.1	17.5	15.1	29.7

3.7.4 Comparison of Gross lumbar Spine Motion and Intervertebral Motion Determined from Vertebral Images and Sensor Images

Table 3.6 shows the differences of rotational and translational gross motions of the whole lumbar spine (from L1 to Sacrum) determined from vertebral images and sensor images. Absolute differences were denoted as a difference between data determined from vertebral body images and sensor images. The percentage differences were also calculated as the absolute difference divided by the magnitude of motion.

Stokes et al (STOKES, IA, BEVINS, TM et al. 1987) reported that surface measurements provided reasonably accurate measurement of the total lumbar motion between surface and radiographic measures if the differences between two measures were less than ± 11.2° or 25 % with a correlation coefficient of 0.58 or above. Lee

YH (LEE, YH, CHIOU, WK et al. 1995) also reported that skin markers measurement is clinically acceptable if R is larger or equal to 0.62. Based on the previous work, the measurement method will clinically acceptable if two above requirements are fulfilled. This standard was used for comparing the testing data from each method with those from vertebral image on Section 3.7. Based on the standard of “acceptability” and “unacceptability” we established, the absolute differences in gross rotations of the spine determined from vertebral images and sensor images were generally small and clinically accepted. For instance, the absolute difference in gross rotations from full flexion to full extension was 8.7 degrees (percentage difference 12.1 %). However, there were clinically unacceptably large differences for the translational movements (more than 400 % as shown in Table 3.6).

These results (Table 3.6) also indicate there was a lot of sliding of Fastrak sensor along the skin surface, but the sliding did not tilt the sensors significantly on X-ray film. The absolute differences in gross rotations of the spine determined from vertebral images and sensor images were positive. It can be explained that the measuring of the motion derived from the sensor images were underestimation compared with motion derived from the vertebral image. Sensor slides along the axis and move forward on the skin. In general, for instance, detecting of L1 to L5 segment movement becomes detecting of L1 to L4 level. Not completely whole spine measuring occurs due to sliding of sensors. The percentage differences of translation determined from vertebral images and sensor images are large which are ranging from 390 to 3050%, however it is relatively small compared to the length of the whole lumbar spine.

Table 3.6 The absolute and percentage differences of rotational and translational gross motions of whole lumbar spine (from L1-Sacrum) determined from vertebral images and sensor images.

		Absolute Differences		Percentage Differences %	
Motion	Posture	Mean	Std. Deviation	Mean	Std. Deviation
Rotation,	Flexion/Extension	8.7	10.3	12.1	15.2
deg	Flexion/Neutral	7.4	6.9	12.8	12.2
	Neutral/Extension	1.0	9.5	-17.0	148.1
Postero-anterior	Flexion/Extension	58.5	14.5	534.2	80.2
translation,	Flexion/Neutral	49.5	13.5	568.7	100.1
mm	Neutral/Extension	9.1	5.9	390.5	138.3
Supero-inferior	Flexion/Extension	-16.0	7.5	727.3	340.8
translation,	Flexion/Neutral	-9.9	6.9	471.4	328.6
mm	Neutral/Extension	-6.1	3.7	3050	1850

Table 3.7 The absolute and percentage differences of rotational and translational gross motions of the whole lumbar spine (from L1 to Sacrum) among five subjects determined from vertebral images and electronic output of the Fastrak machine after curve fitting.

		Absolute Difference		Percentage Differences %
Motion	Posture	Mean	Std. Deviation	Mean
Rotation,	Flexion/Extension	1.02	2.03	2.08
deg	Flexion/Neutral	1.23	3.19	2.73
	Neutral/Extension	0.89	3.14	0.69
Postero-	Flexion/Extension	5.23	3.98	3.84
anterior	Flexion/Neutral	4.78	4.16	0.32
translation,mm	Neutral/Extension	4.02	3.84	4.09
Supero-	Flexion/Extension	5.93	2.55	0.90
Inferior	Flexion/Neutral	4.29	5.87	8.30
translation,mm	Neutral/Extension	6.38	3.38	4.33

3.7.5 Comparison of Gross Lumbar Spine Motion of the Spine Determined from the Vertebral Images and Electronic Output of the Fastrak Machine

The absolute and percentage differences of rotational and translational gross motions of the whole lumbar spine (from L1 to Sacrum) derived from the vertebral images and electronic output of the Fastrak machine among five subjects after curve fitting are shown in Table 3.7. The absolute and percentage differences in gross rotations were less than 1.23 degrees (percentage difference 2.8 %). They were clinically acceptable. Similarly, the mean differences in the translational movements were equal to the magnitude of the movements. Therefore, there were clinically unacceptably large differences in the translational movements. Results also showed that fixed consistent relation established between the sensor images on radiographs and the electronic output of the Fastrak machine. Therefore, motion data obtained from the Fastrak machine are comparable to those obtained on the radiographs. Both data were matched as best as possible and gross rotational motion derived from Fastrak sensors can represent from Fastrak machine at a reasonable accuracy. The availability of motions derived from the sensor images and electronic output of Fastrak machine was tested by comparing the motions derived from the sensor images and electronic output of Fastrak machine.

The absolute and differences of rotational and translational gross motions of whole lumbar spine from L1 to Sacrum determined from vertebral images and electronic output of the Fastrak machine were reported on Table 3.8. Similarly, there were clinically acceptably difference in the rotational movements and unacceptably large differences in the translational movements.

Table 3.8 The absolute and relative differences of rotational and translation gross motions of whole lumbar spine (from L1-Sacrum) determined from vertebral images and electronic output of the Fastrak system.

		Absolute Differences		Percentage Differences, %	
Motion	Posture	Mean	Std. Deviation	Mean	Std. Deviation
Rotation, deg	Flexion/Extension	-2.1	16.7	-2.8	48.5
	Flexion/Neutral	-9.6	13.0	-19.8	52.8
	Neutral/Extension	7.4	10.5	216.3	318.3
Postero-anterior translation, mm	Flexion/Extension	20.8	33.0	143.5	252.8
	Flexion/Neutral	1.7	22.0	32.3	186.3
	Neutral/Extension	19.1	17.3	382.0	278.5
Supero-inferior translation, mm	Flexion/Extension	26.6	57.1	72.4	1408.7
	Flexion/Neutral	-8.2	34.8	-130.4	803.1
	Neutral/Extension	14.9	63.8	1271.4	10300.7

3.7.6 Regression Analysis of the Gross Range of Motion Derived from Vertebral Images and Sensor Images

Regression of gross range of motion derived from vertebral images and the electronic output of the Fastrak machine during the flexion and extension, the flexion and neutral and the neutral to extension motion were shown in the Figs. 3.10 (a) to (c). Regression equations and Correlation coefficients were presented on each graph. The correlation coefficient was decreasing from flexion to extension, flexion to neutral, neutral to extension. R value was high, ranging from 0.772 to 0.871. The significance $p<0.05$ were reported. Statistical significance of the correlation coefficient were demonstrated.

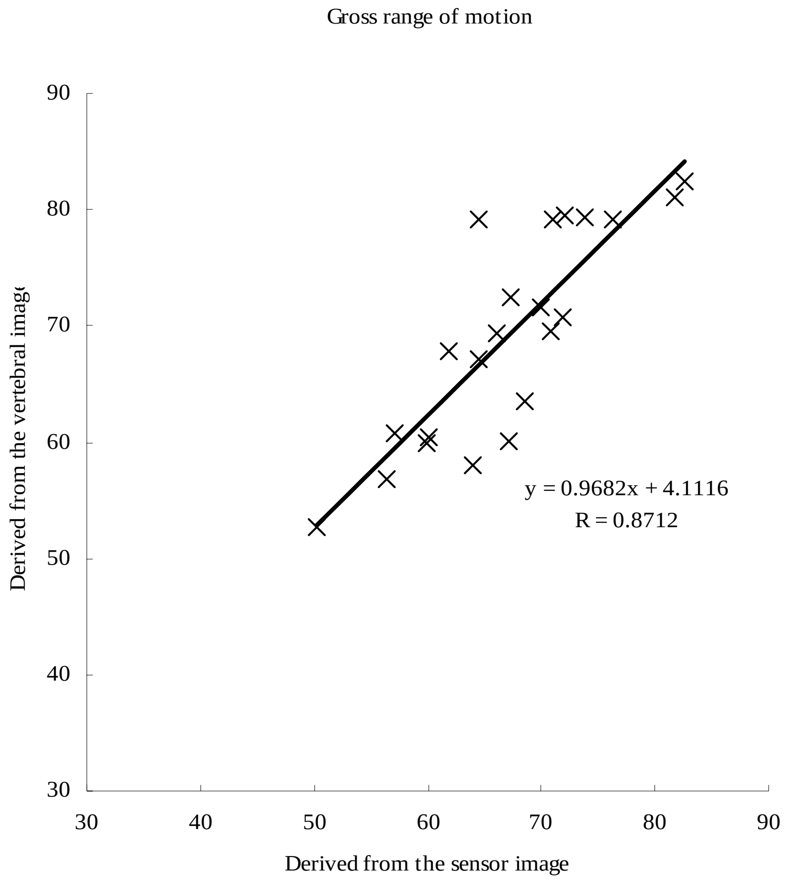

Fig. 3.10a Regression of gross range of motion from vertebral images and sensor images during the flexion and extension motion.

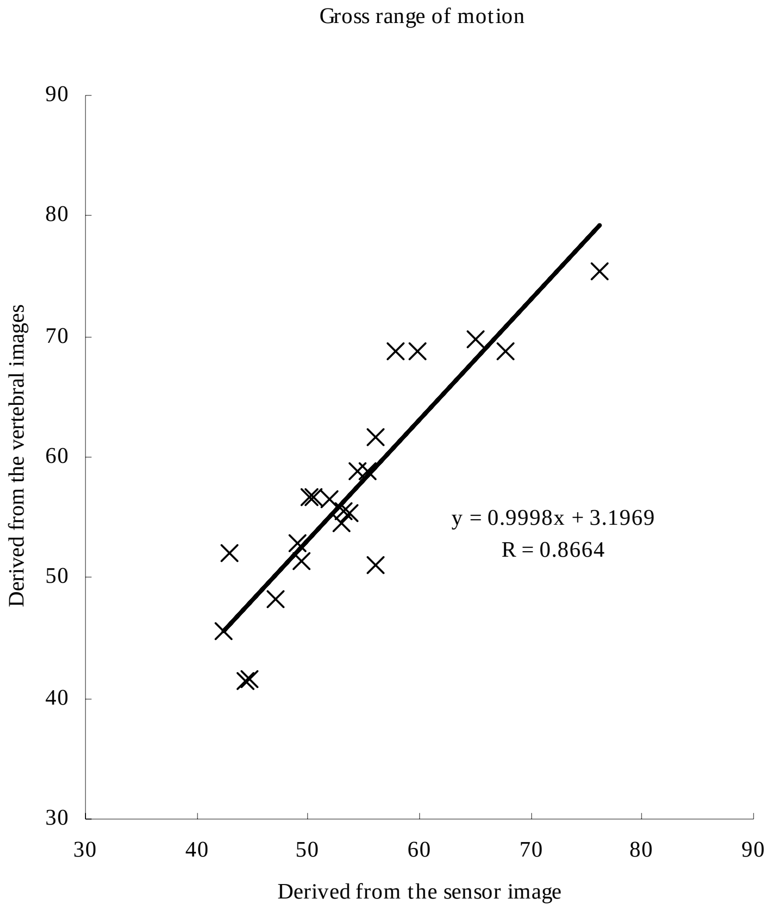

Fig. 3.10b Regression of gross range of motion from vertebral images and sensor images during the flexion and neutral motion.

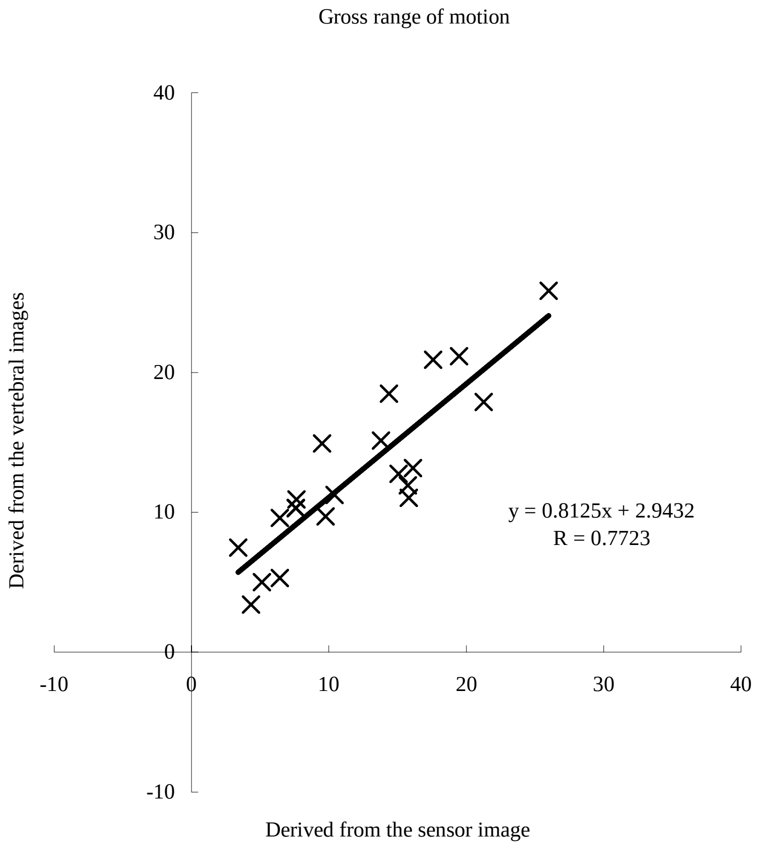

Fig. 3.10c Regression of gross range of motion from vertebral images and sensor image during the neutral and extension motion.

3.7.7 Regression Analysis of the Gross Range of Motion Derived from Vertebral Images and Electronic Output of the Fastrak Machine

Regression of gross range of motion derived from vertebral images and the electronic output of the Fastrak machine during the flexion and extension, the flexion and neutral and the neutral to extension motion were shown in the Figs. 3.11 (a) to (c). The significance $p<0.05$ were reported only in flexion to extension and flexion to neutral, not in neutral to extension.

Compared with section 3.7.6, correlation coefficients were less. Both motions derived from sensor image and electronic output of the Fastrak machine were affected by to the error induced underlying the skin. It is obvious that the relatively large skin error occur in measuring of the gross spine motion using skin-mounted electromagnetic motion sensors. The method was also subject to some system of errors such as less matching of the data film from electronic output of the Fastrak machine to the vertebral image and the background noises.

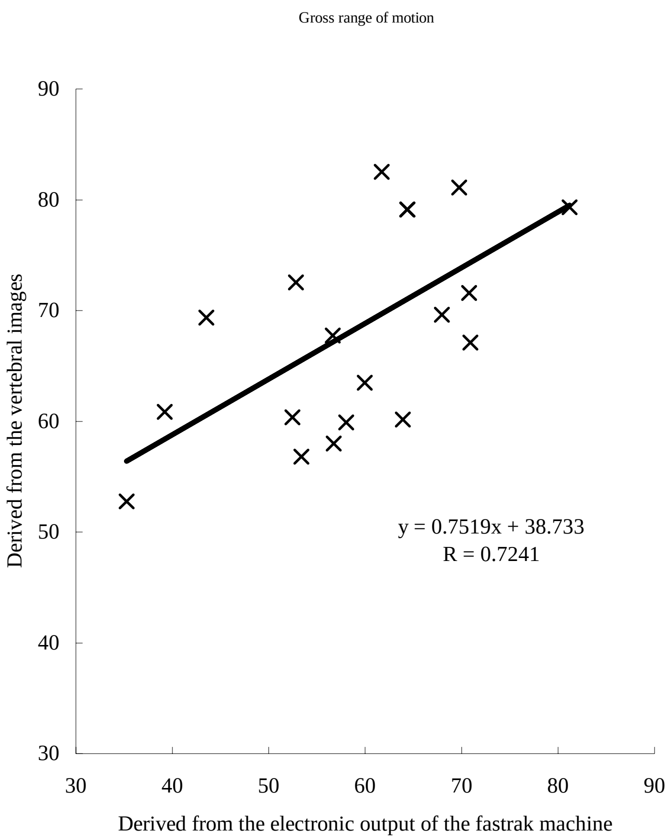

Fig. 3.11a Regression of gross range of motion from vertebral images and the electronic output of the Fastrak machine during the flexion and extension motion.

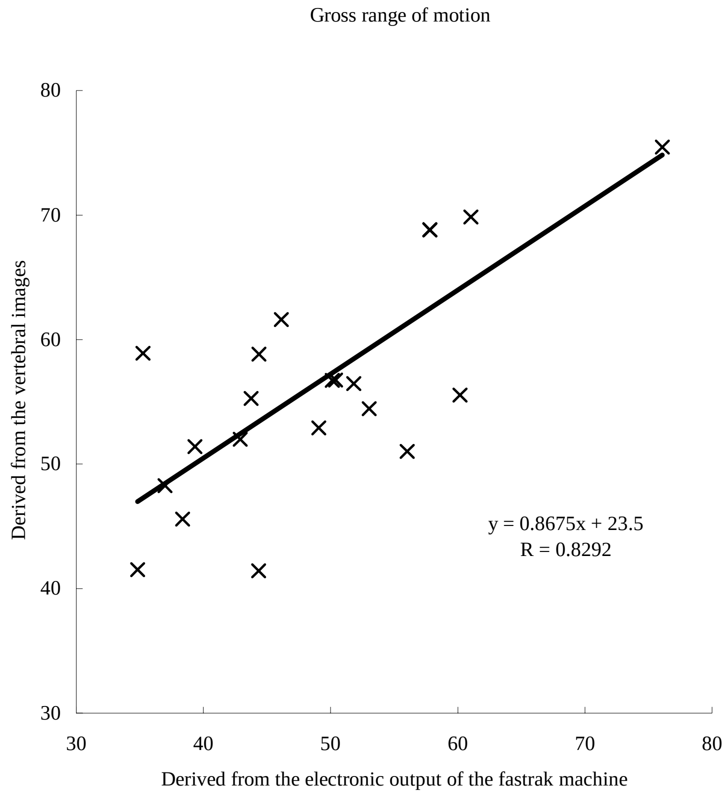

Fig. 3.11b Regression of gross range of motion from vertebral images and the electronic output of the Fastrak machine during the flexion and neutral motion.

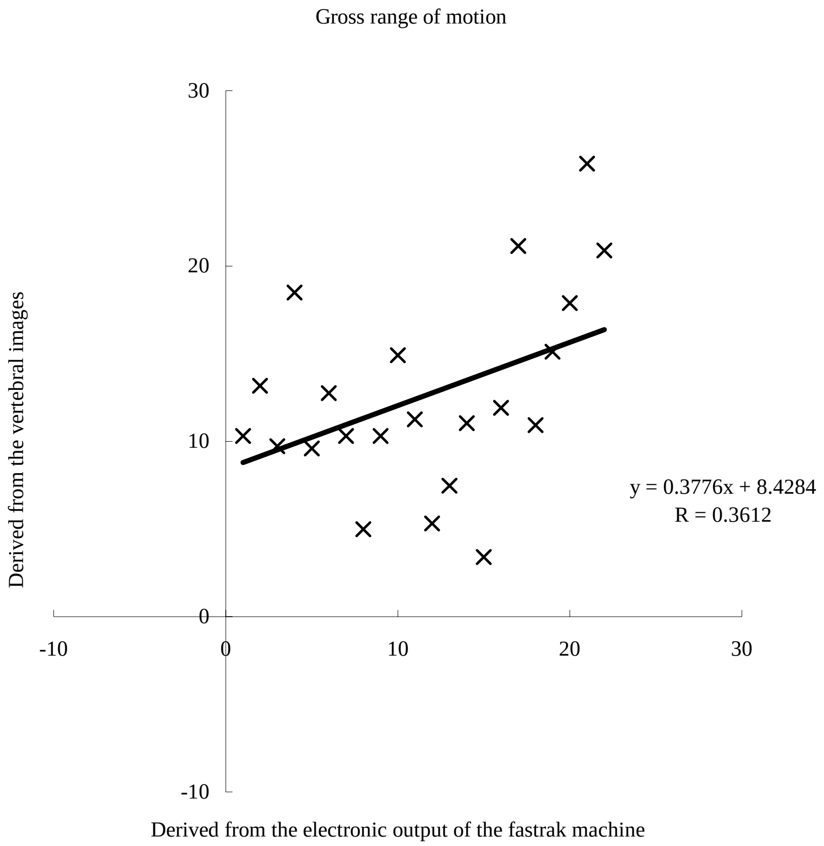

Fig. 3.11c Regression of gross range of motion between vertebral images and the electronic output of the Fastrak machine during the neutral to extension motion.

3.8 DISCUSSION

3.8.1 Gross Motion of Spine

The magnitude of the rotational gross motion of the lumbar spine in the sagittal plane during flexion and extension motion was reported to be 78º (WHITE, AA and PANJABI, MM 1978), 70º (PEARCY, M, PORTEK, I et al. 1984) , 76º (DVORAK, J, PANJABI, MM et al. 1991) and 64º (YAMAMOTO, I, PANJABI, MM et al. 1989). The mean gross rotations of the lumbar spine derived from the vertebral images (69.1º), the sensor images (60.4º) and the electronic output of the Fastrak machine (66.9º) were similar to those reported in previous work.

The magnitude of intervertebral translation was reported to be around 15mm (PEARCY, M, PORTEK, I et al. 1984; DVORAK, J, PANJABI, MM et al. 1991). The postero-anterior translation (X-translation) was two to three times larger than the supero-inferior translations (Y-translation). The measured mean translational motions (2~11 mm) from the vertebral body image were in close agreement with those reported in previous work only. Larger measured mean translational motion from the sensor images and recorded were by Fastrak® system were found. However, measurement of translational motions using skin-mounted sensors was not feasible as there would be large errors as demonstrated by this study. The measurement of translation of spinal motion has extremely high percentage errors due to the small magnitude of the movement (only 1 to 20 mm). The mean total magnitude of sagittal translation of the whole lumbar spine (from L1/2 to L5/S1) was found to be 11 mm and 2.2 mm along posterior-anterior and superior-inferior degrees in this study. The present experimental results indicate there was a lot of sliding of the Fastrak sensors along the skin surface during the performance of spinal motions, but the sliding did not tilt the sensors significantly so that they could still be reliably used to measure gross sagittal rotation of the lumbar spine.

3.8.2 The Intervertebral Movements of the Spine

Difference between data determined from vertebral images and sensor images was shown in Table 3.6. The analysis results showed that the method in using skin-mounted sensors to predict the rotational range of the entire lumbar spine is acceptable for lumbar spines, but not at the intervertebral level. There are unacceptably large errors in intervertebral movements in the data determined from both the sensor images and the electronic outputs of the sensors.

3.8.3 Validity of Surface Measurement

A high linear correlation (R = 0.742 to 0.829) was found between the gross lumbar range of motion derived from the vertebral body images and the electronic output of the Fastrak machine. The correlations were higher for full flexion to full extension and for full flexion to neutral than that for neutral to full extension, as the range of motion of neutral to full extensions were smaller and more difficult to measure. The regression equations provided in this study showed the nature of error induced by skin deformation underlying the sensors. The constant b represent the error associated with the movement of the sensors, and would represent error due to sliding of the sensor. The constant a is the offset error, which is constant regardless of the movement of the sensor. This might represent error introduced by placement of sensors. In future research studies, the regression equation should be used to correct gross motions determined by skin-mounted sensors, but such correction could only be done for young healthy male subjects. It was not unclear if the same error pattern and magnitude would be observed in other population groups.

The major reason for the error associated with skin-mounted sensors is soft tissue deformation. The present study addresses a limitation of previous work, which provided no information about the size of the error due to soft tissue deformation. The present study clearly suggests that skin mounted sensors are not accurate enough to provide information about intervertebral movement as the magnitude of the movement is similar to that of the error due to soft tissue deformation underlying the sensors.

The experiment was performed with a small group of male volunteers. The ethical problem of taking x-rays of normal subjects limited the study to a small sample size. However, the movements of twenty-two subjects were sufficiently consistent to establish a baseline for comparison of movements determined from the vertebral body images, the sensor images and between skin-mounted sensors based measurement.

In this study, we used only male subjects for error analysis of surface measurements. The result of the study would be affect by the gender, ageing, different pathology of the people selected. The outcome of the study would have been different if female subjects included because of the different patterns of movement. The percentage of muscle and fat combination of the tissue will also affect the error size of the study. Patients with large changes in vertebral geometry such as osteropenia, osteropororosis and obesity definitely have an effect on the result. This should explore the research direction of the further development how the intra-variance of the individuals that have affected the results in the study. Some precautions were taken to aware of these issues. Exclusion criteria on all studies were included. Subject with a fracture, dislocation or nay structural defeats of vertebrae were excluded. Warm up exercise done on each subject before examination in order to maintain the normal condition of the flexibility (or Stiffness) of the spine.

3.9 CONCLUSION

The feasibility of surface measurement in intervertebral movements and gross motion measurement were addressed. Experimental validation was conducted to evaluate the validity of method that determines the intervertebral movements of the lumbar spine with given knowledge based on the surface detection method. While the analysis results show that the error of using skin-mounted sensors to predict rotational range of gross motion is acceptable for lumbar spines, the errors associated with gross translational motion ranges are not acceptable. The correlation between the lumbar gross range of motion determined from the vertebral body images and recorded by the sensors suggest that the surface measurement method could be used for measuring full flexion to full extension and full flexion to neutral, but the measurement would be less ideal for neutral to full extension. The regression equation established in this study could be used to correct the measured values for errors produced by skin deformation underlying the sensors.

In addition, the results of this study showed that the skin-mounted sensors are not accurate enough to measure movements at the intervertebral level. This might require the use of radiographic measurements. However, if an alternative surface method could be developed to determine movements of the intervertebral joints using mathematical prediction, there will be widespread applications in assessing a patient's treatment outcomes and the risks of radiation would be avoided. The proposed study in next chapter (Chapter 4) attempted to achieve this goal using an inverse kinematic method which is commonly used in robotic engineering.

CHAPTER 4 PREDICTION OF INTERVERTEBRAL MOVEMENTS USING AN INVERSE KINEMATIC ALGORITHM (INDIRECT METHOD)

4.1 INTRODUCTION

The human spine has redundant degrees of freedom, giving us great flexibility in the performance of a movement. For instance, forward-bending movement of the spine can be accomplished with an infinite number of combinations of configurations of the various intervertebral joints. Inverse kinematics is a method used in robotic engineering for determining joint configurations given a desired position and orientation of the end effector of the robot in achieving a certain goal (CRAIG, JJ 1989; MCCARTHY, JM 1990; ALLARD, P, STOKES, IAF et al. 1995; ZHANG, X and CHAFFIN, DB 1996; ZATSIORSKY, VM 1998). We propose that an inverse kinematic algorithm may be used to determine whether a certain combination of intervertebral joint configurations may be the most feasible and reasonable way of performing forward bending.

The inverse kinematic method has been successfully used to model the movements of various body joints (SOMMER, HJ, 3RD and MILLER, NR 1980; FUJIE, H, MABUCHI, K et al. 1993; JUNG, ES, CHOE, J et al. 1994; ZHANG, X and CHAFFIN, DB 1996; ZATSIORSKY, VM 1998; WANG, X 1999). For instance, Sommer (SOMMER, HJ, 3RD and MILLER, NR 1980) described a spatial inverse kinematic model to predict an *in vivo* wrist joint under typical physiological loading conditions. Fujie et al. (FUJIE, H, MABUCHI, K et al. 1993) developed a 6-axis articulated manipulator with 6 degrees of freedom (DOF) of motion. It modified to control and measure both the force and position of synovial joints for the study of joint kinematics. It performed an anterior-posterior (A-P) translation test on a human cadaveric knee under simulated physiological loading conditions. It showed that the system simulated complex loading conditions and measured the resulting joint kinematics. Jung et al. (1994) (JUNG, ES, CHOE, J et al. 1994) employed a psychophysical cost function (potential function) to define a cost value for each joint movement angle and developed a regression model to predict the perceived discomfort with respect to the joint movement. Zhang (ZHANG, X and CHAFFIN, DB 1996) developed a new optimization-based differential inverse kinematics approach for modeling three-dimensional dynamic seated postures. Wang (WANG, X 1999) also utilized an inverse kinematics algorithm to predict arm postures.

However, the inverse kinematic method has never been applied to model the movements of the spine. This is probably because the spine has unlimited numbers of degrees of freedom, and finding an optimal solution to the inverse kinematic problem would be extremely difficult. However, a solution may be feasible if appropriate constraints could be imposed on the kinematic modelling. For instance, the positions of the most posterior parts of the spinous processes may be determined by surface measurements. Such information may be used to reduce the number of solutions. In addition, an optimisation function may be employed to determine the best solution.

This chapter presents an inverse kinematic model that was employed to determine an optimal intervertebral joint configuration for a given forward-bending posture of the human trunk. The purpose of this study was to evaluate the validity of using an inverse kinematic model to determine intervertebral joint movements with a given knowledge of the total flexion movement of the lumbar spine and the positions of the spinous processes. The lumbar spine was modeled as an open-ended, kinematic chain of five links representing the five vertebrae (from L1 to L5). An optimization equation with physiological constraints was employed to determine the intervertebral joint configuration. Intervertebral movements were measured from sagittal x-ray films of twenty-two subjects to validate the method. The mean differences between x-ray measurements of intervertebral rotations in the sagittal plane and the values predicted by the kinematic model were compared and are summarized in tabular form.

4.2 MODELING

The lumbar spine was modeled as a five-link system from the L1 to L5 vertebrae, which is shown in Fig. 4.1. It was assumed that there were three degrees of freedom (DoF) (one rotation and two translations) for each intervertebral joint. Forward flexion of the spine was assumed to be confined to the sagittal plane (PEARCY, MJ 1985). The Denavit-Hartenberg convention (MCCARTHY, JM 1990; ZATSIORSKY, VM 1998; TAKAYANAGI, K, TAKAHASHI, K et al. 2001) was used to describe the multilink chain. The antero-superior corner of the sacrum was considered to be the origin of the kinematic chain in the global coordinate system. A local coordinate system was defined for each vertebra with the x-axis running from the antero-superior corner to the postero-superior corner of the vertebrae and the y-axis perpendicular to the x-axis (TAKAYANAGI, K, TAKAHASHI, K et al. 2001).

The following information was assumed to be known:

(a) The positions of the most posterior parts of the spinous processes – In this study, the positions were obtained from radiographs. But clinically, these bony landmarks can be easily palpated through the skin surface. Their positions can be predicted from surface measurements (STOKES, IA, BEVINS, TM et al. 1987) or directly measured by non-invasive techniques such as ultrasonic scanning (PORTER, RW, WICKS, M et al. 1978; SUZUKI, S, YAMAMURO, T et al. 1989).

(b) The total movement of whole lumbar spine – This was determined from the changes in the curvature (lordosis) of the lumbar spine during the forward-bending movement. Lumbar lordosis was defined by the angle of intersection between a line running along the inferior border of T12 and a line along the superior border of the sacrum. Clinically, this is referred to as Cobb's method, and could be readily determined by surface measurement techniques.

(c) The geometry of the vertebrae and the length of each link of the kinematic chain – These parameters were obtained from previous studies (TENCER, AF and MAYER, TG 1983; PANJABI, MM, GOEL, V et al. 1992; CHAFFIN, DB, ANDERSSON, G et al. 1999).

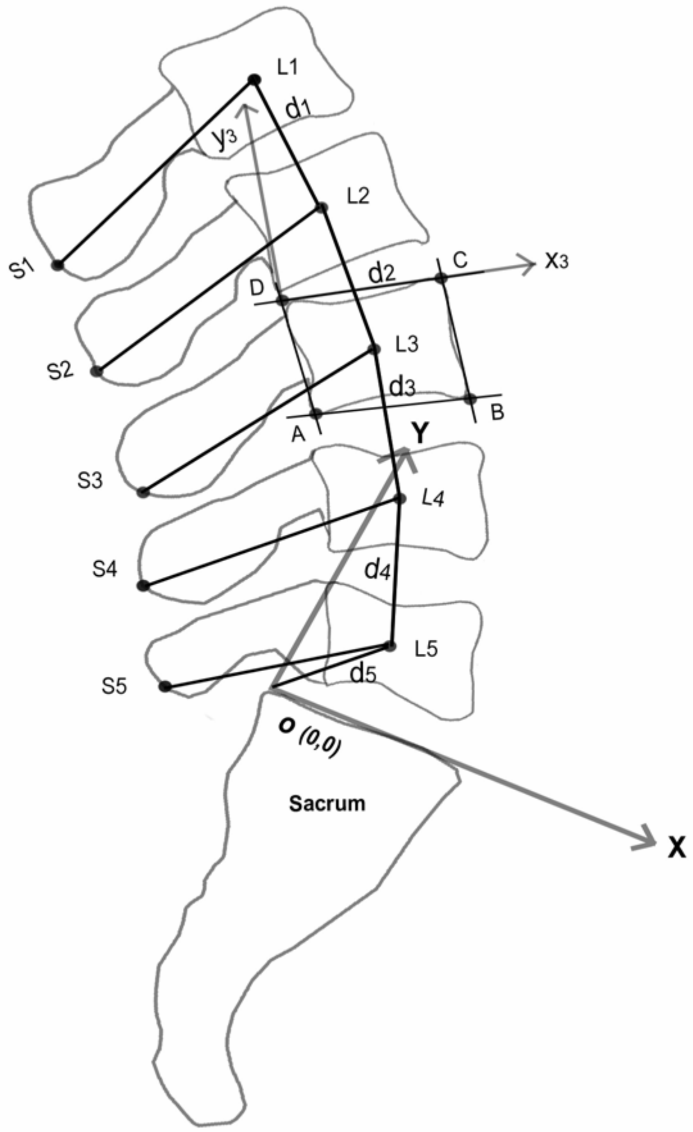

Fig.4.1 Five-line kinematic model of the lumbar spine. Four corners of each vertebra (A.B.C.D) are identified by fitting the vertebral body image with a quadrangle. The local coordinate system of the intervertebral joint (shown for L2/3 segment only) is defined by the x_i-axis joining the posterosuperior and anterosuperior corners of lower vertebra of the joint, with the origin at point D. The y_i-axis is perpendicular to the x_i-axis. The position of the spinous process is denoted as S_i. d_i is the length of the kinematic chain from the i^{th} vertebra to the $(i + 1)^{th}$ vertebra. The global coordinate is shown on the x- and y-axes.

The inverse kinematic problem was to derive the intervertebral joint configuration with the known positions of the spinous processes. The joint angles, θ_I, and the x- and y- translations of the vertebrae (L1 to L5) were the state variables, ω_i. Thus, there were three unknown variables for each joint and, with five joints in the kinematic chain, the total number of unknown variables was fifteen.

The coordinates of the most posterior parts of spinous processes, S_i, were expressed as functions of the state variable, ω_i, which is a function of joint angles, θ_i, and x_i and y_i translations of the i^{th} vertebrae (i=1,2…5) (Appendix I).

$$S_i = f(\omega_i) \qquad (1)$$

where

$$\omega_i = [\theta_i, x_i, y_i]^T$$

In order to derive the variable ω_i with a given S_i, the inverse of the equation would be required. That is,

$$\omega_i = f^{-1}(S_i) \qquad (2)$$

Solving the above equation is difficult. There is more than one solution for a given set of S values. The inverse kinematic problem was therefore solved by the general equation:

$$\dot{\omega} = J^+ \cdot \dot{S} + \left(I - J^+ \cdot J\right)\left(-k\,\frac{\partial P}{\partial \omega}\right)^T \qquad (3)$$

where J was the Jacobian matrix,

$$J(\omega) = \frac{\partial}{\partial \omega} S \qquad (4)$$

$J^{+,}$ the pseudoinverse of J, and I create the identity matrix. The term P, referred to as the potential function, defines the secondary conditions that need to be fulfilled. It eliminates redundancy, accounts for the physiological limits of the intervertebral joints and avoids kinematic singularities. An optimal solution of the inverse kinematic problem was obtained by minimizing the potential function (VAN DEN BOGERT, AJ, SMITH, GD et al. 1994; TILG, B, FISCHER, G et al. 2002).

The following potential functions were employed in this study.

[i] The error (ε) in predicting the total movement of the lumbar spine (γ_o) was minimized. The potential function was

$$P_1(\omega) = \frac{1}{2}\varepsilon^2 \qquad (5)$$

where $\varepsilon = \gamma_0 - \theta_1 - \theta_2 - \theta_3 - \theta_4 - \theta_5$. The following equation was then used to obtain values of θ_i for the error, ε, to be less than a pre-defined value (1 degrees).

$$\frac{\partial P_1}{\partial \omega} = (\gamma_0 - \theta_1 - \theta_2 - \theta_3 - \theta_4 - \theta_5)[1 \quad 1 \quad 1 \quad 1 \quad 1 \quad 0 \quad \dots \quad 0] \qquad (6)$$

[ii] The potential function for constraining the intervertebral rotations and translations (θ_i, x_i and y_i) within the physiological limits of the joints was

$$P_2(\omega) = \left\{ \begin{array}{l} \sum_{i=1}^{5} \frac{1}{2}\left(\theta_{i\,\max} - \theta_i\right)^{-2} + \left(\theta_{i\,\min} - \theta_i\right)^{-2} \\ \sum_{i=1}^{5} \frac{1}{2}\left(x_{i\,\max} - x_i\right)^{-2} + \left(x_{i\,\min} - x_i\right)^{-2} \\ \sum_{i=1}^{5} \frac{1}{2}\left(y_{i\,\max} - y_i\right)^{-2} + \left(y_{i\,\min} - y_i\right)^{-2} \end{array} \right\} \qquad (7)$$

where $\theta_{i\,min}$,$\theta_{i\,max}$, $x_{i\,min}$, $x_{i\,max}$, $y_{i\,min}$, $y_{i\,max}$ are the minimum and maximum values of θ_i, x_i and y_i. The minimum and maximum allowable joint angles are –5 degrees and 22 degrees respectively. These values were based on experimental results reported by previous authors (PEARCY, MJ 1985; SHAFFER, WO, SPRATT, KF et al. 1990; PANJABI, MM, GOEL, V et al. 1992). The minimum and maximum allowable values of the x and y translations are –10mm and 10mm, respectively. Previous studies showed that the intervertebral joints did not exhibit translation beyond these values (WHITE, AA and PANJABI, MM 1978; PANJABI, MM, GOEL, V et al. 1992). It follows that

$$\frac{\partial P_2^T}{\partial \omega} = \left\{ \begin{array}{l} \left(\theta_{i\,\max} - \theta_i\right)^{-3} + \left(\theta_{i\,\min} - \theta_i\right)^{-3} \\ \left(x_{i\,\max} - x_i\right)^{-3} + \left(x_{i\,\min} - x_i\right)^{-3} \\ \left(y_{i\,\max} - y_i\right)^{-3} + \left(y_{i\,\min} - y_i\right)^{-3} \end{array} \right\} \qquad (8)$$

[iii] There were a number of possible solutions for θ_i, x_i and y_i after the potential functions P_1 and P_2 were employed. The Jacobian determinant (P_3) was then used to eliminate those solutions with kinematic singularities. Minimising the determinant would allow convergence of the potential function, P_3, so that an approximate solution of ω could be determined.

$$P_3(\omega) = -\sqrt{\det(J \cdot J^{+})} = -w, P \to P_{\min}, \dot{D} \subset 0 \qquad (9)$$

An iterative refinement algorithm was used to improve the solution (CHEN, K, GIBLIN, P et al. 1999). The positions of the spinous processes were predicted using the approximate solution of ω and equation (1). The residuals (r) of the solution were defined as the difference between the predicted and actual spinous process positions. The solution was accepted if the residual was less than its 2-norm $\|r\|_2$. If not, the inverse kinematic problem was considered to be ill conditioned. Singular value decomposition was employed (GOLUB, GH and VAN LOAN, CF 1996; CHEN, K, GIBLIN, P et al. 1999) to estimate the error. The approximate solution of ω was adjusted accordingly. The new θ_i, x_i and y_i values would then serve as initial values for obtaining another solution of ω using the inverse kinematic equation and the potential functions. This process was repeated until the residual of the solution was less than the 2-norm. The inverse kinematic problem was then considered to be well defined and the solution of ω optimal. The inverse kinematic algorithm for obtaining an optimal solution of ω is summarized in Fig. 4.2.

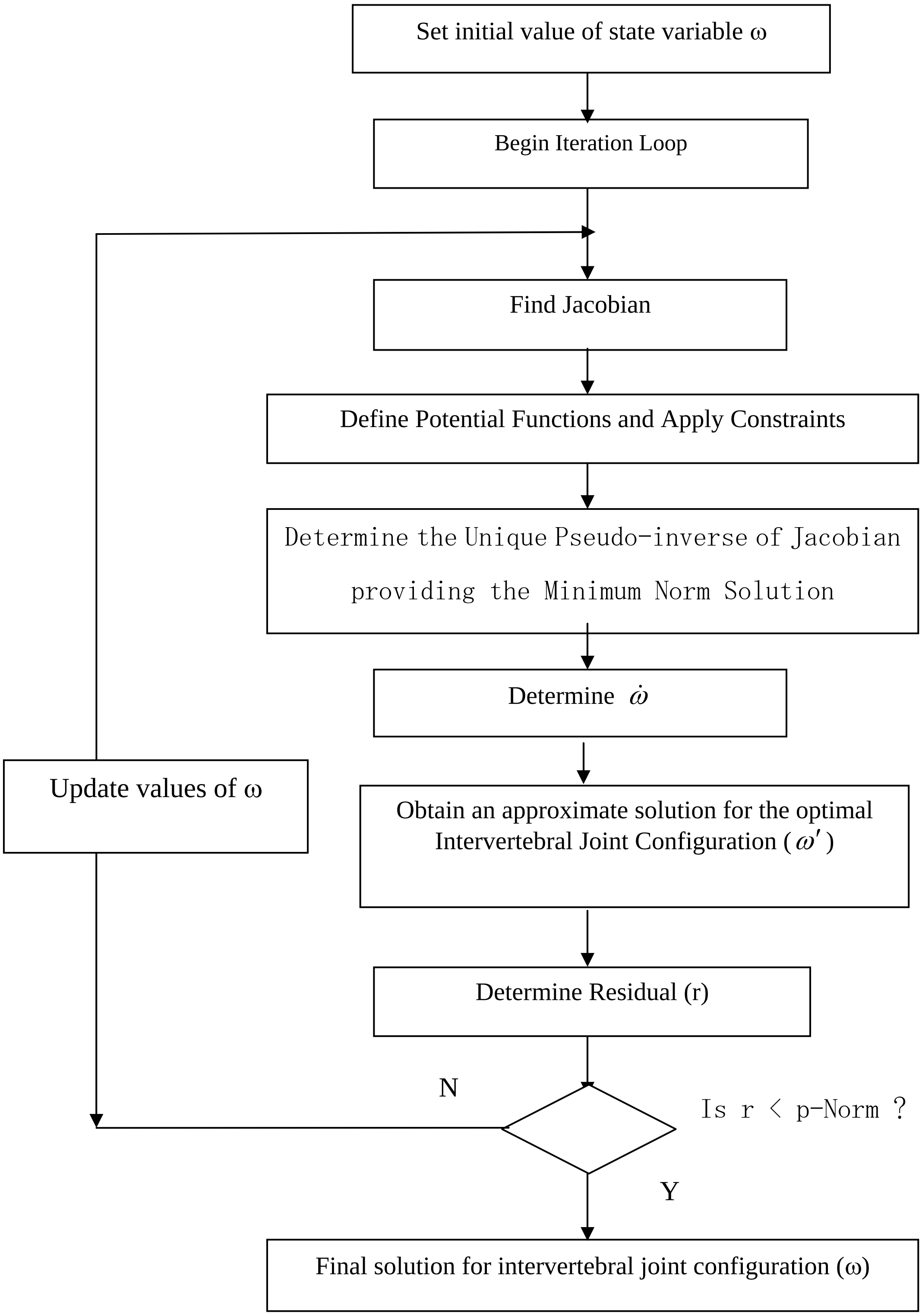

Fig. 4.2 The inverse kinematic algorithm for predicting intervertebral movements of the lumbar spine.

4.3 EXPERIMENTAL VALIDATION

Lateral radiographs of the lumbosacral spines of twenty-two subjects (9 men and 13 women, mean age = 40 ± 14 years) were obtained from the Duchess of Kent Children's Hospital, Hong Kong. They were taken with the lumbar spine in full flexion and extension while standing. The radiographs were either taken during routine clinical examination or used in other research studies. Subjects were diagnosed with non-specific LBP with no pathologies. Subjects who showed any signs of fracture or dislocation, spinal instability, spondylolisthesis, narrowed disc spaces, osteophytes, transitional lumbosacral vertebrae or any structural disorders of the lumbar spine, or those who had previous history of spinal surgery were excluded.

The positions of the vertebrae were identified on the radiograph by fitting quadrangles around the vertebral bodies in Fig. 4.1. The positions of the most posterior parts of the spinous processes were also recorded. The images of the inferior vertebra of a motion segment of the flexion and extension radiographs were superimposed, and the images of the superior vertebra of the segment on the two films were then compared. Intervertebral rotation was determined by the change in the angle of rotation of the superior vertebra. Intervertebral translations along the x- and y- directions were given by the changes in the locations of the centre of the superior vertebra. This measurement method has been described in detail in previous studies (LEE, RYW 1995; LEE, RYW and EVANS, J 1997).

The radiographic measurements of intervertebral movements were repeated five times. Intra-class correlation (ICC) (3,1) was employed to examine the repeatability of measuring the three kinematics parameters among the five measurements as presented in Table 4.2. The ICC value ranged from 0.88 to 0.97 for intervertebral rotation, and from 0.95 to 0.99 and 0.95 to 0.99 for x- postero-anterior and y- supero-inferior translations respectively. The radiographic measurements were considered to be sufficiently reliable and accurate. They were then compared with the intervertebral movements predicted by the inverse kinematic algorithm so that the validity of the algorithm could be established.

4.4 STATISTICAL ANALYSIS

The Statistical Package for Social Sciences (Version 11 for Windows) (SPSS Inc., Chicago, Illinois 60606, USA) was employed for statistical analysis in this study. Linear regression was used to examine the relationship between the radiographic measurements and the values predicted by the inverse kinematic algorithm. Pearson’s product correlation coefficient was determined to assess the degree of association. This analysis was performed for each of the three kinematic variables, namely, the intervertebral rotation, and the intervertebral translations along the x- postero-anterior and y- supero-inferior directions.

4.5 SENSITIVITY ANALYSIS

Previous studies showed that there could be significant inter-subject variations in vertebral geometry, particularly in spines with degenerative changes (MCCARTHY, JM 1990; ZHOU, SH, MCCARTHY, ID et al. 2000). Inaccuracies in the geometry data of the inverse kinematic model might lead to errors in the predicted intervertebral rotations and translations. In addition, the physiological constraints as defined by Eq. (7) were based on normal subjects. The minimum and maximum allowable joint movements might need to be altered in subjects with instability or other pathological diseases. Sensitivity analysis of the model was thus performed by changing the input data by 10 % and evaluating the corresponding changes in the predicted intervertebral movements. The following input data were examined: the length of the kinematic chain, the position of the spinous process, and the physiological constraints of Eq. (7).

4.6 RESULTS

Table 4.1 provides the description statistics of the values obtained by radiographic measurement and those predicted by the inverse kinematic algorithm. The prediction error, which was defined by the differences between the measured and predicted values, and the correlation between the two values are also presented in the Table 4.2. The values are presented separately for each kinematic parameter and for each intervertebral joint.

Table 4.1 Comparison of mean measured and predicted kinematics parameters of the 5 intervertebral joints.

	Motion segment				
Angle of rotation, degree	**L5/S**	**L4/5**	**L3/4**	**L2/3**	**L1/2**
Mean measured results from x-ray film (i)	8.0 (6.0)	10.6 (4.8)	9.0 (3.5)	7.1 (3.3)	5.2 (2.6)
Mean predicted results (j)	6.9 (6.3)	10.5 (5.0)	9.1 (4.0)	6.7 (3.0)	4.7 (3.0)
Mean absolute difference between the measured and predicted results (i – j)	1.6 (1.2)	1.1 (0.8)	1.0 (0.7)	1.0 (0.7)	1.2 (0.9)
Correlation between measured and predicted values	0.95	0.97	0.87	0.91	0.83
X—Postero-anterior translation, cm					
Mean measured results from x-ray film (i)	0.17 (0.19)	0.31 (0.19)	0.27 (0.15)	0.22 (0.17)	0.20 (0.25)
Mean predicted results (j)	0.12 (0.16)	0.27 (0.23)	0.21 (0.19)	0.12 (0.21)	0.16 (0.31)
Mean absolute difference between the measured and predicted results (i – j)	0.14 (0.10)	0.12 (0.08)	0.16 (0.11)	0.11 (0.08)	0.17 (0.12)
Correlation between measured and predicted values	0.15	0.67	0.15	0.34	0.64
Y—Supero-inferior translation, cm					
Mean measured results from x-ray film (i)	0.03 (0.08)	-0.02 (0.08)	0.03 (0.06)	0.05 (0.07)	0.03 (0.08)
Mean predicted results (j)	0.02 (0.11)	0.04 (0.14)	0.03 (0.12)	0.05 (0.12)	0.01 (0.13)
Mean absolute difference between the measured and predicted results (i – j)	0.05 (0.04)	0.08 (0.05)	0.04 (0.03)	0.08 (0.05)	0.05 (0.04)
Correlation between measured and predicted values	0.59	0.08	0.31	0.22	0.64

Table 4.2 Mean measurement error (=1 SD) and the mean intra-class correlation coefficient (ICC) values for the radiographic measurements.

	Mean measurement error				
	L5/S	**L4/5**	**L3/4**	**L2/3**	**L1/2**
Angle of Rotation, deg	0.3	0.4	0.3	0.5	0.3
Postero-anterior x translation, mm	0.02	0.03	0.03	0.06	0.03
Supero-inferior y translation, mm	0.02	0.02	0.02	0.02	0.03
	Mean ICC (3,1)				
Angle of Rotation, deg	0.96	0.96	0.96	0.88	0.92
Postero-anterior x translation, mm	0.99	0.99	0.99	0.98	0.95
Supero-inferior y translation, mm	0.99	0.99	0.99	0.98	0.95

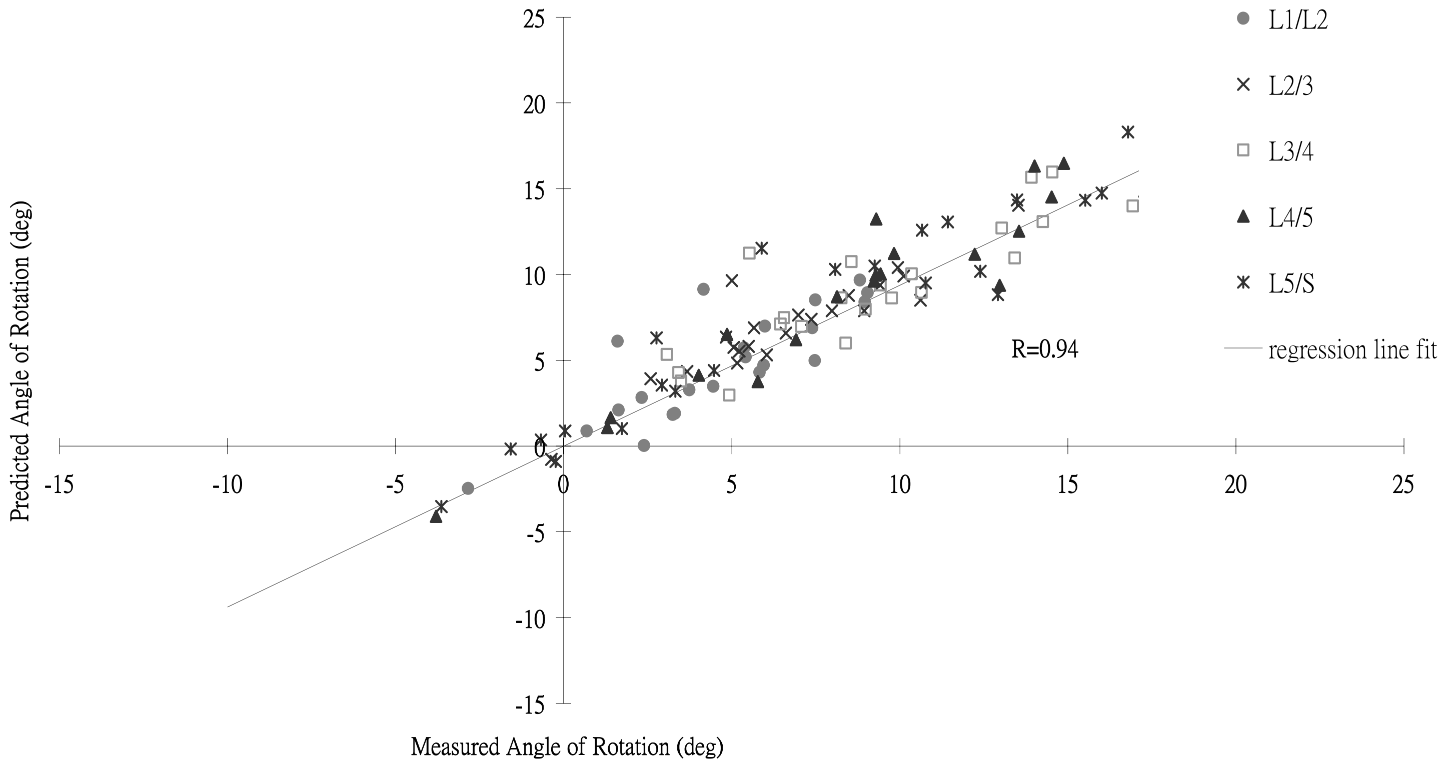

Fig. 4.3 Regression between the measured and predicted intervertebral rotations for different motion segments. (●) L1/L2: (x) L2/L3; (□) L3/L4; (▲) L4/L5: (*) L5/5: (-) regression line fit.

4.6.1 Intervertebral Rotation

The mean predicted values of intervertebral rotations from 4.7 to 10.5 degrees are presented in Table 4.1. The mean predicted error was found to be between 1.0 and 1.6 degrees. Figures 4.3 and 4.4 (a) to (e) illustrate the regressions between the predicted and measured values on the different segmental levels. The correlation between the two sets of values was high, with R values ranging from 0.83 to 0.97 in Table 4.1. The gradients of the regression line fitting are 0.948, 0.965, 0.870, 0.912 and 0.832 on L5-S, L4-L5, L3-L4, L2-L3, L1-L2 respectively, as shown in Fig 4.4 (a) to (e). They are very close to one; the ideal is that the two values are identical. This suggests that the inverse kinematic algorithm can be reliably used to predict intervertebral rotation. The accuracy of prediction varies with different intervertebral segments, with the L1/2 segment being the least reliable.

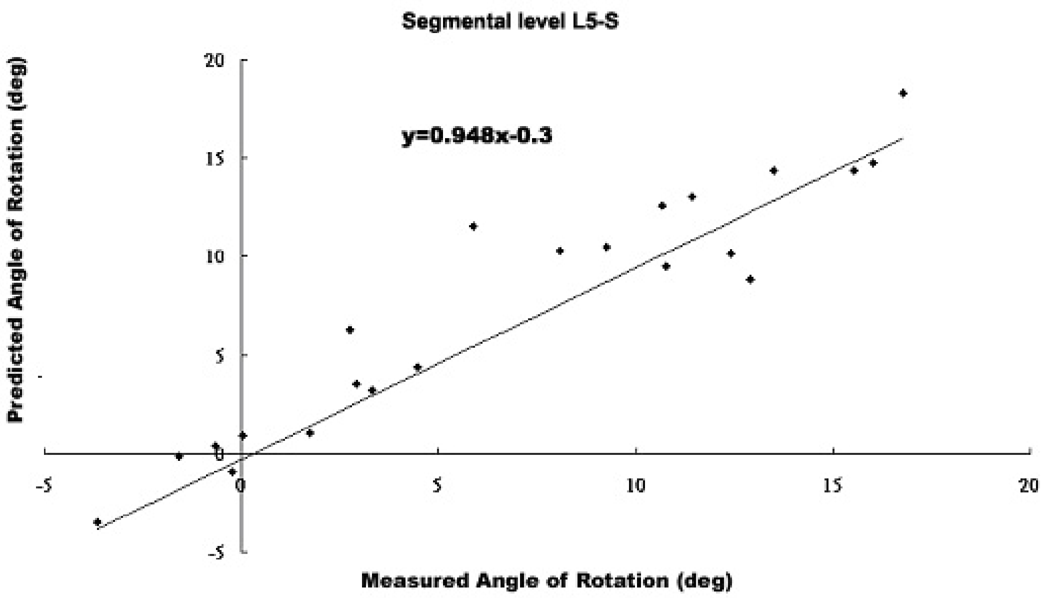

Fig. 4.4a Regression between the measured and predicted intervertebral rotations on L5/S. (-) represents the regression line fit.

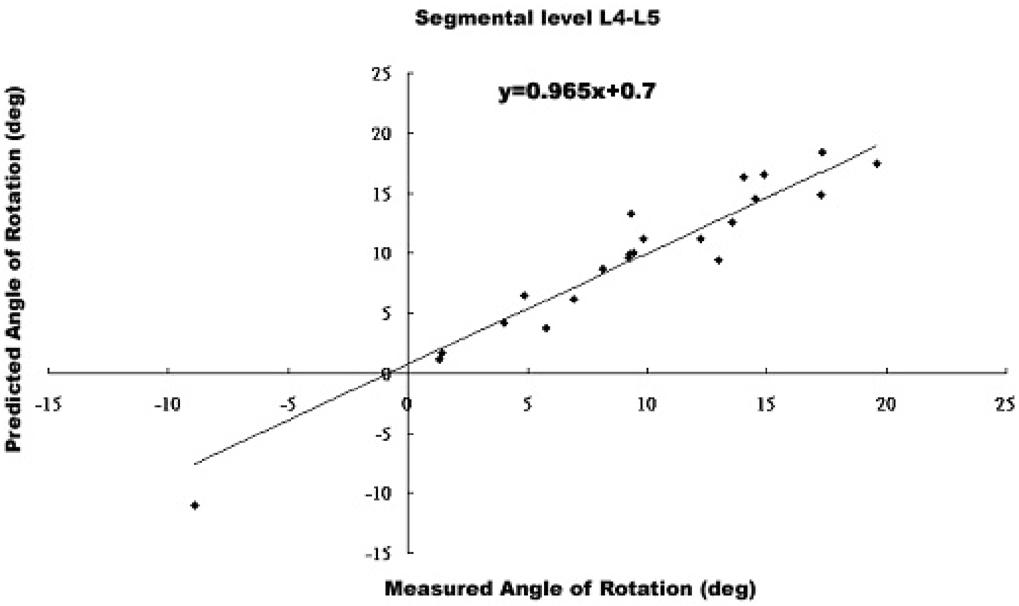

Fig. 4.4b Regression between the measured and predicted intervertebral rotations on L4/L5. (-) represents the regression line fit.

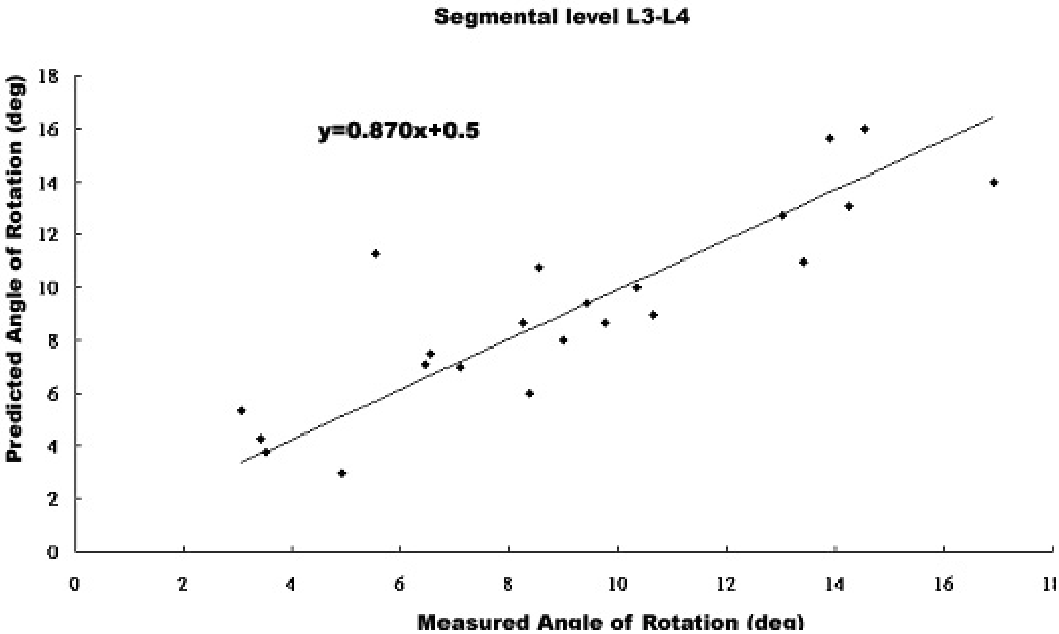

Fig. 4.4c Regression between the measured and predicted intervertebral rotations on L3/L4. (-) represents the regression line fit.

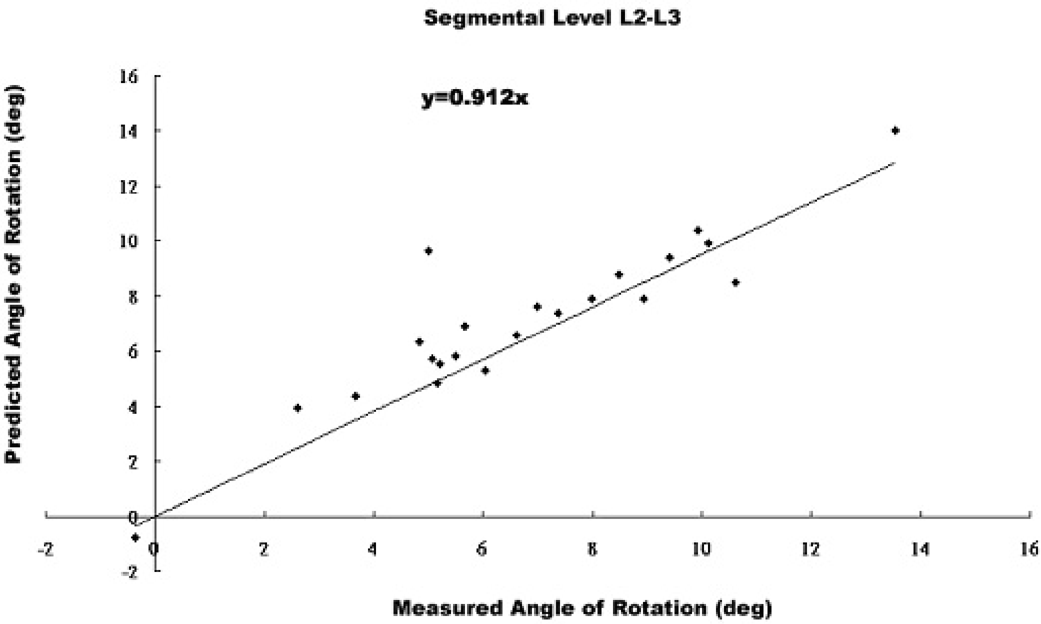

Fig. 4.4d Regression between the measured and predicted intervertebral rotations on L2/L3. (-) represents the regression line fit.

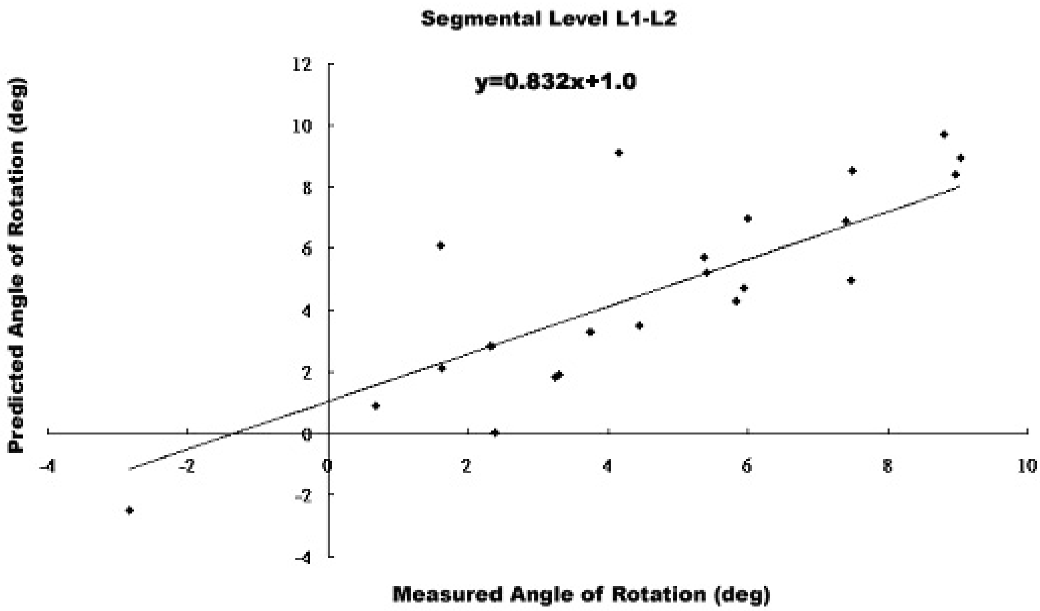

Fig. 4.4e Regression between the measured and predicted intervertebral rotations on L1/L2. (-) represents the regression line fit.

4.6.2 Intervertebral Translation

The mean predicted values of the x- postero-anterior and y- supero-inferior translations ranged 0.12 to 0.27 mm and 0.01 to 0.05 mm, respectively, as given in Table 4.1. The degree of correlation between the predicted and measured values of translations was poor, with R ranging from 0.15 to 0.67 for the x-translation and from 0.08 to 0.64 for the y-translation.

4.6.3 Sensitivity Analysis

Table 4.3 shows the mean percentage changes in the predicted intervertebral movements as a result of changes in the various input data. The mean percentage changes in the predicted movement values due to changes in the length of the kinematic chain, the position of the spinous process and the physiological constraints. The various ± 5 % and ± 10 % input data changes one by one. The changes in the translation movements were the largest. The mean changes in the angle of rotation due to 10 % changes in the kinematic chain length and the spinous process position were 10.4 ± 3.5 % and 12.0 ± 7.1 %, respectively. But the angle of rotation was relatively unaffected by changes in the physiological constraints of Eq. (7).

Table 4.3 Mean percentage changes in the predicted intervertebral movements due to 10 % changes in the input data of the inverse kinematic model.

	Mean Percentage Changes in the Predicted Intervertebral Movements		
Input Data (10% change)	**Angle of Rotation**	**x- postero-anterior translation**	**y- supero-inferior translation**
Length of kinematic chain	10.4% (3.5%)	27.1% (15.0%)	19.62% (10.8%)
Spinous process position	12.0% (7.1%)	30.4% (23.0%)	25.3% (16.7%)
Physiological constraints	7.8% (3.0%)	22.7% (13.2%)	18.9% (6.3%)

4.7 DISCUSSION

4.7.1 Inverse Kinematic Algorithm Prediction

This chapter demonstrates that the inverse kinematic algorithm can be reliably used to predict the intervertebral rotations of the lumbar spine segments but not intervertebral translations. The magnitude of lumbar intervertebral rotations in the sagittal plane was reported to be 13-16 degrees and the magnitude of intervertebral translations was between 1-3mm (WHITE, AA and PANJABI, MM 1978; PEARCY, MJ and HINDLE, RJ 1989; YAMAMOTO, I, PANJABI, MM et al. 1989; PANJABI, MM, GOEL, V et al. 1992). The measured and predicted values of intervertebral rotations were in close agreement with those reported in previous work, but the magnitude of intervertebral translation observed in our study was smaller than the values previously reported. The small magnitude of the translational movement might explain why it was extremely difficult or impossible to predict the movement reliably. In addition, the mean total magnitude of the sagittal rotation of the whole lumbar spine (from L1/2 to L5/S1) was found to be 39.7 degrees in this study. This was similar to results reported in previous studies (WHITE, AA and PANJABI, MM 1978; PEARCY, MJ and HINDLE, RJ 1989).

The differences between the measured and predicted values of intervertebral rotations were generally small (less than 1.6 degrees). The prediction error was found to be high for the L1/2 segment. This could be because the segment was at the end of the kinematic chain, and errors accumulated along the chain. Figure 4.3 shows excellent correlation between the predicted and measured values of intervertebral rotation. The established regression equation may be employed to enhance the accuracy of the prediction. However, it should be pointed out that the present equation may only be applicable to middle-aged subjects with non-specific lower back pain. Different regression equations may have to be established for other population groups.

It is suggested that the inverse kinematic technique can be used to predict intervertebral rotation in a clinical situation when it is not desirable to measure the movements directly using radiographs or other methods with health risks. Another potential application of the results of this study is biomechanical modelling. Past mathematical models of the lumbar spine (MCGILL, SM and NORMAN, RW 1986) made various assumptions about the kinematics of the spine. For instance, it was suggested that during flexion, the relative magnitudes of movements in the various motion segments were 13.2 % for L1/2, 21 % for L2/3, 29 % for L3/4 and 23.6 % for L4/5. It was also assumed that all lumbar segments moved together simultaneously, and that there was a constant relationship between the angle of rotation at each lumbar segment. In this study, it was shown that the distribution of movements was 13 %, 18 %, 23 % and 27 % among the L1/2 – L4/5 segments, which generally agree with the figures provided by (MCGILL, SM and NORMAN, RW 1986). However, in future modelling work, the actual intervertebral rotations could be predicted by the present inverse kinematic model, and no assumptions have to be made regarding the distribution of movements among the segments. The relationship among the various segments does not have to be assumed to be constant throughout the movement. The accuracy of the biomechanical models can be tremendously improved.

Knowledge of the intervertebral translations of the spine may be useful in the clinical assessment of some spinal pathologies such as spondylolysis or spondylolisthesis. Unfortunately, it appears that this can only be reliably determined by radiographic measurement, and the inverse kinematic algorithm was found to be rather unreliable in predicting such movement. This is an area for future research. The kinematic model may be further refined to increase the prediction of such movement, and non-invasive methods may be developed to measure the movement directly.

The inverse kinematic model developed in this study may be modified to determine the intervertebral movements of other regions of the spine. For instance, the lordosis and spinous process positions of the cervical spine may be measured clinically so that the kinematic mechanisms of healthy and painful necks can be studied. However, an inverse kinematic model of the cervical spine is likely to be more complex than the present model as it involves seven motion segments and larger numbers of degrees of freedom of movements.

4.7.2 Potential Functions

In order to determine the inverse kinematics of a redundant kinematic chain, a large number of solutions may be possible and it is necessary to determine the most optimal solution using some potential functions. In this study, one of the potential functions employed is the total movement of the lumbar spine. This is an appropriate choice because the movements of the individual joints should be dependent on the total movements of the spine. It can be argued that in order to minimise energy expenditure and enhance efficiency of movement, a person should perform forward bending of the trunk with as little movement of each intervertebral joint as possible, and the magnitude of the intervertebral movement should not exceed the physiological limits of the joints. Constraints were thus imposed on the kinematic links, and potential functions were employed to minimise the magnitude of the intervertebral movements. The constraints imposed were based on the physiological range of movements reported in previous studies (WHITE, AA and PANJABI, MM 1978; PEARCY, MJ and HINDLE, RJ 1989; YAMAMOTO, I, PANJABI, MM et al. 1989; PANJABI, MM, GOEL, V et al. 1992).

The Jacobian determinant was also employed as a potential function in deriving the inverse kinematic solution. The design of a kinematic mechanism loses at least one degree of freedom when singularity occurs. This happens when the Jacobian determinant becomes zero. The manipulability of a redundant kinematic mechanism would be minimal when the Jacobian determinant is minimised. Convergence of this potential function would allow a solution to be determined.

The fidelity of the solution was examined after the potential functions were applied. This was achieved by predicting the positions of the spinous processes using the solution and comparing the predicted positions with the known positions. An iterative procedure was employed to minimise the residuals, thus ensuring the most optimal solution was obtained. The 2-norm of the residuals was used as the optimisation criteria as it was most computationally efficient when compared to the

1-norm and infinity-norm (GOLUB, GH and VAN LOAN, CF 1996; CHEN, K, GIBLIN, P et al. 1999).

Previous researchers had employed other techniques to solve inverse kinematic problems with redundancy. For instance, as opposed to the algebraic method employed in the present study, Wang (WANG, X 1999) employed a geometric method to predict the arm-reaching posture. The method was based on previously observed behaviours of the arm, and it was able to solve the kinematic problem in a straightforward way. The advantage of this method was that no matrix inverse calculation was required, avoiding the stability and convergence problems occurring near a singularity of the Jacobian. However, due to the complexity and unpredictable nature of spinal motions, previous research has not been able to establish any behavioural rules of intervertebral movements. It is not possible to employ a behaviour-based approach for predicting spinal movements and the pseudoinverse method is thus chosen. The potential functions and the iterative procedure were used in this study to solve the convergence problem.

4.7.3 Sources of Error

It was shown that there would be small changes in the predicted values of intervertebral rotation if there were inaccuracies in the geometric data of the vertebrae. In our pilot study, we measured the actual geometries of the vertebral images and compared them with the anthropometric data employed in the model. The differences between the two sets of data were found to be less than 10 %. The sensitivity analysis showed that such differences would only lead to small errors in the prediction of the intervertebral rotation. However, it was shown the predicted values of intervertebral translation were very sensitive to changes in input data. This might be a reason why the prediction of the translation was inaccurate.

4.7.4 Sensitivity Analysis

The movement prediction might be sensitive to the predetermined parameters of vertebral geometry and physiological constraints. We had therefore performed a sensitivity analysis of the inverse kinematic model. We determined the mean percentage changes in the predicted movement values due to changes in the length of the kinematic chain, the position of the spinous process and the physiological constraints. The various input data changes one by one. The results of the analysis are presented in Section 4.6.3 and Table 4.3. In very beginning of this study, we measured the actual geometry of the vertebral images and compared them with the anthropometric data employed in the model (TENCER, AF and MAYER, TG 1983; PANJABI, MM, GOEL, V et al. 1992; PANJABI, M, CHANG, D et al. 1992b). The differences between the two sets of data were found to be less than 10 %. The sensitivity analysis showed that such differences would only lead to small errors in the prediction of the intervertebral rotation. Results suggested that the angle prediction is less sensitive to the predetermined parameters of the physiological constraints. We agree that the present model may not be appropriate for patients with large changes in vertebral geometry, for instance, subjects with significant spinal deformities. Both the anthropometric parameters and constraining functions would affect the precision of the x- postero-anterior and y- supero-inferior translation prediction (Table 4.3). We suggest that this might explain why the prediction of translation was inaccurate.

The method of Wang et al. (WANG, X 1999) has the advantage that it avoids the singularity issue and the need for matrix inversion. Unfortunately, due to the complexity and unpredictable nature of spinal motions, previous research has not been able to establish any behavioural rules of intervertebral movements. It is therefore not possible to employ the behaviour-based approach of Wang et al. (WANG, X 1999) in the present study.

The present model may not be appropriate for patients with significant vertebral deformities. The geometry of the spines of these patients will be grossly different from the anthropometric data obtained in the literature. Geometric data will have to be determined using radiographs or other imaging techniques for accurate model prediction. On the other hands, the sensitivity analysis showed that the predicted intervertebral rotation was insensitive to changes in the physiological constraints of the kinematic model. The model may therefore be employed for patients with hypo- or hyper-mobility of the spine.

Although radiographic measurements were used as the “standards” for comparison with the values predicted by the inverse kinematic algorithm, it should be pointed out that they were not free from errors. The accuracy of radiographic measurements may be affected by the clarity of the image, the number and positions of the chosen landmarks or markers, the process of tracing and superimposition, the radiographic quality, within- and between-observer variance, measurement method and the magnitude of the measured motion (PEARCY, MJ and HINDLE, RJ 1989; PANJABI, M, CHANG, D et al. 1992b; LEE, RYW and EVANS, J 1997). In this study, every effort was made to minimise the above sources of errors.

In the following chapters, we examine if it is possible to develop more accurate methods for tracing of vertebral contour and measurement of intervertebral movements. This would be particularly helpful when it is desirable to determine intervertebral translations but when the inverse kinematic method would not be reliable enough to predict such movements.

4.8 CONCLUSION

This was the first study to examine the feasibility of using a robotic engineering method to study the kinematics of the intervertebral movements of the lumbar spine. The developed inverse kinematic algorithm was found to be valid for predicting the rotational movements of the intervertebral joint for a given forward-bending movement of the trunk. Such prediction would require knowledge of the total flexion movement of the lumbar spine, the positions of the spinous processes that could be determined by surface measurements and anthropometric data provided from previous studies (TENCER, AF and MAYER, TG 1983; PANJABI, MM, GOEL, V et al. 1992; CHAFFIN, DB, ANDERSSON, G et al. 1999). It is suggested that the technique can be used to predict intervertebral rotations when it is clinically undesirable to measure such movements with radiographs or other methods carrying health risks. The technique will also be of value in biomechanical modeling when kinematic data are required. However, the study demonstrated that the method was unable to predict reliable intervertebral translations. The technique is of little value in the assessment of some spinal pathologies such as spondylolysis or spondylolisthesis when clinicians are required to determine if there is excessive translation of the intervertebral joint. Determination of the translational movement is technically difficult as the magnitude of the movement is small. This would require the use of radiographic techniques which would be further examined in the next chapter.

CHAPTER 5 PILOT STUDIES: SEGMENTATION OF VERTEBRAL BODY IMAGES

This chapter describes two pilot studies which examined the feasibility of using different techniques for segmentation of vertebral body images on radiographs.

5.1 PILOT STUDY I: SEGMENTATION OF THE VERTEBRAE USING THE HOUGH TRANSFORM

5.1.1 Purpose of Study

To study the feasibility of using the Hough Transform (HT) for segmentation of vertebral body image.

5.1.2 Introduction

The Hough Transform was first introduced by Hough in 1962 (HOUGH, PVC 1962). It aimed at describing a set of parameters for particle tracking in a bubble chamber image. The Hough Transform (HT) is a very powerful tool in computer vision offering a unique potential in the automation of visual inspection tasks (HOUGH, PVC 1962; LEAVERS, VF 1993). The theory of the Hough Transform (HT) was explained in section 2.7.2. The HT involves a mapping from geometric features of edge pixels in an image to a multi-dimensional space. For instance, two point, *p* and *q*, on the same straight line are transformed into two straight lines which intercept at the point (*m'*, *c'*) in the Hough space. It has been applied in a wide variety of problems, e.g., line detection (HOUGH, PVC 1962), circle detection (KIMME, C, BALLARD, D et al. 1975) and arbitrary shape extraction (AGUADO, AS, NIXON, MS et al. 1998). The HT has the ability to extract two-dimensional shapes as well as motion parameters (COOPER, R, CARDAN, C et al. 2001). Sklansky (SKLANSKY, J 1978) showed that it provides a result equivalent to that derived by template matching but with less computational effort.

Zheng et al. (SKLANSKY, J 1978; ZHENG, Y, NIXON, S et al. 2000a; ZHENG, Y, NIXON, S et al. 2000b) employed the generalized Hough Transform (GHT) to extract lumbar segments from fluoroscopic images of an artificial spine model. A spatial-temporal HT was designed (ZHENG, Y, NIXON, S et al. 2000c). GHT was also used to detect of corpus callosa of the human undergoing weak affine transformations in images (ECABERT, O and THIRAN, JP 2004). This study examined whether the GHT could be extended to planar radiographic image of the living spine.

5.1.3 Method

5.1.3.1 Fourier description of a shape

The feasibility of the GHT in segmentation of vertebral body image was studied on a lateral radiograph which was taken of a normal healthy subject (age 21, tall 1.74 m, weight 67 kg, Body Mass Index = 22.13 kgm^{-2}). The target vertebral body shape was described by a set of Fourier descriptors, which locate it in an accumulator space from which the object parameters of translation (both in the x- and y- direction), rotation and scale can be determined. A curve $c(t)$ defines the positions of its points on the vertebral contour along it by their components in two orthonormal axes.

$$c(t) = c_x(t)U_x + c_y(t)U_y \qquad (1)$$

where $U_x = [1 \quad 0]^T$ and $U_y = [0 \quad 1]^T$

According to Fourier theory,

$$c(t) = \begin{bmatrix} C_x(t) \\ C_y(t) \end{bmatrix} = a_0 + \sum_{k=1}^{8} \begin{bmatrix} a_{xk} & b_{xk} \\ a_{yk} & b_{yk} \end{bmatrix} \begin{bmatrix} \cos(k\omega) \\ \sin(k\omega) \end{bmatrix} \qquad (2)$$

The good attribute of Fourier descriptors is that they can represent curves, either in closed or open form.

5.1.3.2 Hough Transform Algorithm

Detailed equations are given by Zheng (ZHENG, Y, NIXON, MS et al. 2004). Any curve can be obtained under an affine transformation. It expressed by its two components in the x and y directions. That is

$$\begin{bmatrix} A_x(t) \\ A_y(t) \end{bmatrix} = \begin{bmatrix} x_t \\ y_t \end{bmatrix} + s \begin{bmatrix} \cos(\rho) & -\sin(\rho) \\ \sin(\rho) & \cos(\rho) \end{bmatrix} \begin{bmatrix} C_x(t) \\ C_y(t) \end{bmatrix} \qquad (3)$$

where s represents scale, ρ is the angle of rotation, and x_t, y_t are translations in the x- and y- directions. Normally, the scale factor s can be determined by the magnification factor of the image under radiographic examination. The transformation kernel is defined (AGUADO, AS, NIXON, MS et al. 1998) as

$$\omega(t,s,\rho) = s \begin{bmatrix} \cos(\rho) & -\sin(\rho) \\ \sin(\rho) & \cos(\rho) \end{bmatrix} \begin{bmatrix} C_x(t) \\ C_y(t) \end{bmatrix} \tag{4}$$

For any edge point $P(p_{xi}, p_{yi})$, its translation vector

$$\begin{bmatrix} x_t \\ y_t \end{bmatrix} = \begin{bmatrix} p_{xi} \\ p_{yi} \end{bmatrix} - w(t,s,\rho) \tag{5}$$

A simple matching function is defined as

$$H(a,b) = \begin{cases} 1, & a = b \\ 0, & a \neq b \end{cases} \tag{6}$$

where a and b can be vectors. The HT discrete form defines:

$$S_{DH}(b,s,\rho) = \sum_{i \in D_i} \sum_{\in D_t} H\left(b, \begin{bmatrix} p_{xi} \\ p_{yi} \end{bmatrix} - w(t,s,\rho) \right) \tag{7}$$

where b is the translation vector, $S_{DH}(b,s,\rho)$ is an accumulator array which stores the number of intersections. D_i is the edge points and D_t is the domain of the points in the model shape.

Arbitrary shape extraction is determined by optimization of Eq. (7). Fourier descriptors were used to describe the vertebral body shape. This description was incorporated with the Hough Transform Algorithm from which we can obtain affine transform parameters, i.e., scaling, rotation and translation of the vertebral body images. Hough Transform Algorithm computes all the possible solutions from the data and accumulates them in a solution space. After the number of accumulators is predefined, all the data have been accessed and contributed to the solution space. A peak that receives the largest votes in the solution space is searched and gives the most optimal solutions. The above Hough Transform Algorithm program was written in Visual C++ for the windows 95/NT platform.

The Statistical Package for Social Sciences (Version 11 for Windows) (SPSS Inc., Chicago, Illinois 60606, USA) was employed in this study. Linear regression was used to examine the relationship among the extraction shape of vertebral image derived from the Hough Transform Segmentation and manual. Pearson’s product correlation coefficient was determined to assess the degree of association between segmentation and manual tracing.

5.1.4 Results

5.1.4.1 Extraction of quadrangle on images

A quadrangle was used to represent the vertebral body. The simple synthetic quadrangles on the images were successfully identified by HT algorithm. Figure 5.1 shows the original quadrangle of the spine image. Figure 5.2 shows extraction result of quadrangles by Hough Transform Algorithm. Figures 5.3 (a) and (b) show that different searching results obtained by different number of accumulators.

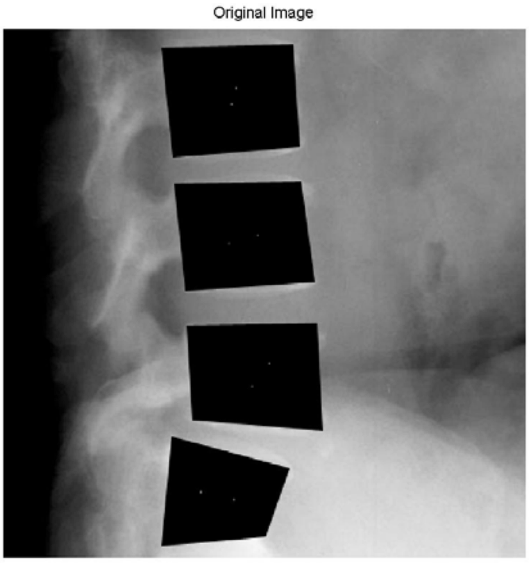

Fig. 5.1 Original image of quadrangles of the spine.

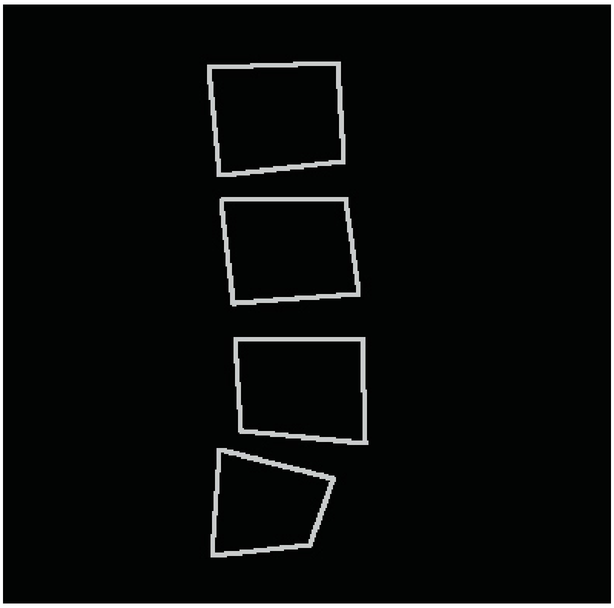

Fig. 5.2 Extraction shape of quadrangles by Hough Transform Algorithm.

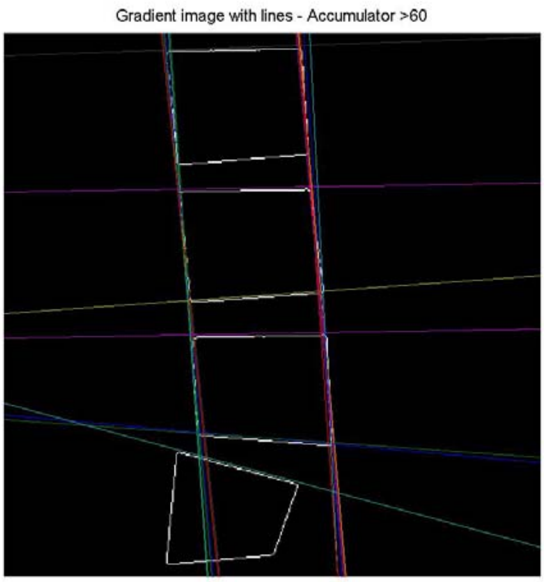

Fig. 5.3a Searching results with different number of accumulator (60).

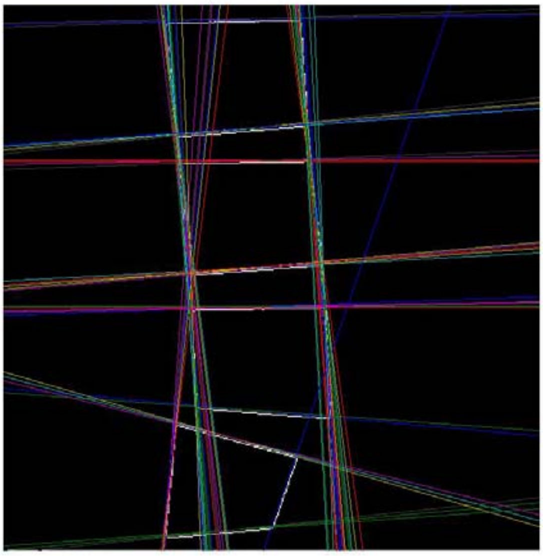

Fig. 5.3b Searching results with different number of accumulator (40).

5.1.4.2 Extraction of vertebral body images

Figure 5.4 shows the original vertebral body image of the spine from L3 to sacrum. Figure 5.5 shows vertebral body image after edge detection. Figure 5.6 shows the extraction result of the vertebral body image. When 16 number of Fourier descriptors parameters were used, 377 edge points on each vertebra were generated.

Fig. 5.4 Original vertebral body images of the spine.

Fig. 5.5 Edge detention of vertebral body image.

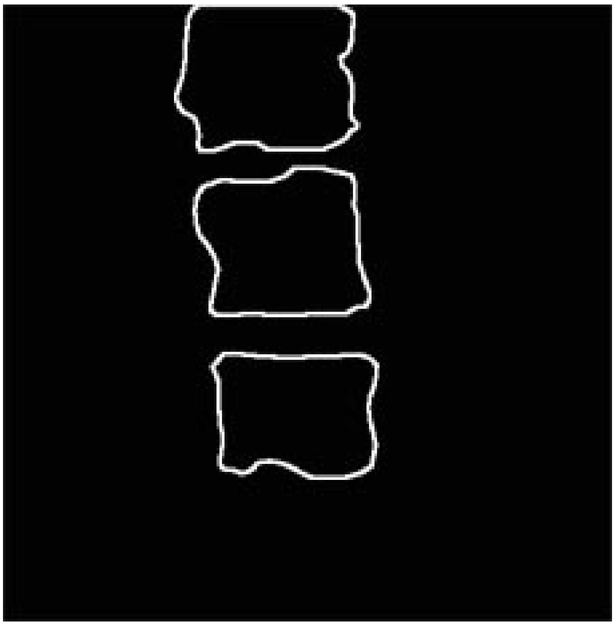

Fig. 5.6 Extraction shape of the vertebral body image by Hough Transform Algorithm.

Fig. 5.7 Superposition of extraction shape (by HT) with the original images.

5.1.4.3 Differences between contours of vertebral body image extracted by Hough Transform Algorithm and manual tracing

The extraction of the vertebral body image by Hough Transform Algorithm was superimposed on the original vertebral body image of the spine from L3 to sacrum (Fig. 5.7). The vertebra contour was also traced manually, and sixty landmark points along this contour were identified. Each of these points corresponded to the points identified by the Hough Transform Algorithm. The average differences in the x- (postero-anterior) and y- (supero-inferior) coordinates of the points identified by GHT and manually were presented in Fig. 5.8. The graphs are shown in polar form from 0 to 360 degrees.

Mean difference and standard deviation of coordinates of the sixty points derived from the extraction shape of vertebral body image by Hough Transform Algorithm and Manual were 1.3 ± 1.0 mm and 3.3 ± 1.7 mm along postero-anterior and supero-inferior directions respectively. Pearson's product correlation coefficient was determined to assess the degree of association between computerised segmentation and manual tracing. The R values were 0.869 and 0.835 along postero-anterior and supero-inferior direction respectively. They were marginally satisfactory.

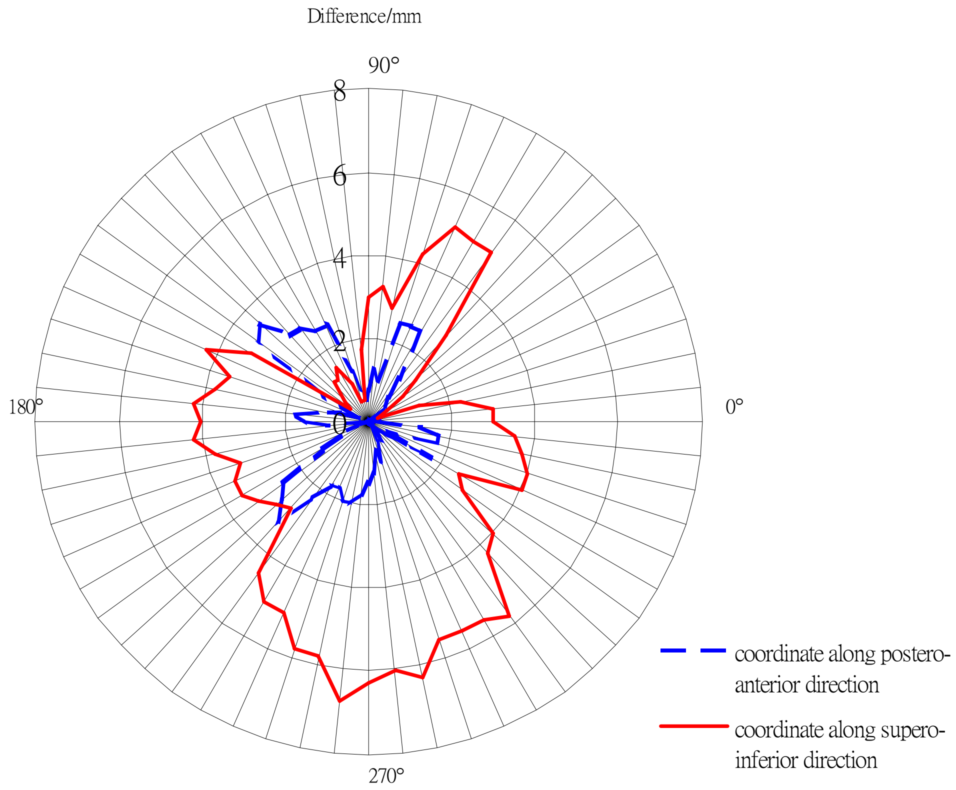

Fig. 5.8 The average difference in the coordinates of the points identified by Hough Transform and manual tracing.

5.1.5 Discussion

The simple quadrangles on the vertebral images were successfully identified by HT algorithm. However, the verterbral body is an arbitrary shape instead of simple quadrangle in real. Shape extraction of the vertebral body image was used by HT algorithm. However, there were large mean differences in HT segmentation and manual tracing, showing that the HT does not obtain satisfactory results. The extraction shape was not located on the contour of the vertebral body images (Fig.5.7).

There are many factors contributing to segmentation errors. First, poor edge detection occurs (Fig.5.5). Edge information is a prerequisite to the implementation of the HT. The HT algorithm can only provide reliable result by good edge detection. Poor edge detection caused by the uneven brightness and poor contrast of image. Secondly, the search is an accumulator-dependent. It varied by the number of accumulators. The numbers of accumulator should be predefined by the researcher manually. As introduced earlier, in order to from the accumulator array, an evaluation criterion should be made in order to increase the values of the arrays cells where they are intersection. More Fourier descriptors provide more reliable results, but longer computational time. However, Zheng (ZHENG, Y, NIXON, MS et al. 2004) reported that 16 Fourier descriptors are sufficient for a refined analysis of the match at the vertebra. Noise of the image increased the difficulty in selecting optimal number of accumulators manually for a large database in order to obtain the good searching results.

It is concluded that the HT algorithm provides unsatisfactory extraction results. Another technique to segment the vertebral image needs to be developed.

5.2 PILOT STUDY II: SEGMENTATION OF THE VERTEBRAE USING THE MORPHOLOGICAL WATERSHED SEGMENTATION ALGORITHM

5.2.1 Purpose of study

To examine the feasibility of the Morphological Watershed Segmentation Algorithm in recognising the shape of vertebrae body image.

5.2.2 Introduction

The watershed algorithm was first introduced by S.Beucher and C. Lantujoul in 1979 (BEUCHER, S and LANTUJOUL, C 1979). The basic idea of their initial approach was to model the gradient image as a topographic surface, which is shown in Figs. 5.9 (a) and (b).

Fig. 5.9a An example of a gradient image (adapted from Chau 2001).

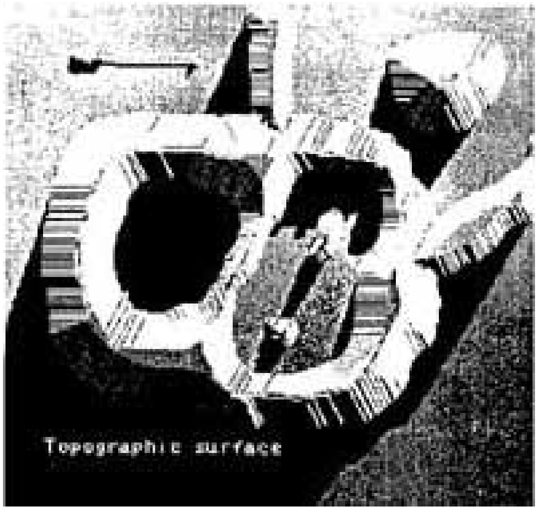

Fig. 5.9b The corresponding topographic surface (adapted from Chau 2001).

In fact, the topographic surface of a gradient image can be considered as a three-dimensional view of the gradient image, such that the gray level of the gradient image becomes the value of the z-axis of the topographic surface. The segmentation algorithm mainly relies on the flooding and dam-building mechanism.

We consider the local minima inside the topographic image as valleys, the so-called catchment basins (Fig. 5.10). Similar to flood water in a valley, each catchment basin will be filled by water according to its gradient level. When the water level goes up, two different catchment basins may merge together.

In order to prevent the region from being merged, a dam will be built across the merging boundary and this dam is called the watershed line. This flooding and dam-building process will be run repeatedly until the water level is higher than the maximum level of the topographic image. When the process finishes, the dams, which are used to prevent the merging of the catchment basins, remain inside the topographic image only. As a result, these dams will form the boundaries of the segments and we can obtain many regions segmented by their own boundaries.

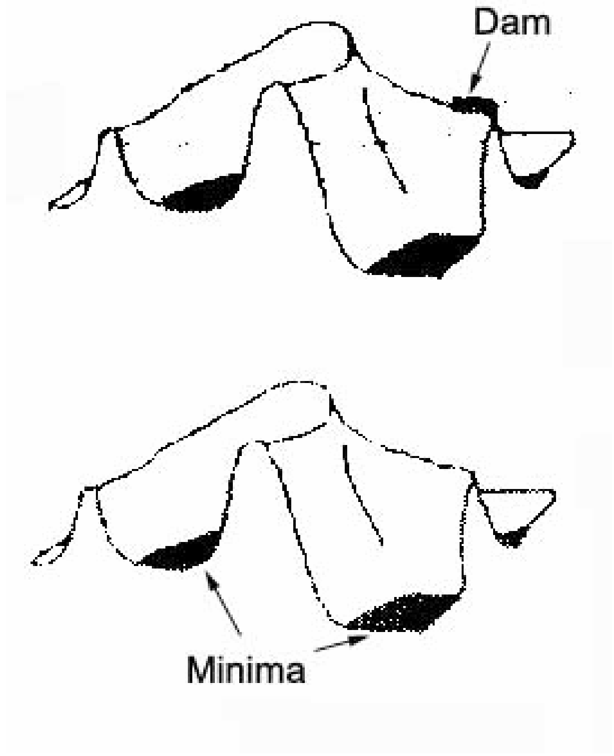

Fig. 5.10 An example of catchment basins (adapted from Chau 2001).

Algorithm generates unpredicted number of catchment basins inside the topographic image. It is called as over-segmentation.

5.2.3 Method

5.2.3.1 Morphological Watershed Segmentation Algorithm Procedure

The feasibility of this approach was investigated in the same radiograph employed in the first pilot study. The grayscale image of the vertebral body (Fig.5.11a) was analysed by the following algorithm.

Step 1: Select the area of interests on the image by manual (Fig.5.11b). Researchers locate the regions in the image that they are interested in.

Step 2: Superimpose the area of interests on the original image to locate the area for segmentation (Fig. 5.11c). The segmentation operated only focus on the areas to be selected.

Step 3: Obtain binary image by thresholding (Fig. 5.11d). Image contains two regions of different gray level separted by an edge when there is an edge pixel. The best estimation of the gradient at that pixel should be the level difference between two regions where on region corresponds to the zero pixels in the binary image and the other corresponds to the one-valued pixels.

In order to resolve the problem of over-segmentation, markers are defined on the topographic image. The Watershed segmentation algorithm becomes guided with markers. The markers (inner and outer) constructed based on the area of interests on the image. The segmentation performs on the area between the outer and inner markers.

Step 4: Build inner marker by erosion (Fig. 5.11e). Inner marker dilate (Fig. 5.11f).

Step 5: Build outer marker by inverting (Fig. 5.11g)

Step 6: Develop boundary image after equalization (Fig. 5.11h).

Step 7: Shape of vertebral body image extract after watershed segmentation. It is shown in the Fig. 5.12.

Fig. 5.11a Original vertebral image.

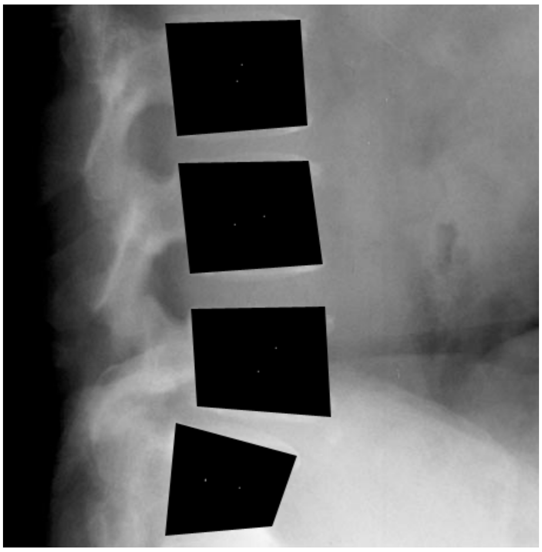

Fig. 5.11b Rough location of area of interests.

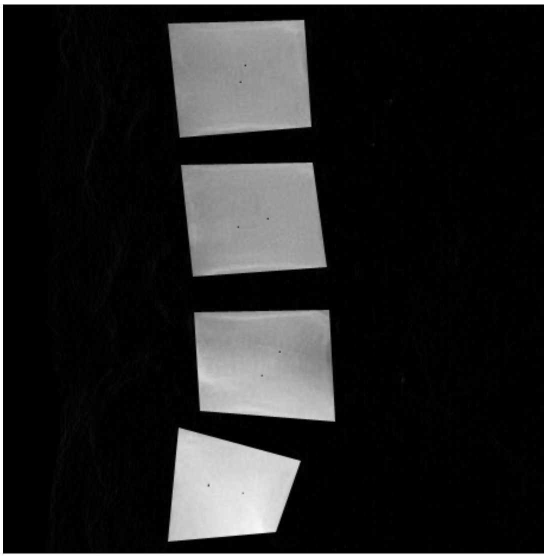

Fig. 5.11c Superposition.

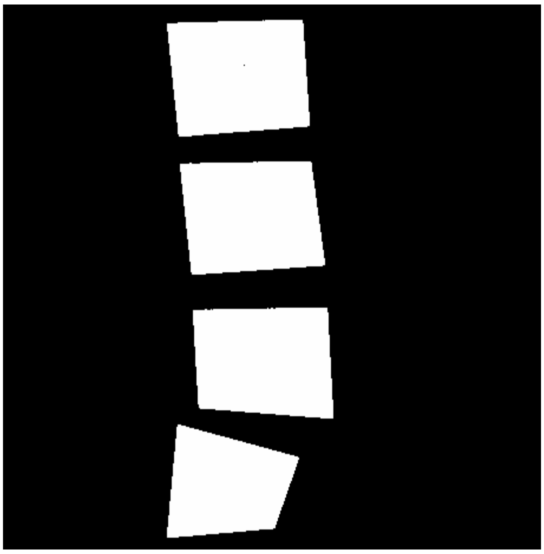

Fig. 5.11d Binary image by thresholding.

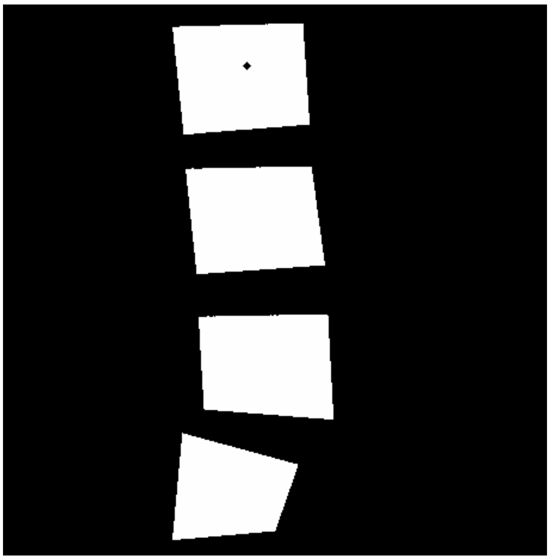

Fig. 5.11e Inner marker by erosion.

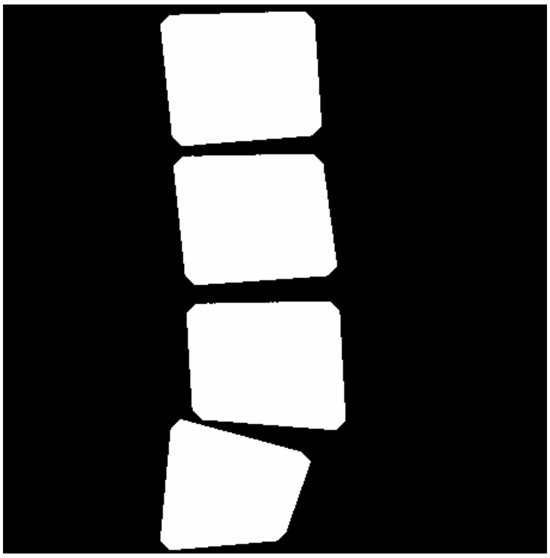

Fig. 5.11f Dilation result.

Fig. 5.11g Outer marker by inverting.

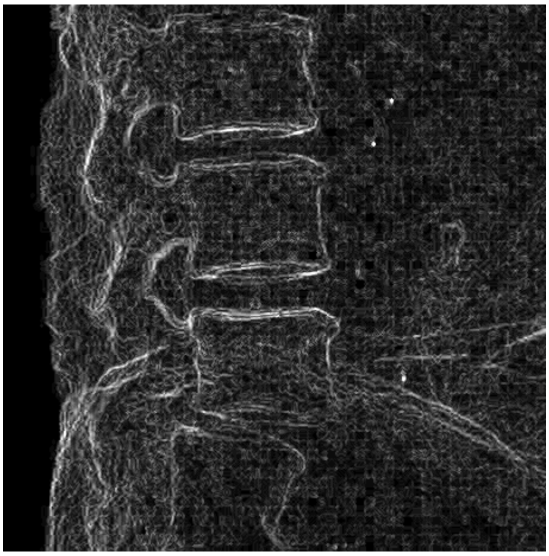

Fig. 5.11h Boundary image after equalization.

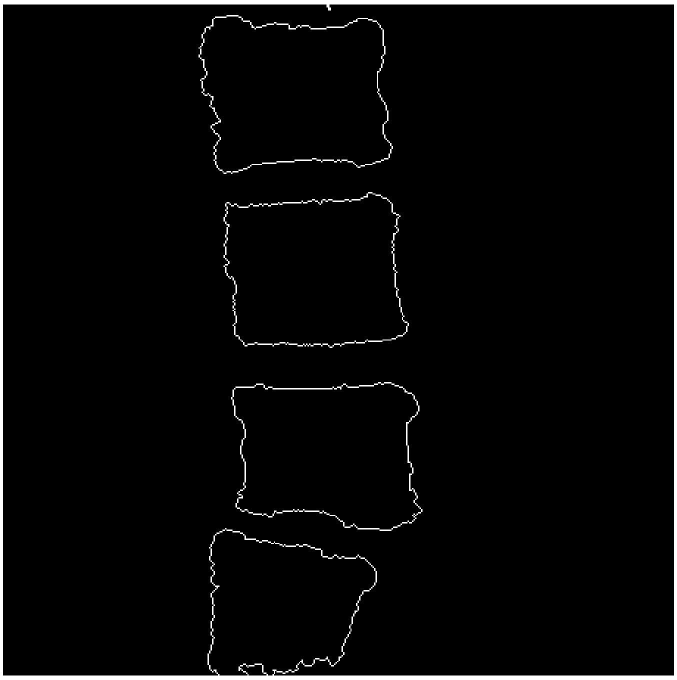

Fig. 5.12 Extraction shape of vertebral body after watershed segmentation.

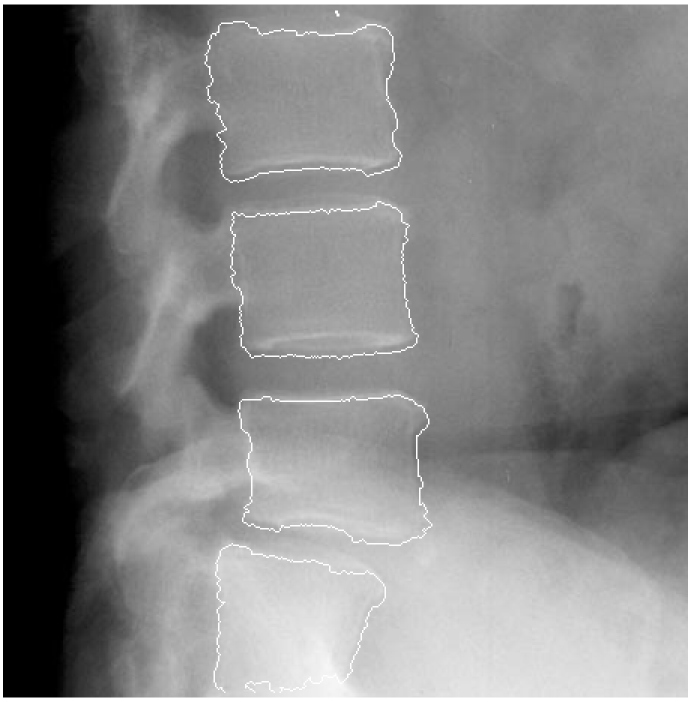

Fig. 5.13 Superposition of extraction shape with the original images after watershed segmentation.

5.2.4 Results

5.2.4.1 Extraction of vertebral body images

Figure 5.11a shows the original vertebral body image of the spine from L3 to Sacrum. Figure 5.12 shows the extraction result of the vertebral body image. The extraction of the vertebral body image by Morphological Watershed Segmentation Algorithm was superimposed on the original vertebral body image of the spine from L3 to Sacrum (Fig. 5.13).

5.2.4.2 Differences of contours from extraction of vertebral body image by Morphological Watershed Segmentation Algorithm and manual by researcher

Similar to section 5.1.4.3, the vertebra contour was divided into sixty parts, from 0 to 360 degrees. Sixty landmark points along the vertebral outline was also traced manually. The average difference of the x- (postero-anterior) and y- (supero-inferior) coordinates of the points on the vertebral contours were presented in Fig. 5.14. The graphs are shown in polar form. Mean difference and standard deviation of coordinates of the sixty points derived from the extraction shape of vertebral body image by Morphological Watershed Segmentation Algorithm and Manual were 2.1 ± 1.9 mm and 3.4 ± 1.8 mm along postero-anterior and supero-inferior directions respectively. Pearson’s product correlation coefficients were 0.634 and 0.571 along postero-anterior and supero-inferior direction respectively. They were marginally satisfactory.

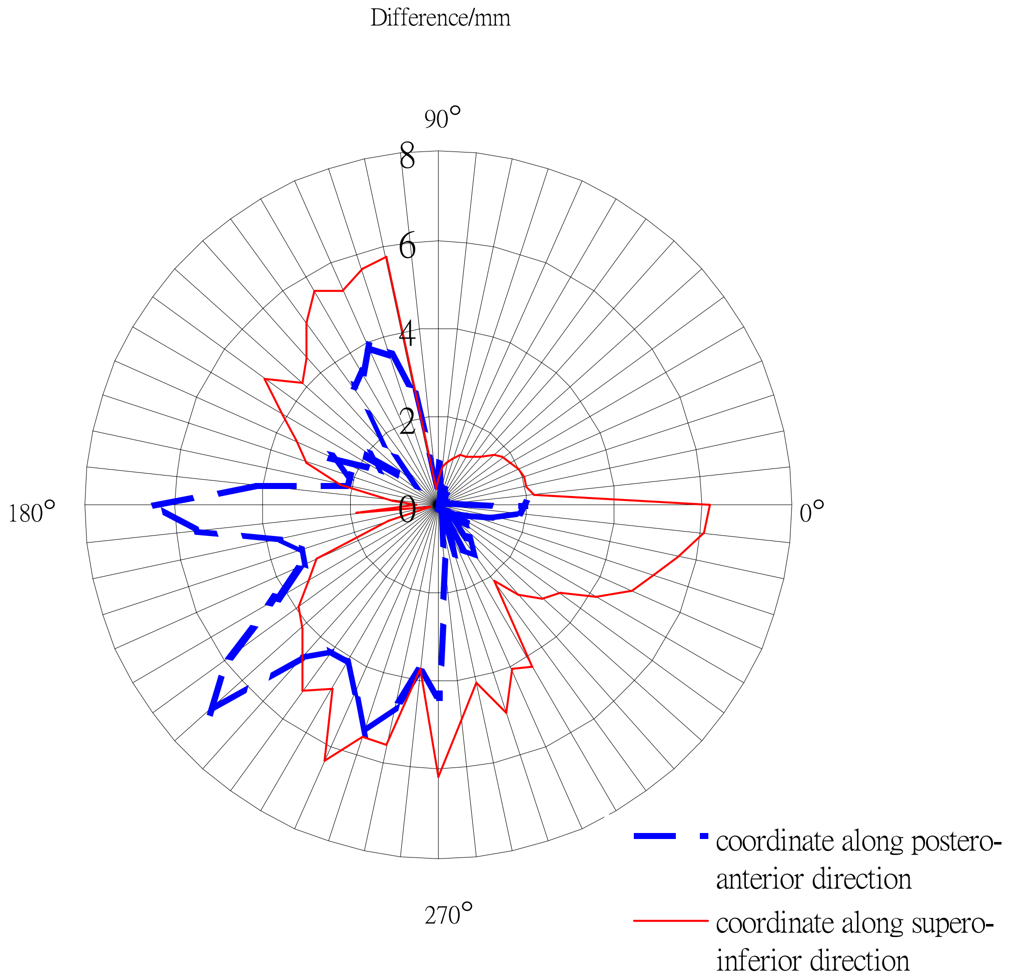

Fig. 5.14 The average difference in the coordinates of the points identified by Morphological Watershed Segmentation and manual tracing.

5.2.5 Discussion

Large differences in the sixty points derived from the Morphological Watershed Segmentation Algorithm and manual tracing were observed. The correlation coefficient values were low. The extraction shape was not located on the contour of the vertebral body images especially on the ventral part of the vertebra (Fig. 5.7). Similar to the performance with the Hough Transform, segmentation of the vertebrae was not very precise. The algorithm is not valid for segmentation of the vertebral body images.

The capture images are corrupted by noise. Over-segmentation occurs from generation of more catchment basins inside the topographic image. The segmentation depends on the area of interests (markers) that varies by users. Algorithm reply on local image information (edges, pixel and gray level) and fail if the region selected is performed too far away from the expected solution. Generally, it is difficult to obtain markers on image. For the defined markers, the properties of images objects are needed to be considered, for example of colour, gray level, texture (CHAU, CC 2001). Dougherty (DOUGHERTY, ER 1992) proposed an automatic defined markers. They are the Morphological operators. The Morphological operators can analyze the image non-linearly such that some rough markers can be obtained based on the gray scale of the image. However, the methods for how to obtain the markers depend much on the types of images. Its application is questionable. Another technique to segment the vertebral image needs to be developed.

5.3 CONCLUSION

Pilot studies explained segmentation approaches, Hough Transform Algorithm and Morphological Watershed Segmentation Algorithm, for extracting vertebrae shape on the radiographic image. The analysis results show that the above two techniques fail due to larger differences. Noise is a common problem in segmentation of the vertebral image. It is unwise to obtain the vertebral shape information from the image as a whole because the poor contrast between the vertebrae and the background, the complexity structure of the vertebrae and the uneven distribution of the image illuminations. The automatic segmentation of the vertebral image should be isolated by human justification. Both techniques (Hough Transform Algorithm and Morphological Watershed Segmentation Algorithm) require pre-defined parameters such as thresholds, number of accumulators and inner and outer markers.

It is concluded that an alternative approach should be adopted for accurate segmentation of vertebral image. Active Contour (other computer vision technique) had been successfully employed in vertebral image extraction (SMYTH, PP, TAYLOR, J et al. 1999), although it did not provide any information on vertebral movements. The Active Contour is recognized as being a powerful tool in shape analysis which gives good results even in the presence of noise and occlusion (LEAVERS, VF 1992; LEAVERS, VF 1993). This algorithm should improve the robustness of image segmentation by using shape constraints. The next study reported in this thesis (Chapter 6) will explore the effectiveness of the Active Contour Method. And investigate if it would provide a better shape extraction of the vertebral body compared with the above two techniques. The studies also examine the use of a Genetic Algorithm to provide information about vertebral motion. In Chapter 6, the repeatability of the Active Contour would be compared with the results reported in these pilot studies.

CHAPTER 6 COMPUTERISED RADIOGRAPHIC MEASUREMENT

6.1 INTRODUCTION

Radiography has been used for image-based measurement of spinal angles (COOPER, R, CARDAN, C et al. 2001), and planar and serial biplanar radiography have provided data documenting static and range-of-motion of the spine in three planes (PEARCY, M, PORTEK, I et al. 1984; PEARCY, MJ 1985; PANJABI, M, CHANG, D et al. 1992b; SIMONIS, C, ALLEN, R et al. 1993; COOPER, R, CARDAN, C et al. 2001; ROGERS, BP, HAUGHTON, VM et al. 2002). While radiography is advantageous for direct measurement of the position and movements of bony structures, it is subjected to measurement error. These may result from poor imaging and difficulty in finding landmarks of bony structures that permit reliable identification. X-ray techniques are considered the most accurate clinical method of lordosis measurement and kinematic movements, although this has traditionally introduced the problems of radiation dosage and the accuracy and laboriousness of handling data from anatomical landmarks.

Intervertebral movements are determined from changes in the positions of the radiographic images of the vertebrae in the two postures (STOKES, IA, MEDLICOTT, PA et al. 1980; STOKES, IA, WILDER, DG et al. 1981; PEARCY, M, PORTEK, I et al. 1984; PEARCY, MJ 1985; DVORAK, J, PANJABI, MM et al. 1991; PANJABI, MM, GOEL, V et al. 1992; FROBIN, W, BRINCKMANN, P et al. 1996; FROBIN, W, BRINCKMANN, P et al. 1997; SMYTH, PP, TAYLOR, J et al. 1999). This involves computer digitization of bony landmarks such as the vertebral body corners and manual superimposition of radiographic images, which is labour intensive and time consuming. It is also technically difficult to identify the vertebral shape or bony landmarks accurately. Previous research reported that the measurement errors for intervertebral rotations and translations were 1.5-3 degrees and 1.4-4 mm, respectively (STOKES, IA, MEDLICOTT, PA et al. 1980; STOKES, IA, WILDER, DG et al. 1981; PEARCY, M, PORTEK, I et al. 1984; PEARCY, MJ 1985; DVORAK, J, PANJABI, MM et al. 1991; PANJABI, MM, GOEL, V et al. 1992; FROBIN, W, BRINCKMANN, P et al. 1996; FROBIN, W, BRINCKMANN, P et al. 1997; SMYTH, PP, TAYLOR, J et al. 1999). Previous researchers have attempted to employ various methods to address the above problems. For instance, an image of the vertebral body may be matched with a template and intervertebral movements determined from correlation of templates obtained from different films (PANJABI, MM, GOEL, V et al. 1992; SIMONIS, C, ALLEN, R et al. 1993; MUGGLETON, JM and ALLEN, R 1997; ZHENG, Y, NIXON, MS et al. 2003; ZHENG, Y, NIXON, MS et al. 2004). However, fitting the vertebral image with a template often requires long processing times. The template-matching method (PANJABI, M, CHANG, D et al. 1992b; SIMONIS, C, ALLEN, R et al. 1993; MUGGLETON, JM and ALLEN, R 1997; COOPER, R, CARDAN, C et al. 2001; ZHENG, Y, NIXON, MS et al. 2004) is also error prone due to out-of-plane motion, which is unavoidable in radiographic films taken in the clinical environment. The Generalized Hough Transform (GHT) (MUGGLETON, JM and ALLEN, R 1997; ZHENG, Y, NIXON, MS et al. 2003; ZHENG, Y, NIXON, MS et al. 2004) is one of the methods used for fitting vertebral images with a template. It has been used to identify arbitrary shapes, such as the vertebral body, by detecting embedded straight lines in images (ULRICH, M, STEGER, C et al. 1996; TEZMOL, A, SARI-SARRAF, H et al. 2002). Matching of vertebral images in different films can then be done by appropriate scaling and changes in the positions and orientations of the images. Since the GHT is not a deformable template method, matching of vertebral shapes is often not ideal because optical distortion and out-of-plane motion can alter the vertebral shapes in different films. The limitations of the GHT had been discussed in Chapter 5.

Other computer vision techniques have also been employed in vertebral image extraction (SMYTH, PP, TAYLOR, J et al. 1999). Algorithms, such as Active Shape Modeling, improve the robustness of image segmentation by using shape constraints. This method requires appropriate initial parameter values, which are obtained after analysis of some previous images. The vertebral body corners may be used as shape constraints as they are prominent bony landmarks and are generally not subjected to distortion in a lateral projection due to axial rotation and lateral tilt of the spine (FROBIN, W, BRINCKMANN, P et al. 1996; FROBIN, W, BRINCKMANN, P et al. 1997; SMYTH, PP, TAYLOR, J et al. 1999). Cootes et al. (COOTES, TF, HILL, A et al. 1994; HILL, A, COOTES, TF et al. 1994) described a technique to use Active Shape Models for building compact models of the shape and appearance of human organs in medical images. The model was demonstrated by locating ventricles in a three-dimension Magnetic Resonance Image (MRI) of the brain and tracking the left ventricle of the heart in an echocardiogram sequence.

The Active Shape Model (ASM) had been used for the measurement of vertebral shapes on lateral DXA scans of the spine for detecting of osteoporotic fractures (STOKES, IA, MEDLICOTT, PA et al. 1980). The ASM was proposed to be a robust tool for measuring vertebral shape on normal spine DXA scans. Our intention in using ASM was to automatically extract more shape information both accurately and more rapidly than manual analysis. An ASM measured the shape of the full vertebral contour rather than the shape described by only four points. A method had been successfully developed to evaluate the petal shape of P. sieboldii using principle component scores obtained from standardized elliptic Fourier descriptors (STOKES, IA, MEDLICOTT, PA et al. 1980; YOSHIOKA, Y, IWATA, H et al. 2004; YOSHIOKA, Y, IWATA, H et al. 2005). The method described an overall shape mathematically by transforming coordinate information concerning its contours into Fourier coefficients and summarizing Fourier descriptors by principal component analysis.

We investigated the feasibility of the same technique for describing vertebral shapes. The Active Shape Method is useful for identifying the contour of the vertebral body, but additional mathematical procedures are required to compute intervertebral movements by matching images from different films. Developments in technology have created the opportunity to overcome these problems. The literature (MINNE, HW, LEIDIG, G et al. 1988; ROGERS, BP, HAUGHTON, VM et al. 2002) review clearly showed that there is a strong need to develop an automatic method for vertebral morphometry of reliable vertebrae shapes and a precise determination method for spinal kinematics that can be used routinely in clinical assessments.

6.2 AIM OF STUDY

The purpose of this study was to develop a method to identify the contour of the vertebral body in radiographic films using the Active Shape Method and to determine intervertebral movements from changes in positions of vertebral body positions using a Genetic Algorithm. It is hoped that the present method would increase the accuracy of measurement and significantly reduce the data processing time associated with manual digitization of landmarks and matching of images.

6.3 AUTOMATIC MEASUREMENT OF INTERVERTEBRAL MOTIONS ON X-RAY FILMS

Automatic measurement of spinal motions involves two steps (1) Active shape model for identifying the contour of the vertebral body in radiographic films, and (2) a Genetic Algorithm for determining intervertebral movements from changes in positions of vertebral body positions.

6.3.1 Active Shape Model (ASM)

An Active Shape Model (ASM) (BLAKE, A and ISARD, M 1998; VISUAL AUTOMATION LIMITED, C 1998; SMYTH, PP, TAYLOR, J et al. 1999), a general contour method from the field of computer vision, is used to locate and measures the shapes of vertebrae in images. This method seeks the best object segmentation within a small neighborhood of beginning points. An ASM contains two separate components. Vertebral shape is described by means of a point distribution model (PDM) with seventy-three landmark points along the vertebral contour, which is generated by performing statistical analysis of the object shapes observed over the set of training images. Then, principal component analysis is performed on the set of training profiles for that landmark point, which is a mean profile plus a set of modes of profile variation. Using the ASM Toolkit (Visual Automation, Ltd. (VISUAL AUTOMATION LIMITED, C 1998)) which is an add-on of the MATLAB mathematical software system, we conducted research on the effectiveness of ASM for segmenting lateral radiographs of the lumbosacral spine. The detailed mathematical equations were given in previous works (COOTES, TF, HILL, A et al. 1994; SMYTH, PP, TAYLOR, J et al. 1999).

The shape of the vertebral body image was described as a function of the sets of Fourier descriptors. Fourier descriptors were used to represent the vertebral shape (COOTES, TF, HILL, A et al. 1994; SMYTH, PP, TAYLOR, J et al. 1999; ZHENG, Y, NIXON, MS et al. 2003; ZHENG, Y, NIXON, MS et al. 2004). A curve, $c(t)$, defines the positions of points on the vertebral contour along it by components in two orthonormal axes.

$$c(t) = c_x(t)U_x + c_y(t)U_y$$

where $U_x = [1 \quad 0]^T \quad U_y = [0 \quad 1]^T$

According to Fourier theory,

$$c(t) = \begin{bmatrix} C_x(t) \\ C_y(t) \end{bmatrix} = a_0 + \sum_{k=1}^{8} \begin{bmatrix} a_{xk} & b_{xk} \\ a_{yk} & b_{yk} \end{bmatrix} \begin{bmatrix} \cos(k\omega) \\ \sin(k\omega) \end{bmatrix} \tag{1}$$

$$\begin{cases} a_{xk} = \dfrac{1}{8}\sum_{i=1}^{16} x_i \cos(k\omega_i) \\ b_{xk} = \dfrac{1}{8}\sum_{i=1}^{16} x_i \sin(k\omega_i) \\ a_{yk} = \dfrac{1}{8}\sum_{i=1}^{16} y_i \cos(k\omega_i) \\ b_{yk} = \dfrac{1}{8}\sum_{i=1}^{16} y_i \sin(k\omega_i) \end{cases}, \qquad (2)$$

where a_0 represents the translating effect, the transformation matrix is the rotating effect and the scale effect is the unit. The scaling effect is eliminated by a magnification factor.

To operate ASM, the template is placed within an image, with the goal of converging to a target object by rotating, translating, scaling, and deforming. The template initially becomes the “current shape”. ASM is an iterative process where, at each step: (1) grayscale values from the image are sampled at lines normal to each landmark point on the current shape; these sampled values are compared to the expected grayscale values at each landmark point, and the landmark point is then replaced with the sample point that most closely corresponds to the expected value; (2) the shape model is used to constrain the shape produced by the grayscale model to lie within reasonable distance of the shapes represent by the shape model; and (3) updated position, orientation, and scale are estimated. When the difference between the current shape and the previous shape become sufficiently small, the algorithm has converged. Figures 6.1 (a), (b) and (c) illustrate the lateral radiographs of the lumbosacral spines in a flexion posture, the process of placing an ASM template on the image and the resulting, converged segmentation of the lateral radiographs of the lumbosacral spines on extension posture, respectively. The ASM search on lumbosacral images is also shown in Figs 6.1 (a) to (c).

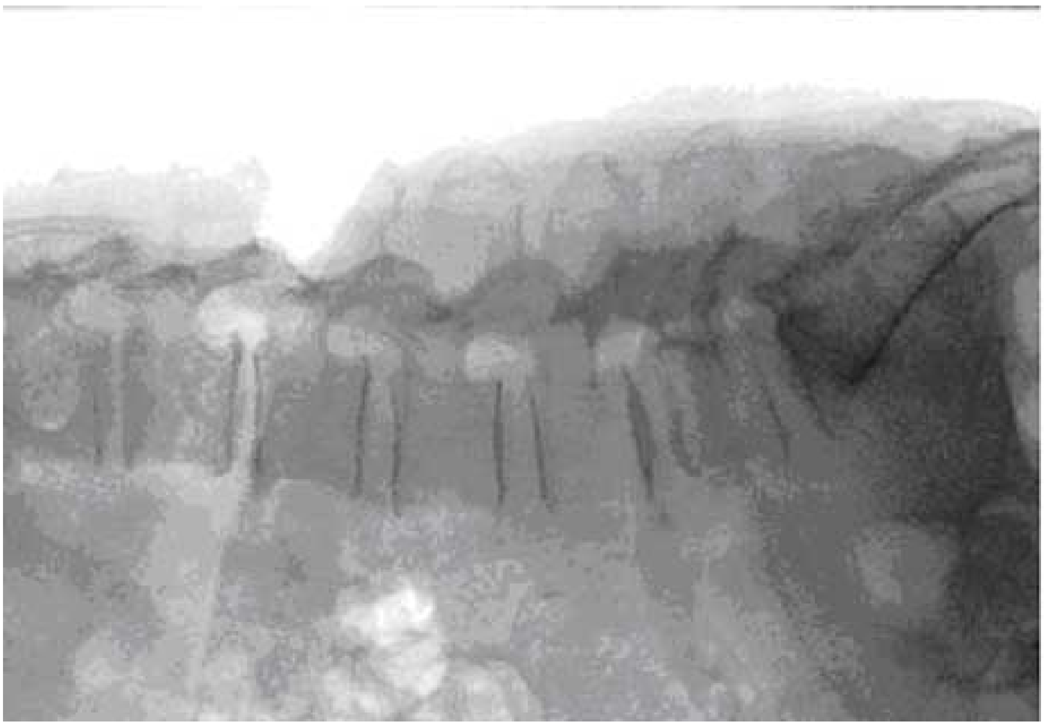

Fig. 6.1a Original lumbosacral spine on X-ray film.

Active Shape Models allow rapid, powerful and robust image searching. The advantage of ASM search over other techniques lies in the model description of shape and the expected shape variation. An active shape model has the following components: statistics describing the grey-level landscape around each landmark point and statistics describing the principal ways in which the modeled shape can vary. An ASM seeks to fit each landmark point to an image structure by matching its grey-level description, while maintaining an acceptable overall shape. The search is an iterative refinement of the model poses and shape parameters to give a better match between grey-level descriptions and image structures.

The following procedure describes the use of the ASM Matlab Toolkit Application in finding and tracking vertebra in an image.

(a) Selecting Training Images: The first step in model construction is to collect a set of training images. These should contain a typical and representative spectrum of the type of object that is to be modeled. Images with poorly defined or partially hidden objects should be avoided. At least 60 images are required to build our model;

(b) Labeling Images: For each training image, we have a set of points (landmarks) describing the object shape. In our vertebra images, we have selected seventy-three consecutive marked landmarks on each vertebra in every image (flexion and extension). The average distance between two adjacent points ranges from 1 to 1.5mm. The vertebrae contour is well represented; and

(c) Build shape model: Construct three types of files that pertain to the shape model. The point file contains the coordinates of points describing a vertebra contour. The parts file (*.parts) encodes the connectivity between points (which points are connected to each other, open or closed boundaries). The shape model data file (*.smd) contains locations of training images and their respective point files, the names of the training images, point files and parts files to be used, and the model building parameters. The shape model is built by composing the three types of files.

The ASM is applied to locate the vertebral shape in the flexion and extension images. A file containing 438 rows (six vertebra from L1 to Sacrum and 73 points for each vertebra), 6 columns (two Cartesian coordinates along the postero-anterior and supero-inferior directions, three postures of flexion-standing-extension) were generated for each subject.

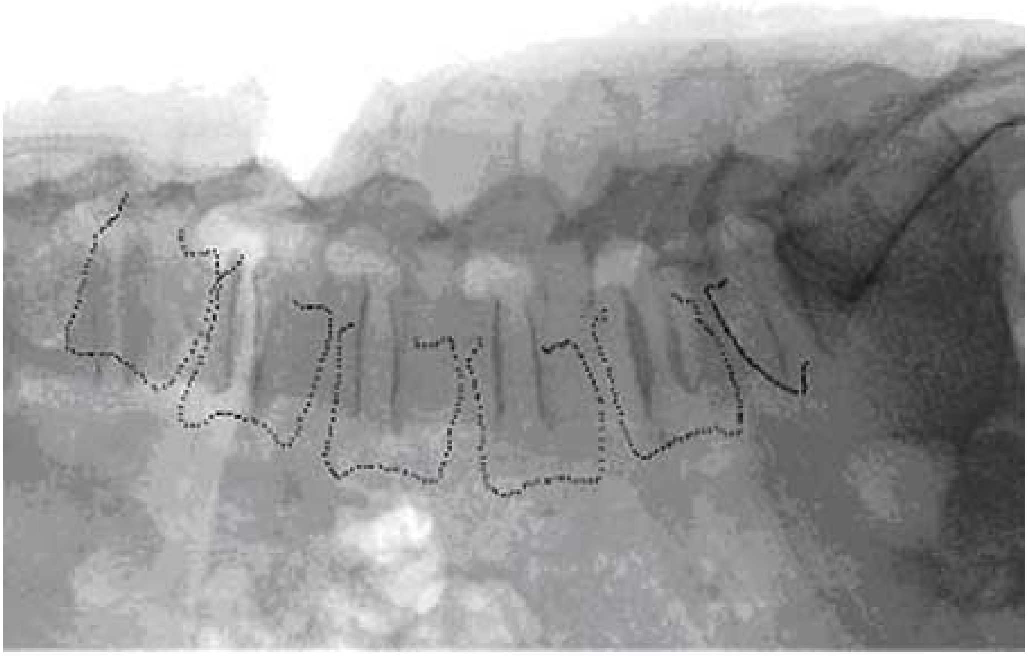

Fig. 6.1b Starting ASM search positions of vertebrae on lateral lumbosacral image.

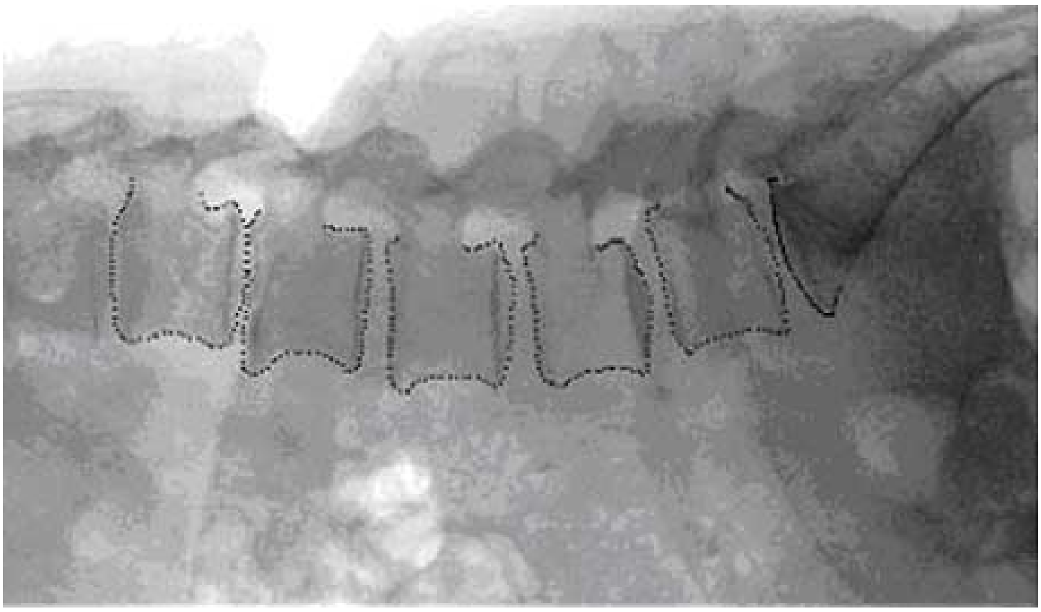

Fig. 6.1c Final ASM search positions of vertebrae on lumbosacral image after convergence.

6.3.2 Genetic Algorithm (GA)

Genetic algorithms (GA) (THE MATHWORKS INC 1994) belongs to a class of stochastic search methods, operates on a population of solutions. The relative motions between two vertebrae in images are determined by searching for the 'best' matched value of the coefficient of correlations with GA. GA includes 4 components in this study.

1) Encoding

The relative angle of rotation and translations between two vertebrae in images were the solutions. The GA encodes 32 bits solutions (rotation & translations of vertebral contours between two radiographic images) in a structure, so called a genome or chromosome.

Table 6.1 Interpretation of 32 bits solution of GA

	Range of Motion	**Accuracy**	**No. of digits**	**Explanation**
Rotation, deg	± 90	0.1	11	2^{11} = 2048 >1800
X or Y Translation, mm	± 50	0.1	10	2^{10} = 1024 >1000
Total			> 31	32 bits variable

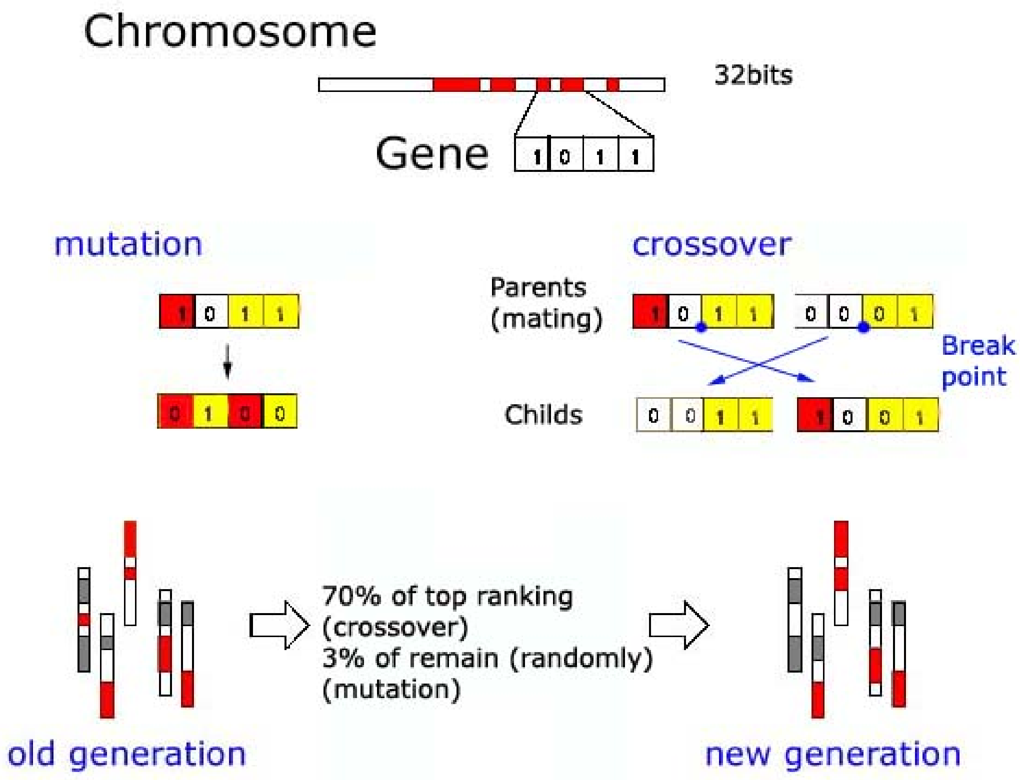

Fig. 6.2 GA generate a new individuals from old generation.

2) Selection criteria

In the beginning, GA created 100 individuals by totally random. There is the fitness function in GA that determines how 'good' each individual is and the best individuals for mating to keep the population evolving. The fitness function maximizes cross coefficient R value. Bifulco (BIFULCO, P, CESARELLI, M et al. 1995) reported that cross-correlation is a similarity cross-correlation measures. GA uses the following two selection criteria to picks the best chromosome: (a) Top 70% ranking of R value to do crossover; (b) Then, random 3% remain individuals on that population to do mutation. Fig. 6.2 shows that GA creates a population of genomes then applies crossovers and mutations to the individuals in the population to generate a new individuals.

3) Terminal condition

Searching will terminate in order to satisfy the following conditions: 100 times loop, the best individual remained unchanged, similarity among individual close to 1.

4) Decoding

The relatives motions between vertebrae on two images are determined after decoding.

The Genetic Algorithm (GA) optimizes the measure of similarity of vertebral contours between the flexion and extension radiographic images. Correlation coefficients (the R values) were employed to examine the reliability of vertebra contours between flexion and extension. GA performs the highest cross-correlation coefficient mapping between vertebra in the flexion and extension postures. The process is started on the sacrum and then repeated for vertebra L5, L4, L3, L2 to L1. Segmental motion is depicted by superimposing images of the stationary underlying vertebra from L1 to L5 and comparing the positions of identical points on the images of the fully flexed with the extended position. The Genetic Algorithm Toolbox (THE MATHWORKS INC 1994) for MATLAB® was developed at the Department of Automatic Control and Systems Engineering of The University of Sheffield, UK, in order to make GAs accessible to the control engineer within the framework of an existing computer-aided control system design package.

The flowchart of the genetic algorithm is shown in Fig. 6.3. The GA algorithm works as follows:

(i) Create an initial population: The segmentation of flexion images generated by the ASM provides an initial approximation of vertebral locations.

(ii) Declaration of parameters: The angle of rotation and translations of the vertebrae along the postero-anterior and supero-inferior directions are outcome variables.

(iii) Evaluate all of the individuals (apply some function or formula to the individuals): the coefficient of correlations on GA is determined. The cross-correlation coefficients between two images on different segmental levels are chosen as a measure of the vertebral contours between the flexion and extension radiographic images.

(iv) Select a new population from the old population based on the fitness of the individuals as given by the evaluation function. By scaling, rotating and translating, the relative motions (rotation and translations) between two vertebrae in the images are determined.

(v) Apply some genetic operators (mutation and crossover) to members of the population to create new solutions.

(vi) Evaluate these newly created individuals.

(vii) Repeat steps iii-vii until the termination criteria has been satisfied: one hundred times of searching conducted.

(viii) Output solution: The intervertebral motions (rotation and translations) between two vertebrae on images are determined by using searching of the ‘best’ value of the coefficient of multiple correlations in GA.

Output Arguments:

% P - the best solution found during the course of the run.

% endPop - the final population.

% bestsols - a trace of the best population.

% traceInfo - a matrix of best and means of the GA for each generation.

Input Arguments:

% x, y - the coordinates of points on vertebra contour for flexion, standing and extension images.

% bounds - a matrix of upper and lower bounds on the variables.

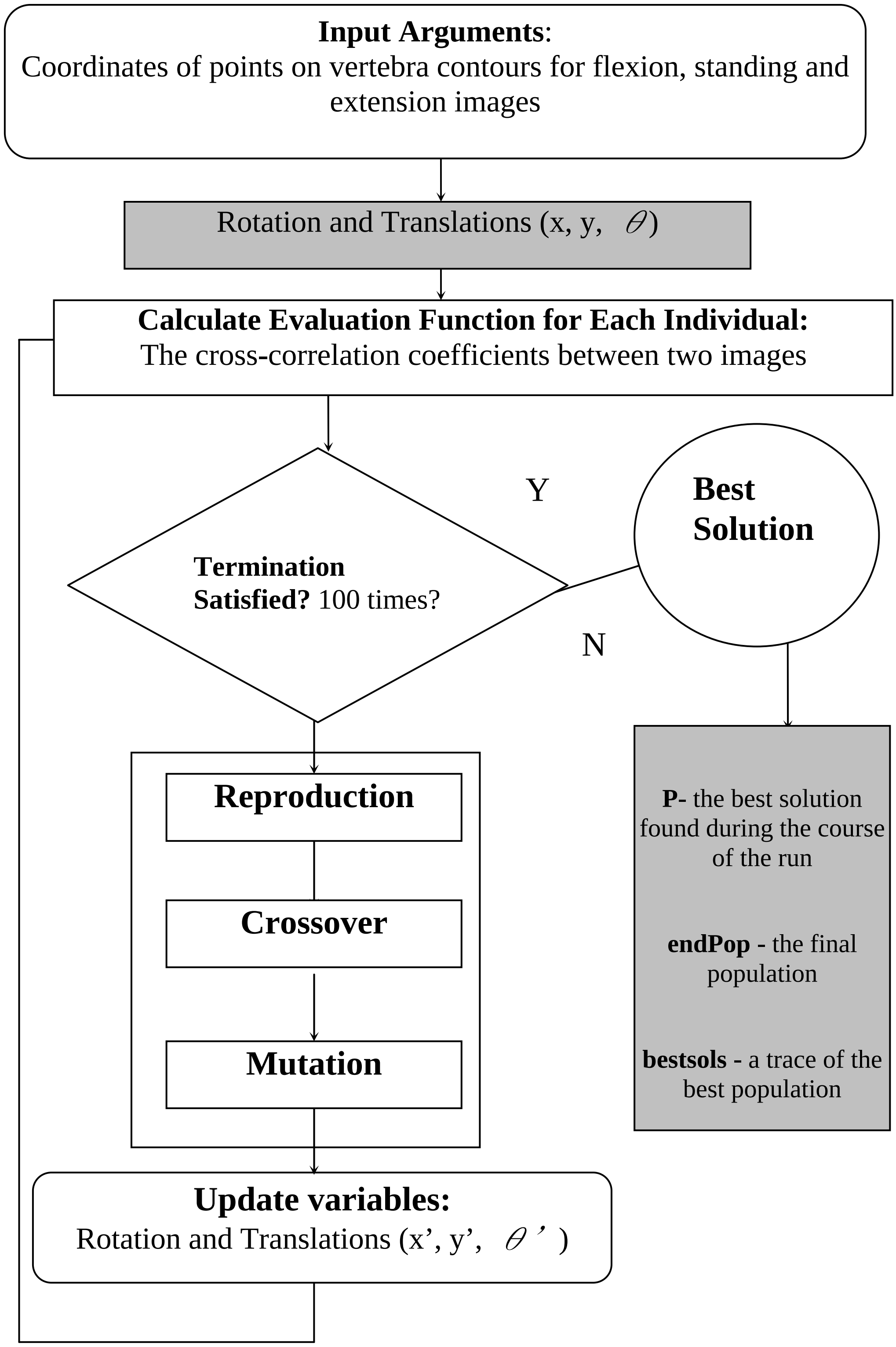

Fig. 6.3 Flowchart of the Genetic Algorithm.

6.4 Manual Measurement of Intervertebral Motions on X-ray Films

The manual measurement method has been described in detail in previous studies (LEE, RYW 1995; LEE, RYW and EVANS, J 1997). The rotation motion was determined by the angle of rotation of the vertebra in relation to the lower vertebra of the fully flexed position with the fully extended position. The translation motions were described by postero-anterior and supero-inferior translation of location of the centre of the vertebra in relation to the lower vertebra. Intervertebral movements are then computed by comparing the positions of the vertebrae in the radiographs taken in the neutral and flexion posture.

Each of the vertebrae (L1 to L5) is identified manually by marking the four body corners. Fitting a quadrangle around the vertebral body allows tracing of the positions of the vertebrae. Segmental motion is depicted by superimposing images of the stationary underlying vertebra from L1 to L5 and comparing the positions of identical points on the images of the fully flexed with the extended position. A radiographic oblique ruler (5 mm apart) was placed on the subject’s backs to allow for scaling of the X-rays to account for the magnification factor. Manual locations of the four corners of the traced quadrangles and ASM search on lumbosacral images are shown in Fig. 6.4.

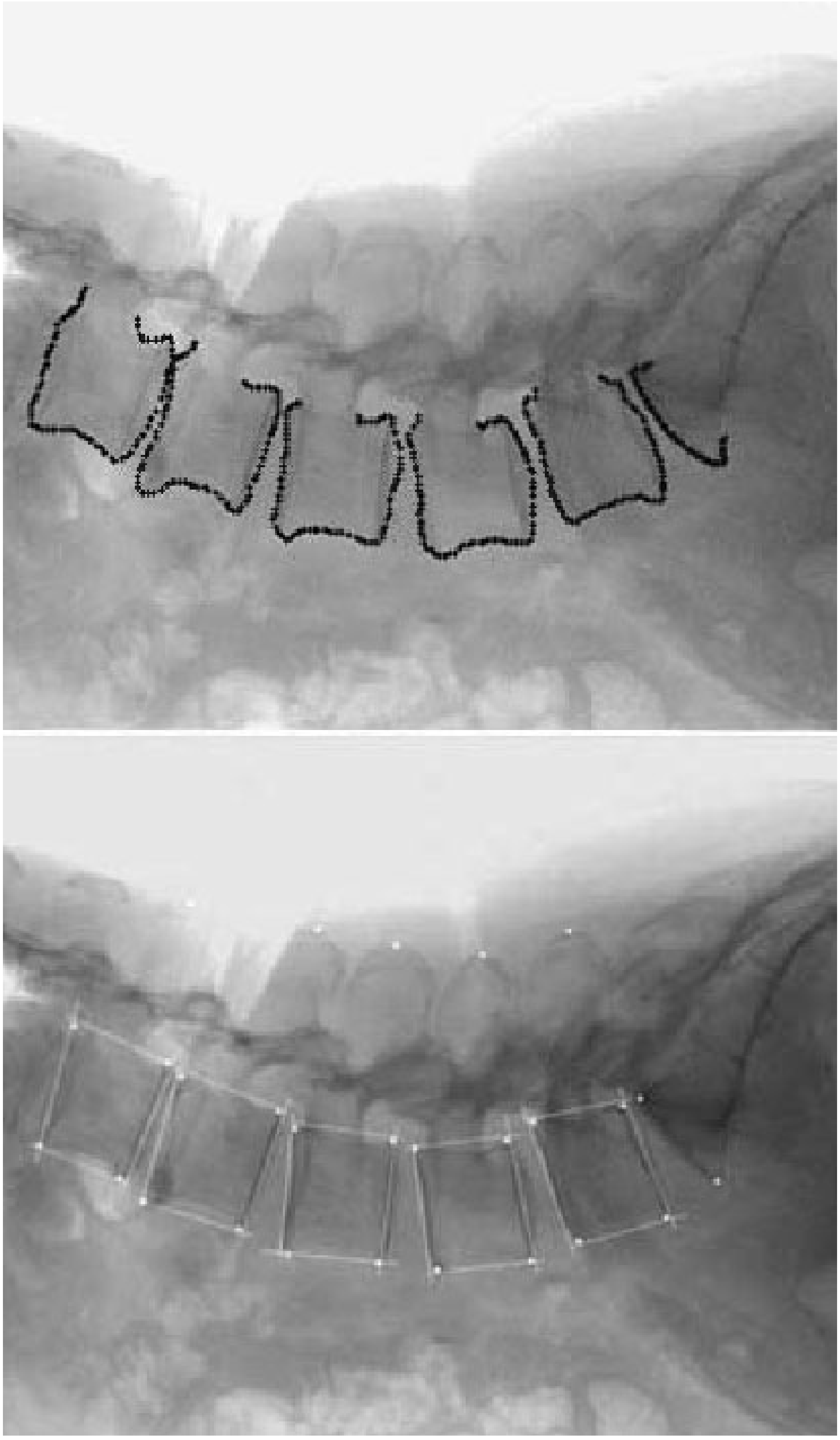

Fig. 6.4 Manually located quadrangles (Bottom) and ASM search (Top) on lumbosacral images.

6.5 EXPERIMENTAL VALIDATION

Twenty-two healthy male volunteers (21 ± 1 years old, 1.75 ± 0.03 m tall, 67.9 k ± 45 g weight, Body Mass Index, 22.2 ± 1.5 kgm^{-2}) were recruited from the Duchess of Kent Children's Hospital, Hong Kong. Lateral radiographs of their lumbosacral spines were taken in full flexion and extension while standing. Subjects who showed any signs of fracture or dislocation, spinal instability, spondylolisthesis, narrowed disc spaces, osteophytes, transitional lumbosacral vertebrae or any structural disorders of the lumbar spine, or those who had previous history of spinal surgery were excluded. The study was approved by the Ethics Committee of Department of Rehabilitation Sciences, The Hong Kong Polytechnic University. Subjects were informed about the experimental procedure and any potential risks prior to the attainment of a written consent form (Appendix III).

The angle of rotation, postero-anterior translation and supero-inferior translation of the vertebrae on inter-segmental levels from L1 to the sacrum were determined and compared between the manually located four corners of quadrangles in the images and the automatic method using ASM and GA. The above measurements were repeated five times and the mean errors (defined as the standard deviations of the measurements) among repeated measures were studied.

6.6 RESULTS

6.6.1 Intervertebral Movements

Ranges of intervertebral motion for the flexion-extension movement are presented in Table 6.2, together with published data of previous research (WHITE, AA and PANJABI, MM 1978; PEARCY, M, PORTEK, I et al. 1984; YAMAMOTO, I, PANJABI, MM et al. 1989; DVORAK, J, PANJABI, MM et al. 1991). The mean values showed a similar range of motion progressively from L1 to L5. The greatest motion was seen at L4/5 and L1/2 had the least range of motion.

Table 6.2 Summary of lumbar spine rotations (flexion and extension) on the sagittal plane, compared with previous results.

	Year		Case	**Range of Motion (Degree)**					
				L1/2	**L2/3**	**L3/4**	**L4/5**	**L5/S**	**Total**
White[1]	1978	In vitro	—	12.0	14.0	15.0	17.0	20.0	78.0
Pearcy[2]	1984	In vivo	11	13.0	14.0	13.0	16.0	14.0	70.0
Yamamoto[3]	1989	In vitro	10	10.1	10.8	11.2	14.5	17.8	64.4
Dvorak[4]	1991	In vivo	10	11.9	14.5	15.3	18.2	17.0	76.9
Current study	2005	In vivo	22	10.5	13.2	14.2	17.9	12.8	68.6

[1]White AA and Panjabi MM (1978) Clinical Biomechanics of the Spine. Philadelphia, J.B., Lippincott.

[2]Pearcy M, Portek I and Shepherd J (1984) Three-dimensional x-ray analysis of normal movement in the lumbar spine. Spine 9(3): 294-7.

[3]Yamamoto I, Panjabi MM, Crisco JJ and Oxland T (1989) Three-dimensional movements of the whole lumbar spine and lumbosacral joint. Spine 14(11): 1256-60.

[4]Dvorak J, Panjabi MM, Chang DG, Theiler R and Grob D (1991) Functional radiographic diagnosis of the lumbar spine. Flexion-extension and lateral bending. Spine 16(5): 562-71.

6.6.2 Analysis of Errors in the Automatic Radiographic Measurements

An error is defined as the standard deviation of the five repeated measurements obtained from an individual. The mean measurement error and the intra-class correlation coefficient (ICC) values of the manually located four corners of the quadrangles and ASM search of five repeated measures of radiographic measurements are presented in Table 6.3.

The mean errors of the automatic method in determining sagittal rotation and x-posteroanterior and y-superoinferior translations were found to be less than 0.15 degrees, 0.014mm and 0.012mm, respectively. The mean error of the manual method involved in determining sagittal rotation and x- posteroanterior and y- superoinferior translations were 0.5 degrees, 0.06 mm and 0.03 mm, respectively. These values were higher than the errors associated with the automatic method.

Table 6.3 Mean measurement error (= 1 SD) and intra-class correlation coefficient (ICC) values of manual 4 corners of the quadrangles and ASM search in five repeated measures of radiographic measurements.

	Mean measurement error					**Mean ICC (3,1)**				
Manual 4 corner quadrangles	**L5/S**	**L4/5**	**L3/4**	**L2/3**	**L1/2**	**L5/S**	**L4/5**	**L3/4**	**L2/3**	**L1/2**
Angle of Rotation, deg	0.28	0.41	0.32	0.48	0.34	0.96	0.96	0.96	0.88	0.92
x-posteroanterior translation, mm	0.02	0.03	0.03	0.06	0.03	0.99	0.99	0.99	0.98	0.95
y-superoinferior translation, mm	0.02	0.02	0.02	0.02	0.03	0.99	0.99	0.99	0.98	0.95
	Mean measurement error					**Mean ICC (3,1)**				
ASM Search	**L5/S**	**L4/5**	**L3/4**	**L2/3**	**L1/2**	**L5/S**	**L4/5**	**L3/4**	**L2/3**	**L1/2**
Angle of Rotation, deg	0.15	0.08	0.10	0.12	0.13	0.996	0.999	0.997	0.997	0.995
x-posteroanterior translation, mm	0.014	0.008	0.007	0.010	0.013	0.999	0.999	1.00	1.00	0.999
y-superoinferior translation, mm	0.012	0.010	0.010	0.009	0.011	0.997	1.00	1.00	1.00	0.999

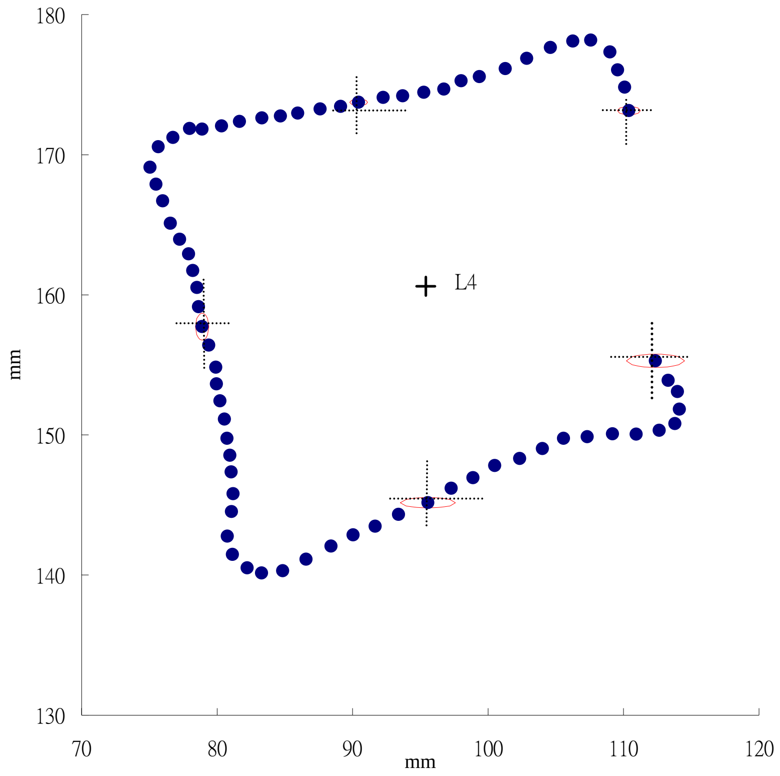

Fig. 6.5 Measurement of ASM reproducibility. Two orthogonal lines show directions along x- and y- axes where errors are measured. The x-axis is posteriorly formed by the superior endplate of the inferior vertebrae and the y-axis superiorly perpendicular to the x-axis. The elliptic areas show the distributions of automatically marked points on the contours of the vertebra.

Using same approach with Smyth (SMYTH, PP, TAYLOR, J et al. 1999), manually marked 73 landmark points on each vertebra in every image in consultation with a radiologist, and compared the converged ASM vertebra boundaries with the manually-marked boundaries. Seventy-three landmark points per vertebrae around the contour of the vertebra shape were marked for the ASM method. Further, to estimate how these errors would compare with reproducibility errors occurring when acquiring boundary markings manually with multiple human readers. Five readers independently mark six boundary points on L5 vertebra, and computed variances in point placement across these readers. The elliptic areas shown in Fig. 6.5 illustrates the error size of the automatically five reading marked (which number are 1, 16, 37, 58 and 73 respectively) points on the contour of L5 vertebrae.

The average variance of the x- and y- coordinates of the points on the vertebral contours among five repeated measures are presented in Figs. 6.6 (a) and (b). The graphs are shown in polar form. Axes of x and y are along the postero-anterior and supero-inferior direction respectively. The vertebra contour was divided into seventy-three parts, from 0 to 360 degrees, with 72 to 144 degrees omitted. This is because no vertebra boundary lies in that zone. The maximum errors of the x and y coordinates are 3.7 and 2.6mm, respectively. The maximum x- and y-coordinates errors occur at L1.

6.6.3 Time of Shape Detection between Manual and Automatic Method

The estimate time of a single shape detection in the automatic method ranged from 2 to 3 minutes. Conventional radiographic measurements (manually locating four corners of the quadrangles) normally take almost 20 minutes for each image.

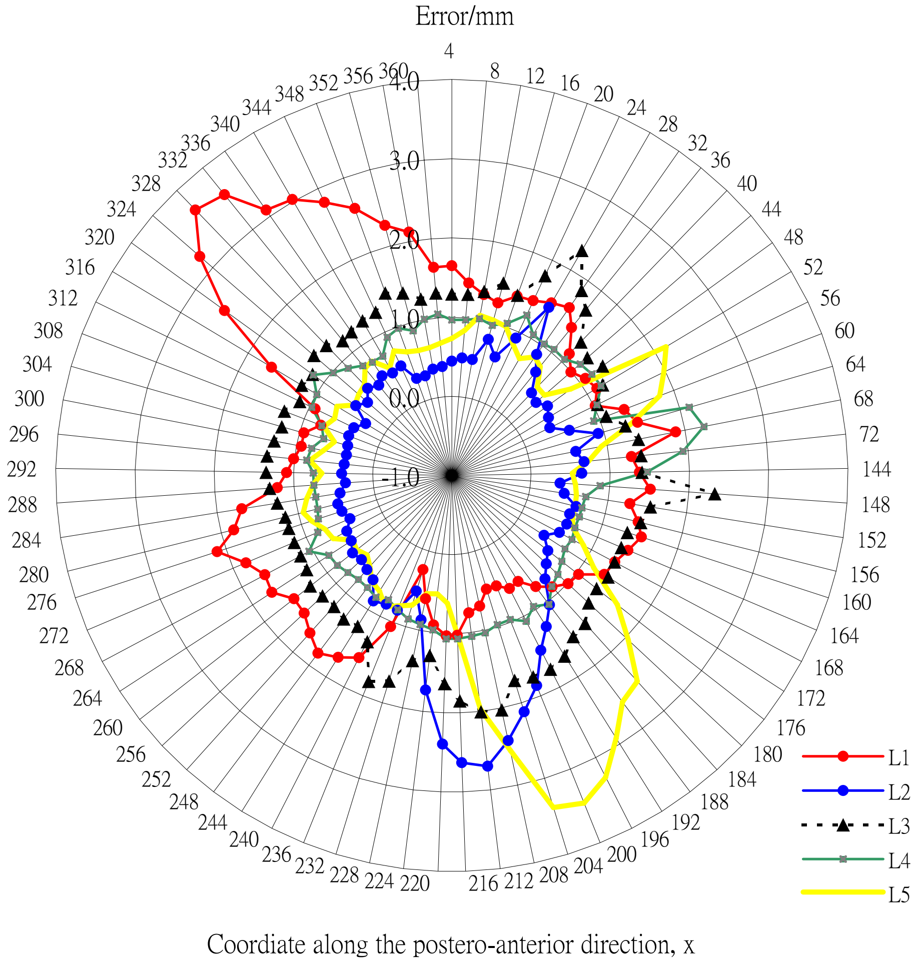

Fig. 6.6a Mean errors of vertebral contours among five repeated measures on different levels in polar form. Coordinate is along with postero-anterior direction.

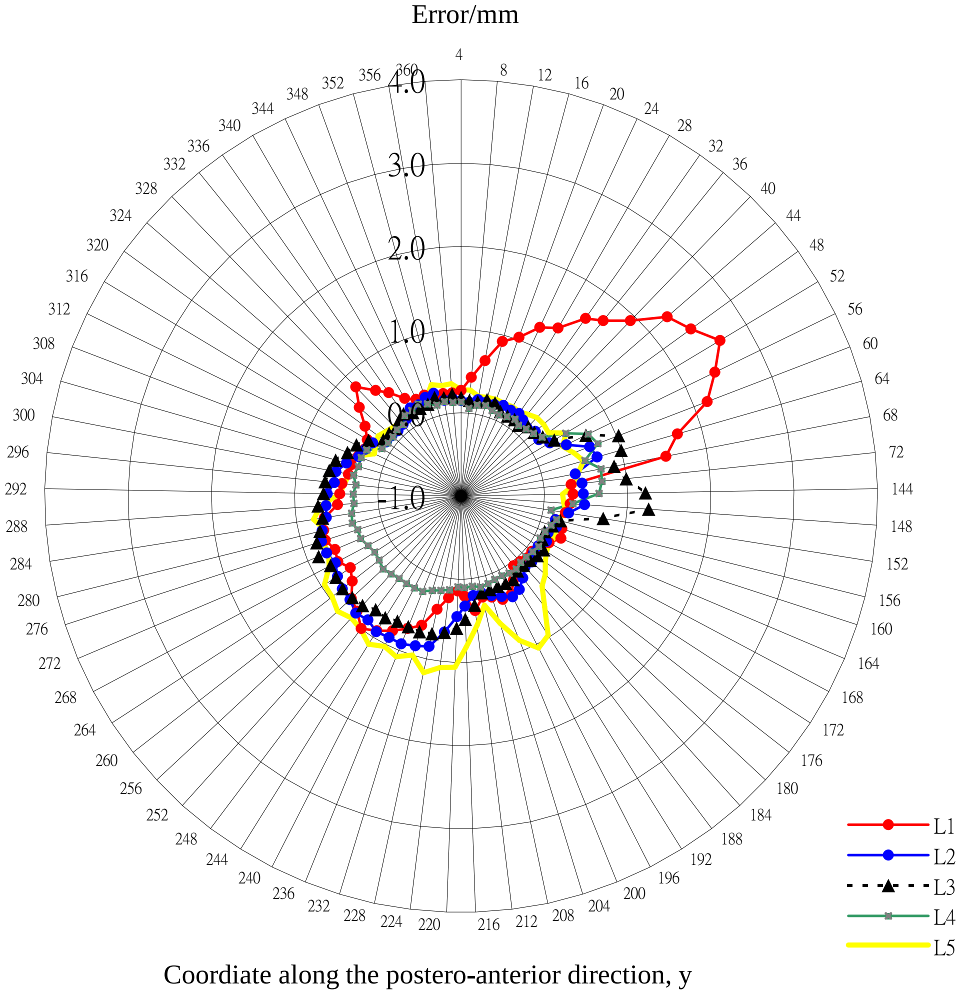

Fig. 6.6b Mean errors of vertebral contours among five repeated measures on different levels in polar form. Coordinate is along with supero-inferior direction.

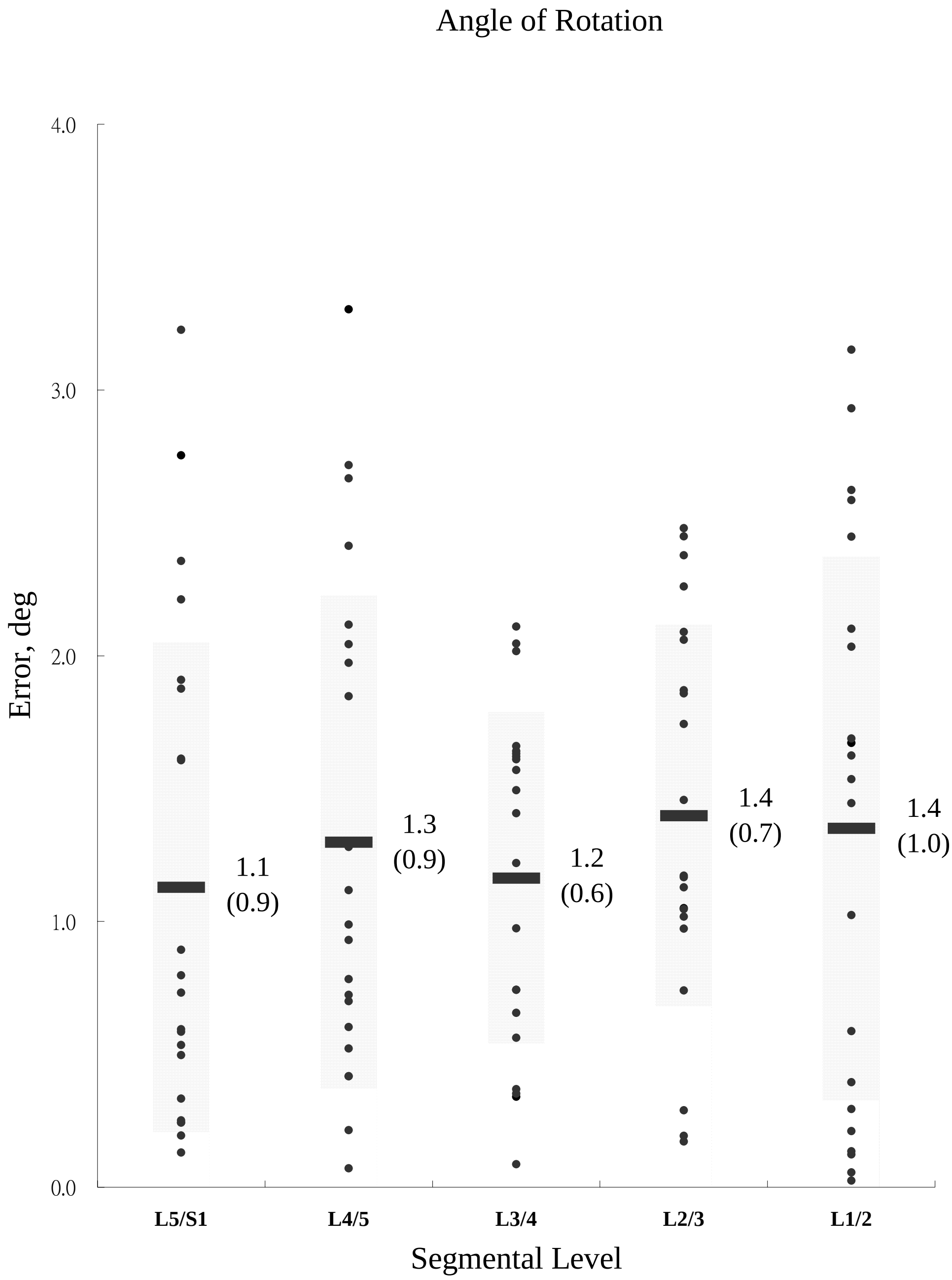

Fig. 6.7a The absolute mean and standard deviation errors of rotation angle determined from manual and automatic method.

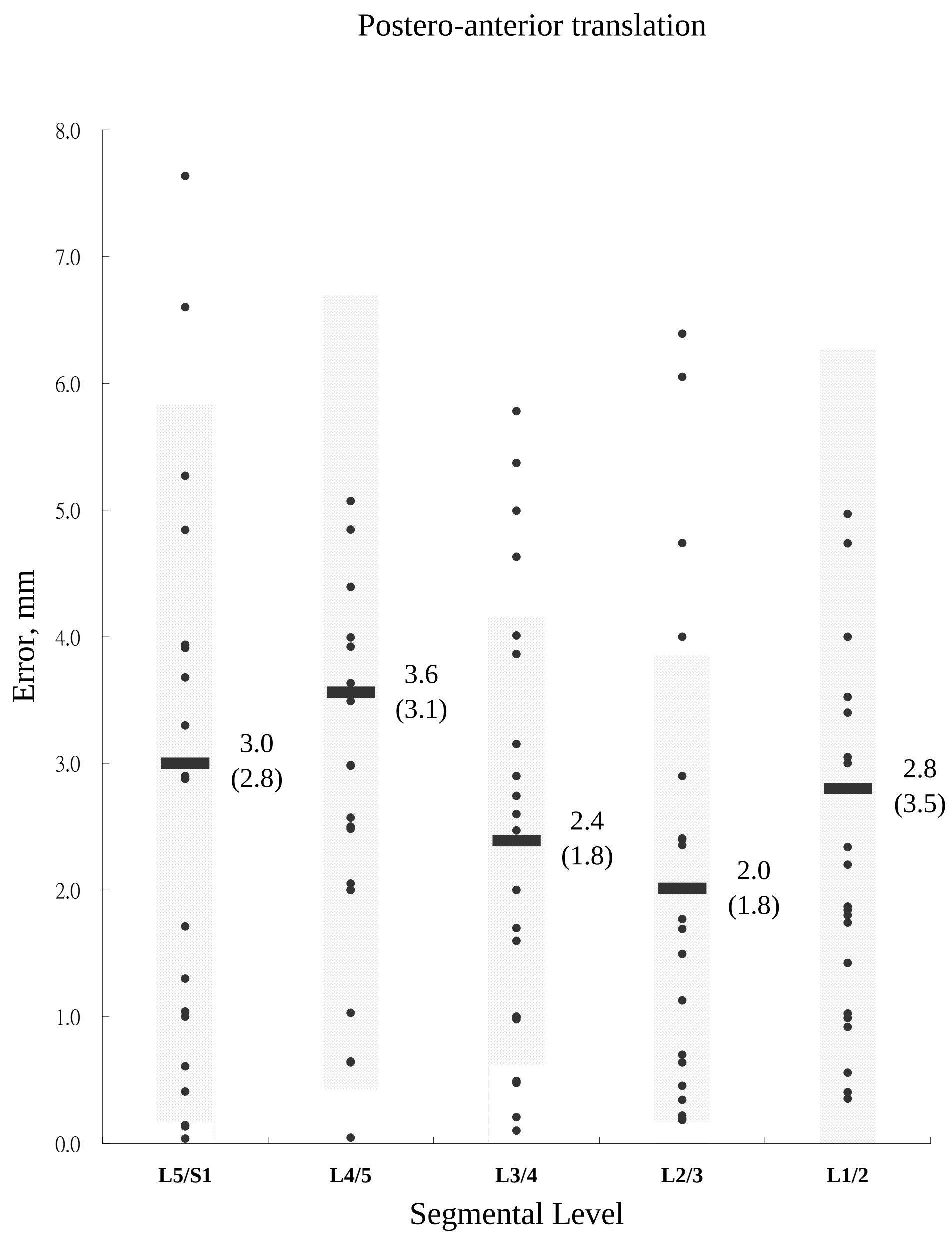

Fig. 6.7b The absolute mean and standard deviation errors of postero-anterior translation determined from manual and automatic method.

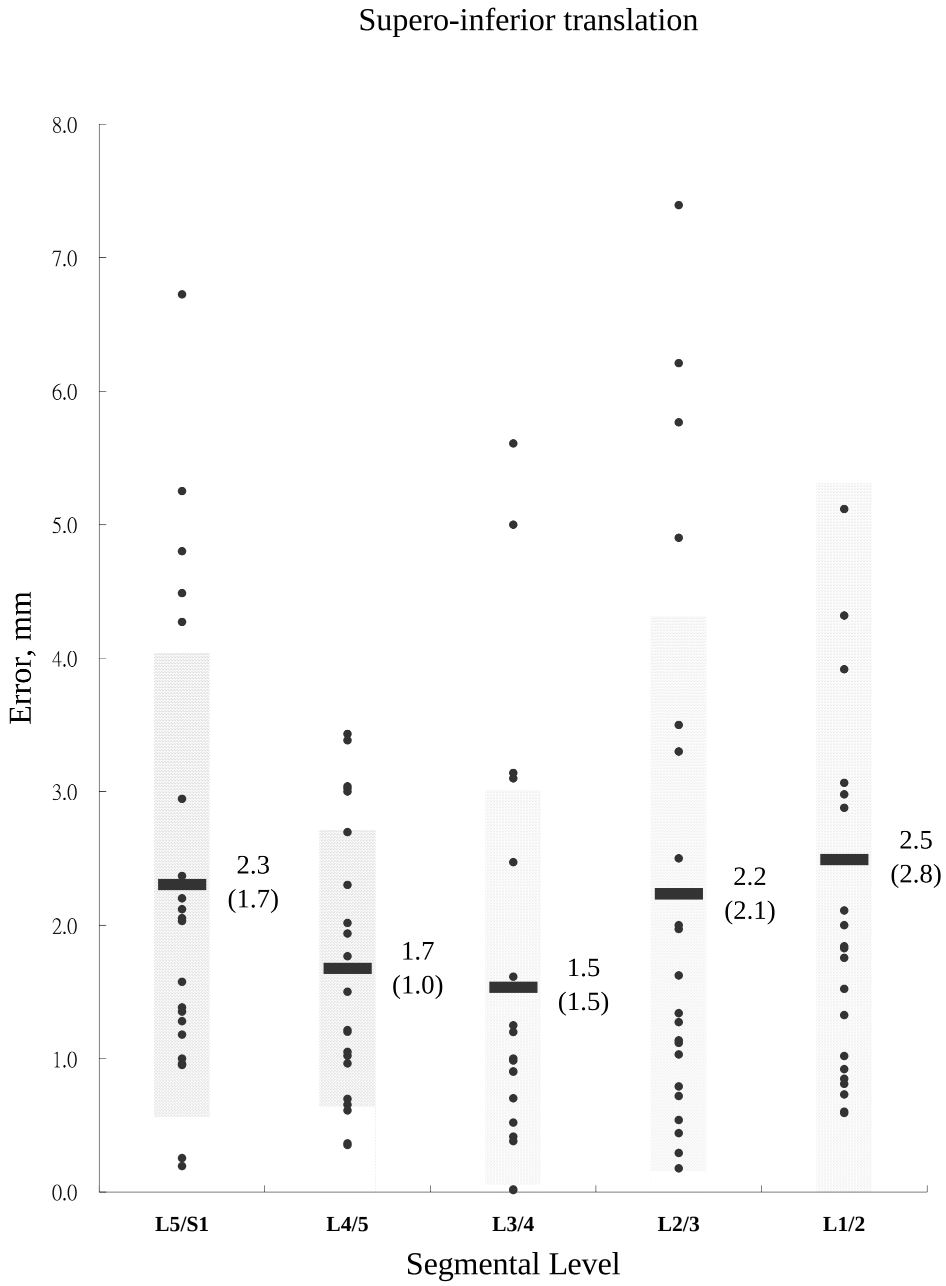

Fig. 6.7c The absolute mean and standard deviation errors of supero-inferior translation determined from manual and automatic method.

6.6.4 Consistent of Vertebral Shapes in Different X-ray Films

The mean values and standard deviations of the correlation coefficients for the 73 points on the flexion and extension films are shown in Fig. 6.8. The values ranged from 0.994 to 0.997, indicating that the shapes of the vertebrae were highly consistent in the two films and that there were little out of plane motions of the vertebrae.

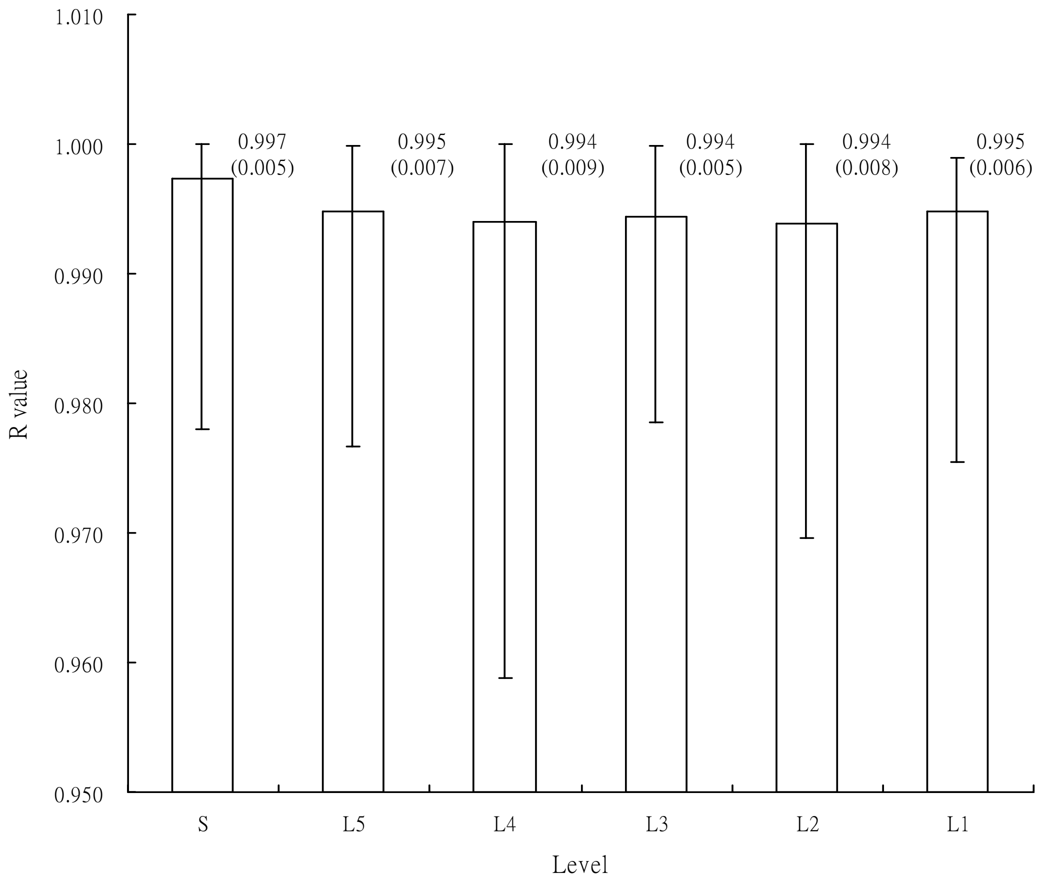

Fig. 6.8 Mean (SD) correlation coefficients of the automatically detected points on the vertebral outline in the flexion and extension films.

6.6.5 Comparison between Manual and Automatic Methods

Table 6.4 shows the comparison of kinematics parameters among subjects as determined by the automatic and manual methods. The mean and standard deviation of the kinematics of the four corners of the quadrangles and the ASM method for each vertebral level are summarized. The mean differences in the angles observed between the two methods were 1.1, 1.3, 1.2, 1.4 and 0.4 degrees for the L5/S to L1/2 segmental levels, respectively. The mean differences in intervertebral translations were also small (from 0.5 to 1.2 mm) for the various intervertebral joints.

6.6.6 Differences of Contours of Vertebral Body Image Extracted by Active Contour and Manual

The extraction of the vertebral body image by Active Contour was superimposed on the original vertebral body image of the spine. The vertebra of L4 was chosen because it located on the middle of the image (less distortion and much clear). The L4 vertebra contour was also traced manually, and sixty landmark points along this contour were identified. Each of these points corresponded to the points identified by the Active Contour. Mean difference and standard deviation of coordinates of the sixty points derived from the extraction shape of vertebral body image by Active Contour and Manual were 0.7 ± 0.8 mm and 0.9 ± 0.8 mm along postero-anterior and supero-inferior directions respectively (Table 6.5). Pearson's product correlation coefficient was determined to assess the degree of association between computerised segmentation and manual tracing. The R values were 0.969 and 0.935 along postero-anterior and supero-inferior direction respectively (Table 6.6). They were satisfactory.

Table 6.4 Comparison of the mean (SD) of the kinematics parameters determined by the manual and automatic methods.

	Motion segment				
Mean Angle of rotation, degree	**L5/S**	**L4/5**	**L3/4**	**L2/3**	**L1/2**
Manual (i)	13.7	17.7	13.8	14.0	9.7
	(5.8)	(4.6)	(3.5)	(3.8)	(4.8)
Automatic (j)	12.8	17.9	14.2	13.2	10.5
	(6.1)	(4.8)	(3.6)	(4.0)	(4.6)
Mean absolute difference (i-j)	1.1	1.3	1.2	1.4	0.4
	(0.9)	(0.9)	(0.6)	(0.7)	(1.0)
X-Postero-anterior translation, mm					
Manual (i)	1.4	2.9	2.5	2.4	2.0
	(1.0)	(0.9)	(0.8)	(0.6)	(1.1)
Automatic (j)	1.3	3.8	2.7	2.4	2.1
	(1.3)	(1.4)	(1.1)	(1.1)	(1.9)
Mean absolute difference (i-j)	1.0	1.2	0.8	0.7	0.9
	(0.9)	(1.0)	(0.6)	(0.6)	(1.2)
Y- Supero-inferior translation, mm					
Manual (i)	1.0	0.9	0.1	-0.2	0.1
	(0.7)	(0.7)	(0.6)	(0.5)	(1.0)
Automatic (j)	0.6	0.9	0.2	0.2	0.3
	(0.8)	(0.7)	(0.9)	(1.2)	(1.3)
Mean absolute difference (i-j)	0.8	0.6	0.5	0.7	0.8
	(0.6)	(0.3)	(0.5)	(0.7)	(0.9)

6.7 DISCUSSION

The magnitude of lumbar intervertebral rotations in the sagittal plane was reported to be 13-16 degrees and the magnitude of intervertebral translation was between 1-3mm (WHITE, AA and PANJABI, MM 1978; PEARCY, M, PORTEK, I et al. 1984; YAMAMOTO, I, PANJABI, MM et al. 1989; DVORAK, J, PANJABI, MM et al. 1991). The intervertebral movements observed in our study agree with those reported in previous work.

6.7.1 Repeatability Analysis

The repeated measures analysis reveals standard deviations of less than 0.5 degrees for intervertebral rotations and less than 0.25 mm for translation (MUGGLETON, JM and ALLEN, R 1997). The mean errors for the automatic method for determining the sagittal rotation and x-posteroanterior and y-superoinferior were smaller than the errors reported in previous studies using the manual method. The mean value reported were 1 degree, 0.6 mm and 0.8 mm for sagittal rotation posteroanterior and superoinferior translations (LEE, RYW and EVANS, J 1997).

The automatic method were not only more accurate but proved to be more convenient because the whole procedure from import of the image data to determining the vertebra’s contours lasted 2 to 3 minutes compared with 20 minutes for the conventional method. The optimal solution was generated by 2 minutes computation time of GA. It suggested that there are small relative angle of rotation and translations between two vertebrae on images. The searching was close to the best solution while it starts. GA is an appropriate searching method in this study.

Both results were considered to be accurate and the efficiency of the automatic method was sufficiently improved.

Larger errors were found in the dorsal contours of the vertebral image. This phenomenon was explained by Brinckmann et al. (FROBIN, W, BRINCKMANN, P et al. 1996; FROBIN, W, BRINCKMANN, P et al. 1997). The full set of dorsal vertebral contours is not visible in a large percentage of radiographs due to overlay from other structures or due to deficient film quality. The dorsal delineation of the vertebral image is complicated due to the dorsally concave shape of the vertebral body and the insertion of the pedicle. The contour is more distinct at L2 to L5 and usually less at L1. The ventral corners on the L1 vertebra are subject to large distortion as it lies on the boundaries of the image and far beyond from the centre of the radiographic image which is tightly focused.

The mean correlation coefficients of the 73 points identified in the flexion/extension films were higher than 0.994. This showed that no distortion and out-of-plane movement occurred. The measurements will be inaccurate if there are distortion and out-of-plane motion. Higher correlation coefficients (R values) showed that ASM successfully converged the vertebra between flexion and extension from L1 to sacrum.

6.7.2 Segmentation of Vertebral Image Extracted by Hough Transform Algorithm, Morphological Watershed Segmentation Algorithm and Active Contour

Differences of contours of vertebral body image extracted by Hough Transform Algorithm and manual tracing was described in Section 5.1.4 and differences of contours of vertebral body image extracted by Morphological Watershed Segmentation Algorithm and manual tracing was described in section 5.2.4. Differences of contours of vertebral body image extracted by Active Contour compared with the results reported in pilot study (Chapter 5) and summarized in Tables 6.4 and 6.5. Less difference and higher correlation coefficients implied that Active Contour is a much better measuring method than the Hough Transform Algorithm and Morphological Watershed Segmentation Algorithm MWSA methods described in the earlier chapter.

Table 6.5 Differences of the vertebral body image (L4) between Hough Transform Algorithm (HT), Morphological Watershed Segmentation Algorithm (MWSA), Active Contour (AC) and manual.

Difference between manual	Coordinate along postero-anterior direction, X/mm				Coordinate along supero-inferior direction, Y/mm			
	Mean	SD	Median	Max.	Mean	SD	Median	Max.
HT	1.3	1.0	1.3	3.5	3.3	1.7	3.3	6.8
MWSA	2.1	1.9	1.5	7.0	3.4	1.8	3.6	6.3
AC	0.7	0.8	1.0	2.1	0.9	0.8	1.1	2.2

Table 6.6 Mean intra-class coefficient (ICC) values between Hough Transform Algorithm (HT), Morphological Watershed Segmentation Algorithm (MWSA), Active Contour (AC) and manual.

R value between manual &	Coordinate along postero-anterior direction	Coordinate along supero-inferior direction
HT	0.869	0.835
MWSA	0.634	0.571
AC	0.969	0.935

6.7.3 Advantages of Automatic Measurement

The automatic measurements of intervertebral movements were reliable and accurate. They compared favourly with the values obtained by the manual method. Cootes et al. (COOTES, TF, HILL, A et al. 1994; VISUAL AUTOMATION LIMITED, C 1998; SMYTH, PP, TAYLOR, J et al. 1999) first described the ASM technique for modelling human organs in medical images. The present study had successfully extended this method to locate and measure the shapes of vertebrae in images.

Almost every object of interest in the human body can vary in size, shape and appearance. This variability causes difficulties in automatically identifying and segmenting structures. Manual radiographic measurement of vertebrae is inadequate for the evaluation of continuous shape variation, as it cannot eliminate the subjectivity of human visual judgments, which result in unacceptable human errors.

The automatic method we developed was based on the technique for building compact models of the shape and appearance of flexible objects and it proved to be accurate for determining intervertebral movement of the lumbar spine. It is simple, fast, easy to operate and it provides adequate and accurate results. The automatic methods may be clinically used for shape recognition in diseases like fracture or osteoporosis. The automatic method significantly increases the clinical feasibility of the radiographic method for determining intervertebral movements.

6.7.4 Further Improvements

As a local search technique, the ASM needs a reasonable start position. The global search of a Genetic Algorithm (GA) was implemented to find good but approximate solutions rapidly. The two techniques are separate but complementary. The ASM search was conducted and it suggested a solution in a non-optimal area of the search space. The GA was applied as a refinement procedure. Each of the populations of solutions for a GA is assessed by evaluating an objective function, which measures the evidence for a given hypothesis. The multiple correlation coefficients were an objective function of GA in our study.

However, it is attractive to consider combining the two techniques in another approach. In the GA literature, it has been suggested that incorporating heuristic information and local optimization techniques within a GA search can improve the performance significantly. The basis of this approach is that the GA can locate the optimal area in the search space while the ASM embedded within the GA can determine the local minimum. The present method could be further improved in future work. The ASM can be embedded within the GA search directly. Applying a single iteration of the ASM procedure each time the objective function is evaluated requires minimal extra work and leads to significant improvements in the rate of convergence of the GA and the quality of the final fit.

Due to ethical reasons, we purposely restricted our study to male subjects where the gonads could be adequately protected. Unnecessary exposure of subjects to large doses of radiation were avoided with the use of image intensifier. Another limitation of this study is that although plain functional radiographs may reveal static states at two points of maximum flexion and extension positions, they do not provide information on detailed motion during flexion and extension. Zheng (ZHENG, Y, NIXON, MS et al. 2003; ZHENG, Y, NIXON, MS et al. 2004) used dynamic-motion analysis to try to evaluate the pattern of lumbar motion during flexion in patients with degenerative spondylolisthesis or lumbar spine instability and compared the results with those of asymptomatic volunteers. In future work, the automatic method will be extended to videofluroscopy, because the automatic tracking algorithm minimizes the computational effort.

6.8 CONCLUSION

This study demonstrated the accuracy and feasibility of using the active shape method (ASM) and a genetic algorithm (GA) to determine intervertebral movements. The ASM technique is governed by the range of vertebral shapes and appearances contained within the set of images used to train the model. Any vertebrae with a shape similar to those in the training set should be easily located with the ASM. An overall deformable shape was described mathematically by transforming coordinate information concerning its contour into Fourier descriptors and summarizing by principal component analysis. A quantitative evaluation method of a deformable vertebral shape by Fourier descriptors and principal component analysis was established. The genetic algorithm (GA) can provide a reliable method to determine intervertebral movements of the spine. The spinal motion values determined by the automatic method was similar to those determined by manual digitisation of vertebral corners, but the automatic method is easy, simple and fast. The automatic method will reduce errors occurring on the manual identification of landmark and superimposition of images. Measurement errors in the image registration method proved to be significantly smaller than those of the manual method. In conclusion, automatic detection of the image of vertebral contours revealed a new ability to precisely describe the shape of the lumbar vertebrae and measure the intervertebral movements of the lumbar spine from radiographic images.

CHAPTER 7 GENERAL DISCUSSION

7.1 SURFACE MEASUREMENT OF SPINAL KINEMATICS TECHNIQUE

Non-invasive surface distraction methods, either using markers or sensors attached to the skin, are used to measure motions of the lumbar spine. Chapter 3 describes a methodology that employs skin-mounted sensors to predict the rotational and translational motion ranges of a lumbar spine performing flexion and extension, flexion to neutral and neutral to extension movements. Section 3.8.1 described that the mean relative difference between surface method and radiographic method (ranging from 12 to 17 %) of the gross range of motion observed was acceptable. A high linear correlation (R = 0.742 to 0.829) was found between the gross lumbar range of motion derived from the vertebral body images and the electronic output of the Fastrak machine (section 3.8.4). It is possible to measure gross movements of the entire lumbar spine from skin-mounted sensors.

Dvorak and Panjabi (DVORAK, J, PANJABI, MM et al. 1991) reported that spinal disorders have been associated with limited intersegmental mobility. It is thus necessary to clinically determine the intervertebral movements of the lumbar spine related to pathology. Chapter 3 showed that skin-mounted sensors method was not accurate enough to measure intervertebral rotation motions. Prediction results of translational motion range either in segmental level or entire whole spine were not acceptable. Non-invasive surface measurements suffer from errors due to relative movements between the soft tissues (the skin) and vertebrae and the identification of surface landmarks. Section 3.7.4 indicated there was a lot of sliding of Fastrak sensor along the skin surface, but the sliding did not tilt the sensors significantly. Determination of the intervertebral movements of the surface measurement is not reliable.

7.2 NON-INVASIVE METHOD OF MEASURING OF THE INTERVERTEBRAL MOVEMENTS (INDIRECT METHOD)

An alternative surface method (Chapter 4) was developed to determine movements of the intervertebral joints using mathematical prediction (Inverse kinematic). In the first part of study (Chapter 4), an inverse kinematic model was employed to determine an optimal intervertebral joint configuration for a given forward-bending posture of the human spine. In order to determine the inverse kinematics of a redundant kinematic chain, a large number of solutions may be possible and some functions were used to determine the most optimal solution. An optimization equation with physiological constraints was employed to determine the intervertebral joint configuration. The appropriateness, physical meaning and feasibility of those functions were addressed in section 4.7. Such prediction would require knowledge of the total flexion movement of the lumbar spine, the positions of the spinous processes, which could be determined by surface measurements, and anthropometric data provided from previous studies (TENCER, AF and MAYER, TG 1983; PANJABI, MM, GOEL, V et al. 1992; CHAFFIN, DB, ANDERSSON, G et al. 1999). A sensitivity analysis of the inverse kinematic model using predetermined parameters of vertebral geometry was performed. Experimental validation was performed using lateral radiographs of the lumbosacral spines of twenty-two subjects (9 men and 13 women, 40 ± 14 years old). The differences between the measured and predicted values of intervertebral rotations were generally small (less than 1.6°). The Pearson product-moment correlations were found to be high (section 5.6.1) for prediction of intervertebral rotation, but poor for intervertebral translation (section 5.6.2). The inverse kinematic algorithm can be used to reliably predict the intervertebral rotations of the lumbar spine segments but not to predict intervertebral translations. The latter would require the use of radiographic measurements.

7.3 AUTOMATIC MEASUREMENT OF LUMBAR SPINAL KINEMATICS FROM LATERAL RADIOGRAPHS (DIRECT METHOD)

Radiographic measurements of intervertebral motion are prone to large error if not properly done. The accuracy of radiographic measurements may be affected by the clarity of the image, the number and positions of chosen landmarks or markers, the process of tracing and superimposition, radiographic quality, within- and between-observer variance, measurement methods and the magnitude of the measured motion (BROWN, RH, BURSTEIN, AH et al. 1976; PEARCY, MJ and HINDLE, RJ 1989; DVORAK, J, PANJABI, MM et al. 1991; PANJABI, MM, CHANG, D et al. 1992; LEE, RYW and EVANS, J 1997). Manual tracing and superimposition were satisfactory for determination of intervertebral motions, but the process was rather time-consuming.. In order to speed up the process, the pilot studies (Chapter 5) studied the feasibility of two segmentation approaches, Hough

Transform Algorithm and Morphological Watershed Segmentation Algorithm, for extracting vertebrae shape on the radiographic image. However, section 6.7.2 explained that Active Contour has a much higher accuracy than these methods.

The purpose of Chapter 6 was to develop an automatic method to identify the contour of the vertebral body in radiographic films using the Active Shape Model (ASM) and to determine the intervertebral movements from changes in positions of vertebral body positions using a Genetic Algorithm (GA). Fourier descriptors were used to represent the shapes of the vertebral bodies. It was employed for segmentation of vertebral body image, providing a rapid and accurate measurement of vertebral shape using Fourier descriptors. Vertebral images of the flexion and extension films were then superimposed mathematically using the Genetic Algorithm (GA). A Genetic Algorithm was then utilized to determine the intervertebral movements of the lumbar spine. The accuracy and feasibility of an Active Shape Model (ASM) and Genetic Algorithm (GA) for measuring the intervertebral movements of the lumbar spine were presented (section 6.7). Only small mean errors in determining sagittal rotation and postero-anterior and supero-inferior translations (section 6.6.2). The mean differences between manual tracing and the automatic method were less than 1.4 degrees; the mean differences in posterior-anterior displacement and superior-inferior displacement observed between two methods were less than 1.2 mm and 0.8 mm, respectively (section 6.6). The automatic radiographic measurement technique employed in the study was highly accurate in measuring intervertebral movements, as demonstrated by the error analysis.

Correlation coefficients (R values) ranging from 0.994 to 0.997 between flexion and extension images were reported in section 6.6.4. These results indicate that no image distortion and out-of-plane movements occur. The use of active contour in automatic measurement of intervertebral movement was not only accurate but also convenient as the whole process only required 2 to 3 minutes (section 6.6.3) compared to about 20 minutes for the manual digitisation method. The above results show that the technique could be reliably employed to quantify intervertebral translations as well as rotations using flexion-extension radiographs.

7.4 CONTRIBUTIONS TO SCIENTIFIC AND CLINICAL COMMUNITIES

The inverse kinematic model is a significant breakthrough in the prediction of intervertebral movements of the lumbar spine. It makes the determination of intervertebral rotation possible even with the use of skin-mounted sensors only. It has never been applied in the case of the spine before. This is probably because the spine has an unlimited number of degrees of freedom, and finding an optimal solution to the inverse kinematic problem would be extremely difficult. However, this study showed that a solution would be feasible if appropriate constraints could be imposed on the kinematic modeling. For instance, the positions of the most posterior parts of the spinous processes may be determined by surface measurements. Such information may be used to reduce the number of solutions. In addition, an optimisation function may be employed to determine the best solution. The study shed light on the mechanical mechanism employed by the lumbar spine in performing an activity. It clearly shows that the various motion segments do not move in fixed proportions of the gross motions, and each spine moves in a different way so that previous regression technique was unable to predict intervertebral motions satisfactorily. However, according to the inverse kinematic model, the spine moves according to some potential functions so that the motion was most mechanical efficient. The study increases our understanding of why the spine moves in a certain manner. It will be used to examine how the interaction among the intervertebral joints may be altered by mechanical disorders of the spine.

Another potential application of an inverse kinematic model is to biomechanical modeling. Past mathematical models of the lumbar spine (ADAMS, MA, DOLAN, P et al. 1988) made various assumptions about the kinematics of the spine, as described (Section 5.7.1). The present inverse kinematic model could predict the actual intervertebral rotations, and no assumptions have to be made regarding the distribution of movements among the segments. The relationship among the various segments did not have to be assumed to be constant throughout the movement. The accuracy of the biomechanical models can be tremendously improved by using the inverse kinematic method, which is commonly used in robotic engineering. This pioneering work, which uses the robotics approach to solve a significant clinical problem, will have a very strong impact on the scientific community and clinical profession.

Widespread clinical use of radiographic measurement is not likely due to its risk of radiation. Studies have been conducted in this project to investigate and validate the methods to be valid in a wide variety of lumbar measurement tools. Reliability, reproducibility, safety and cost are often cited as improved by two proposed existing measurement methods. According to Cunningham (CUNNINGHAM, BW, GORDON, JD et al. 2003), "...a nonroentgenographic method of measuring postural curves would be an excellent clinical and research tool if the method was inexpensive, expedient, reliable, and valid." The present study (Chapter 5) demonstrates that the inverse kinematic algorithm can be used to reliably predict the intervertebral rotations of the lumbar spine segments. It is suggested that the inverse kinematic technique can be used to predict intervertebral rotation in a clinical situation when it is not desirable to directly measure the movements using radiographs, for instance, in the case of pregnancy.

One advantage of skin-mounted sensors method against radiographic method is to provide dynamic three-dimensional motions. For radiographic measurement, it only measure static range of movement, and in such circumstance, the relationship between two-dimensional assessments of movement and function of the musculoskeletal system is difficult to ascertain. The present study showed that surface measurement was accurate in measuring the three-dimensional gross motion of the spine. This provides dynamic information which is otherwise impossible, and can be very useful for functional assessment of low back pain which often affects the velocities and accelerations of the spine (MARRAS, WS and WONGSAM, PE 1986).

The present study (Chapter 6) developed a reliable automatic measurement method for intervertebral movements of the lumbar spine that can be used routinely in clinical assessment. Since most radiographs are now clinically obtained in digital forms, the present technique would be very convenient and required very little time for analysis. The results (Chapter 6) showed that the accuracy and efficiency of measurement of intervertebral rotations and translations are enhanced by the Active Shape Model (ASM) and Genetic Algorithm (GA) method. Lumbar spine x-ray segmentations have been obtained at a useful level by using this deformable model in an interactive and automatic system for digitized lumbar spine images. In a feasibility study of this work, ASM was found to be effective in the analysis of digitized radiographs of the lumbar spine. The automatic method measured rotation and translations of lumbar vertebrae with sufficient accuracy and precision to detect abnormalities in clinical conditions. It has proved useful in a wide variety of clinical applications.

Based on the results of this study, the following clinical guidelines were developed to help clinicians decide the appropriate method of measurement of spinal motions. Figure 7.1 presents a flowchart that summarises the decision process. The indirect method of inverse kinematics should be chosen for prediction of the intervertebral rotations of the lumbar spine if the risk of radiation is high (e.g. pregnancy) or if very high accuracy is not required. The direct method of radiographic measurement, to be assisted by active contour and the genetic algorithm, should be the method of choice if very high accuracy is required (1 degree of rotation or 1 mm for translation) and if both intervertebral translations and rotations have to be determined.

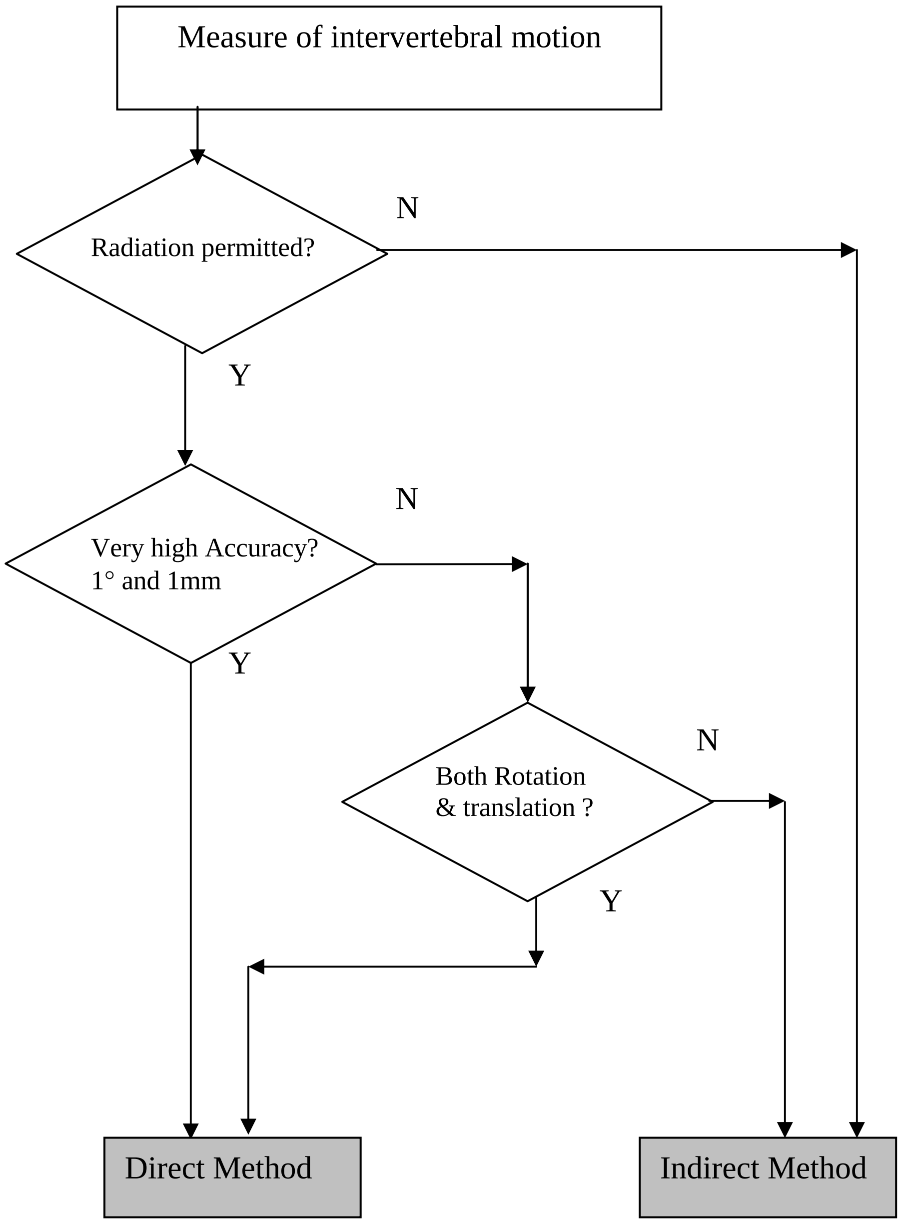

Fig. 7.1 Choice of methods to determine intervertebral movements in clinical practice. Direct Method — X-Ray Measurement and Indirect Method — Inverse Kinematic Method.

7.5 SUGGESTIONS FOR FUTURE STUDIES

The inverse kinematic model developed in this study may be modified to determine intervertebral movements of other regions of the spine. For instance, we can consider the cervical spine. The lordosis and spinous process positions of the cervical spine must be measured clinically so that the kinematic mechanisms of healthy and painful neck conditions can be studied. However, an inverse kinematic model of the cervical spine is likely to be more complex than the present model as it involves seven motion segments and a larger number of degrees of freedom of movements.

In future studies, the inverse kinematic model may be employed for patients with lower back pain, not only normal spines (Chapter 5). This will increase the robustness of the models, and increase our understanding of mechanisms of back pain at the segmental level. The true precision and accuracy of the inverse kinematic method for measuring the intervertebral movements of the lumbar vertebrae should be examined. Ideally, the accuracy may be tested on a phantom containing a rotating and translating lumbar vertebra. In the phantom, the method should have a very high accuracy of 0.1 degrees or 1mm. The method after validation by the phantom will have sufficient accuracy and precision to detect clinically significance differences in patients with or without LBP. Zhang (ZHANG, YM, VOOR, MJ et al. 1998) developed a new intervertebral motion device (IMD). Using the IMD, nine human lumbosacral spine specimens (L3-S1) were test under a simulated physiological load on an MTS (Model 858 Bionix, MTS System Corp.) The root-mean-square error of the IMD was

0.092 mm in axial translation, 0.065 mm in shear translation, and 0.091 degrees in rotation. However, it is very difficult and expensive to build such simulator. It is very difficult to construct a phantom containing a precise and friction-free three-dimensional joint mechanism similar to the intervertebral joint.

The methods developed in the study may also be applied to patients with osteoporosis or other diseases. It will enhance our understanding of the mechanical behaviour of the osteoporotic spine and degeneration of the vertebrae by ageing. It is very essential to develop new clinical methods that could minimise the cost of health care delivery. The kinematic behaviour of the osteoporotic spine should be evaluated by an inverse kinematic model and the performance of measurement should be improved by the automatic method with medical imaging procedures. It would be important to develop a more efficient method that is able to provide kinematic information with acceptable accuracy.

Likewise, the automatic measurement of the vertebrae using ASM and GA may be extended to the patient population. For instance, osteoporotic patients and patients with extensive osteoarthritis may be studied to study how the disease process affects the kinematic mechanisms. The active shape model has been used in the measurement of vertebral shape on lateral DXA scans of the spine for detecting osteoporotic fractures (STOKES, IA, MEDLICOTT, PA et al. 1980). The robustness of ASM for measuring vertebral shape in normal spine DXA scans was analysed. We should conduct further studies on the vertebrae extraction of patients with osteoporotic lumbar spines. Our intention in using of ASM was to automatically extract more shape information both accurately and more rapidly than in the study by

Stokes et al. (STOKES, IA, MEDLICOTT, PA et al. 1980). The automatic methods will be used in clinical applications to detect the morphology of the vertebrae. The feasibility of using Fourier descriptors and principle component for petal shape detection was reported (YOSHIOKA, Y, IWATA, H et al. 2004; YOSHIOKA, Y, IWATA, H et al. 2005). The petal shape variation was evaluated successfully and the symmetrical and asymmetrical elements of the overall shape variation were detected. In future work, a quantitative evaluation method of the vertebrae shape by Fourier descriptors, principle component analysis and the active shape method will be established. If the vertebral morphometry measured by ASM are successfully developed, the method should be able to evaluate the segmental instability of patients' spines.

It is suggested that incorporating heuristic information and local optimization techniques within a GA search can improve the performance of the algorithm significantly. The basic approach is that the GA can locate the optimal area in the search space while the ASM embedded within the GA can determine the local minimum. In future work, a new combination of ASM and GA will be developed. The ASM protocol can be embedded within the GA search directly. Applying a single iteration of the ASM procedure each time the objective function is evaluated requires minimal extra work and leads to significant improvements in the rate of convergence of the GA and the quality of the final fit.

7.6 CONCLUSION

Clinicians and researchers have long been interested in quantifying spinal motions. Several techniques have been previously employed to measure spinal motion with varying degrees of success. X-ray techniques are considered the most accurate clinical method of segmental measurement and kinematic movements, although this method has the problems of radiation dosage and the accuracy and laboriousness of handling data. Various techniques have restrictions that limit their utility in clinical environments. Accuracy, reliability, safety and cost are often the limitations of existing measurement methods. In the literature review, we summarized the existing methods used to determine the intervertebral movements of the lumbar spine. It provided an appraisal of the methods of measurement of the intervertebral movements of the lumbar spine. There is a need to further develop measurement techniques. The thesis presents details of a series of experimental studies that examined the methods to determine intervertebral movements of the lumbar spine. The objective of the first study emphasis on how to measure gross motions as well as intervertebral motions of the spine using skin-mounted electromagnetic sensors. The main achievement was to predict the intervertebral angular movement of the spine by an inverse kinematic algorithm using information derived from skin-mounted sensors. Results of Chapter 3 reported that skin-mounted sensors only can measure gross rotational motions. Results (Chapter 4) suggested that an inverse kinematic model using information derived from skin-mounted sensors measured both gross and intervertebral rotational motions. Non-invasive, precise and reliable objective measuring methods were proposed in Chapters 3 and 4. This study evaluates the performance of a non-invasive range of motion assessment method to predict the rotational and translational movements of the lumbar spine. Moreover, error analysis of the skin-mounted measurement method was presented.

The objective of the second study emphasis on how to measure intervertebral translation motions not only rotational motions of the spine. The method of measurement should be based on a tool or device that is applicable in real working environments as well as laboratory settings. In addition, the method should be allow for quick measurements that will permit screenings of large groups. Techniques proposed to enhance the accuracy and efficient of the measurement. The feasibility of a proposed method of measuring intervertebral movements of the lumbar spine was evaluated by experimental validation.

Therapists should be aware of the accuracy, reliability and safety issues if an appropriate measurement technique is to be chosen and the clinical data is to be interpreted appropriately. A guideline for clinicians in the choice of methods for determining intervertebral movements in routine clinical settings is presented. It is concluded that the inverse kinematic model would be clinically useful when only information about intervertebral rotation is required. However, the automatic method of segmentation and tracing of vertebral images should be employed when knowledge of intervertebral translations is required and when highly accurate measurements are desired. The proposed methods overcome some of problems of existing methods. It is hoped that this thesis has contributed to our body of knowledge by developing valid and accurate methods of spinal motion analysis, which are often required in clinical assessment of back pain. The technique developed will stimulate further researches which will further enhance our understanding how spinal pathologies affects the kinematic mechanisms of the spine.

■ APPENDIX I INVERSE KINEMATICS

A1 MODELING

The lumbar spine will be modelled as a five-link system from the L1 to the L5 vertebra with the L5/S1 joint to be the origin of the kinematic chain. Using the Denavit-Hartenberg convention, the matrix $[T_{k+1,k}]$ comprises a position vector of the end point of the chain, the T12/L1 joint (P_x,P_y), as well as a rotation matrix..

$$\left[T_{S1,L1}\right]=\left[T_{S1,L5}\right]\left[T_{L5,L4}\right]\left[T_{L4,L3}\right]\left[T_{L3,L2}\right]\left[T_{L2,L1}\right]$$

where $[T_{S1,L1}]$ is the homogeneous transform.

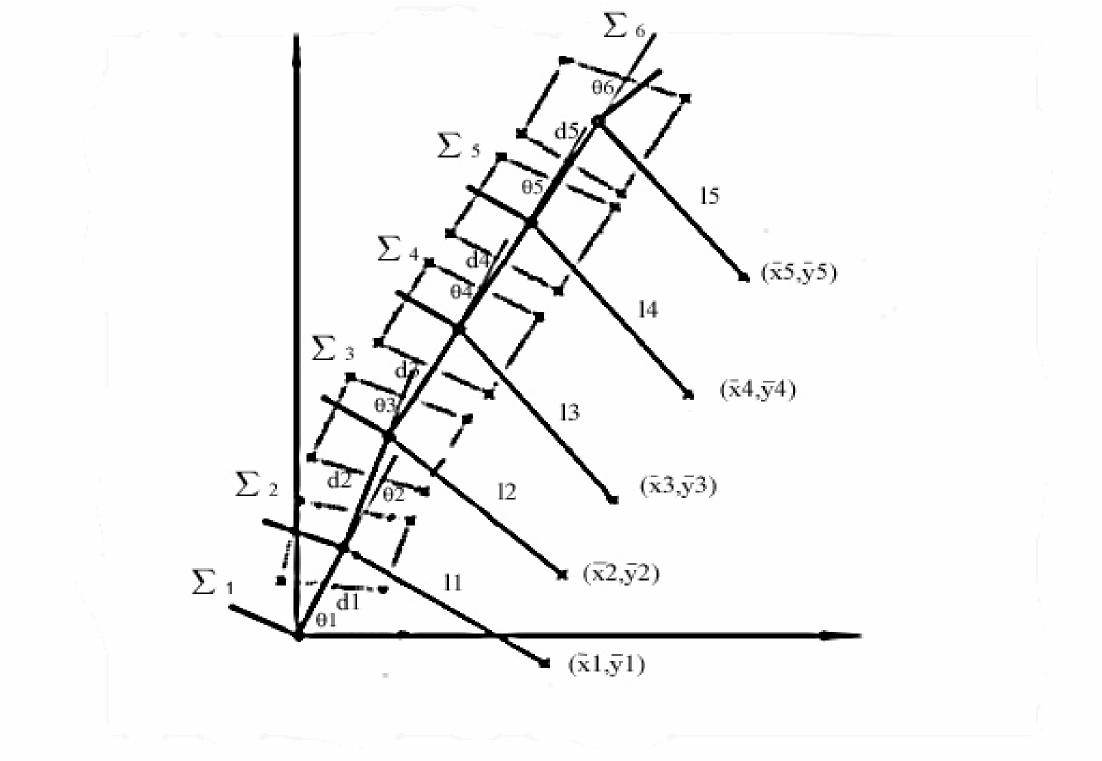

Fig.A A Five-link lumbar spine system

The lumbar spine was modelled as a five-link system from the L1 to the L5 vertebra with the L5/S1 joint to be the origin of the kinematic chain. $(\bar{x}_i, \bar{y}_i)$ is the Cartesian coordinates of the most posterior part of the spinous processes of the vertebra i th. The formula for all the position of $(\bar{x}_i, \bar{y}_i)$ are follow:

$$\bar{x}_5 = d_1 c\theta_1 + d_2 c\theta_{12} + d_3 c\theta_{123} + d_4 c\theta_{1234} + (p_{x56} + d_5) c\theta_{12345} + l_5 c(\theta_{12345} + \alpha_5)$$

$$\bar{y}_5 = d_1 s\theta_1 + d_2 s\theta_{12} + d_3 s\theta_{123} + d_4 s\theta_{1234} + (p_{y56} + d_5) s\theta_{12345} + l_5 s(\theta_{12345} + \alpha_5)$$

$$\bar{x}_4 = d_1 c\theta_1 + d_2 c\theta_{12} + d_3 c\theta_{123} + (p_{x45} + d_4) c\theta_{1234} + l_4 c(\theta_{1234} + \alpha_4)$$

$$\bar{y}_4 = d_1 s\theta_1 + d_2 s\theta_{12} + d_3 s\theta_{123} + (p_{y45} + d_4) s\theta_{1234} + l_4 s(\theta_{1234} + \alpha_4)$$

$$\bar{x}_3 = d_1 c\theta_1 + d_2 c\theta_{12} + (p_{x34} + d_3) c\theta_{123} + l_3 c(\theta_{123} + \alpha_3)$$

$$\bar{y}_3 = d_1 s\theta_1 + d_2 s\theta_{12} + (p_{y34} + d_3) s\theta_{123} + l_3 s(\theta_{123} + \alpha_3)$$

$$\bar{x}_2 = d_1 c\theta_1 + (p_{x23} + d_2) c\theta_{12} + l_2 c(\theta_{12} + \alpha_2)$$

$$\bar{y}_2 = d_1 s\theta_1 + (p_{y23} + d_2) s\theta_{12} + l_2 s(\theta_{12} + \alpha_2)$$

$$\bar{x}_1 = (p_{x12} + d_1) c\theta_1 + l_1 c(\theta_{12} + \alpha_1)$$

$$\bar{y}_2 = (p_{y12} + d_1) s\theta_1 + l_1 s(\theta_{12} + \alpha_1)$$

Differentiating w.r.t states variables

$$\{\theta_1, \theta_2, \theta_3, \theta_4, \theta_5, P_{x12}, P_{y12}, P_{x23}, P_{y23}, P_{x34}, P_{y34}, P_{x45}, P_{y45}, P_{x56}, P_{y56}\}$$

$$\frac{\partial \bar{x}_5}{\partial \theta_1} = -d_1 s\theta_1 - d_2 s\theta_{12} - d_3 s\theta_{123} - d_4 s\theta_{1234} - d_5 s\theta_{12345} - l_5 s(\theta_{12345} + \alpha_5)$$

$$\frac{\partial \bar{x}_5}{\partial \theta_2} = -d_2 s\theta_{12} - d_3 s\theta_{123} - d_4 s\theta_{1234} - d_5 s\theta_{12345} - l_5 s(\theta_{12345} + \alpha_5)$$

$$\frac{\partial \overline{x}_5}{\partial \theta_3} = -d_3 s\theta_{123} - d_4 s\theta_{1234} - d_5 s\theta_{12345} - l_5 s(\theta_{12345} + \alpha_5)$$

$$\frac{\partial \overline{x}_5}{\partial \theta_4} = -d_4 s\theta_{1234} - d_5 s\theta_{12345} - l_5 s(\theta_{12345} + \alpha_5)$$

$$\frac{\partial \overline{x}_5}{\partial \theta_5} = -d_5 s\theta_{12345} - l_5 s(\theta_{12345} + \alpha_5)$$

$$\frac{\partial \overline{x}_5}{\partial P_{X56}} = c\theta_{12345}$$

$$\frac{\partial \overline{x}_5}{\partial P_{X45}} = \frac{\partial \overline{x}_5}{\partial P_{X34}} = \frac{\partial \overline{x}_5}{\partial P_{X23}} = \frac{\partial \overline{x}_5}{\partial P_{X12}} = 0$$

$$\frac{\partial \overline{x}_5}{\partial P_{y56}} = \frac{\partial \overline{x}_5}{\partial P_{y45}} = \frac{\partial \overline{x}_5}{\partial P_{y34}} = \frac{\partial \overline{x}_5}{\partial P_{y23}} = \frac{\partial \overline{x}_5}{\partial P_{y12}} = 0$$

$$\frac{\partial \overline{y}_5}{\partial \theta_1} = d_1 c\theta_1 + d_2 c\theta_{12} + d_3 c\theta_{123} + d_4 c\theta_{1234} + d_5 c\theta_{12345} + l_5 c(\theta_{12345} + \alpha_5)$$

$$\frac{\partial \overline{y}_5}{\partial \theta_2} = d_2 c\theta_{12} + d_3 c\theta_{123} + d_4 c\theta_{1234} + d_5 c\theta_{12345} + l_5 c(\theta_{12345} + \alpha_5)$$

$$\frac{\partial \overline{y}_5}{\partial \theta_3} = d_3 c\theta_{123} + d_4 c\theta_{1234} + d_5 c\theta_{12345} + l_5 c(\theta_{12345} + \alpha_5)$$

$$\frac{\partial \overline{y}_5}{\partial \theta_4} = d_4 c\theta_{1234} + d_5 c\theta_{12345} + l_5 c(\theta_{12345} + \alpha_5)$$

$$\frac{\partial \overline{y}_5}{\partial \theta_5} = d_5 c\theta_{12345} + l_5 c(\theta_{12345} + \alpha_5)$$

$$\frac{\partial \overline{x}_5}{\partial P_{y56}} = s\theta_{12345}$$

$$\frac{\partial \overline{x}_5}{\partial P_{X56}} = \frac{\partial \overline{x}_5}{\partial P_{X45}} = \frac{\partial \overline{x}_5}{\partial P_{X34}} = \frac{\partial \overline{x}_5}{\partial P_{X23}} = \frac{\partial \overline{x}_5}{\partial P_{X12}} = 0$$

$$\frac{\partial \overline{x}_5}{\partial P_{y45}} = \frac{\partial \overline{x}_5}{\partial P_{y34}} = \frac{\partial \overline{x}_5}{\partial P_{y23}} = \frac{\partial \overline{x}_5}{\partial P_{y12}} = 0$$

$$\vdots$$

where $c\theta_i$, $s\theta_i$, $c\alpha_{i-1}$, $s\alpha_{i-1}$, $c\theta_{ii+1}$, $s\theta_{ii+1}$ denote $\cos\theta_i$, $\sin\theta_i$, $\cos\alpha_{i-1}$, $\sin\alpha_{i-1}$, $\cos(\theta_i + \theta_{i+1})$ and $\sin(\theta_i + \theta_{i+1})$ respectively.

A1.1 DERIVATION OF THE JACOBIAN OF AN OPEN CHAIN

The structure equation of an open kinematic chain defined a multi-parameter motion, $[F(\theta)]\langle M \rightarrow F\rangle$, of the end effector (McCarthy 1990). The Transform that defines frame $\{i\}$ relative o the frame $\{i-1\}$ was determined. The 4x4 transformation matrix from link (i-1) to link i was a function of the four link parameters. These link parameters are valid: a_i = the distance from $\hat{Z}_i$ to $\hat{Z}_{i+1}$ measured along $\hat{X}_i; \alpha_i$ = the angle between $\hat{Z}_i$ to $\hat{Z}_{i+1}$ measured about $\hat{X}_i; d_i$ = the distance from $\hat{X}_{i-1}$ to $\hat{X}_i$ measured along $\hat{Z}_i; \theta_i$ = the angle between $\hat{X}_{i-1}$ to $\hat{X}_i$ measured about $\hat{Z}_i$;

The general form of

$$T_i^{i-1} = \begin{bmatrix} c\theta_i & -s\theta_i & 0 & a_{i-1} \\ s\theta_i c\alpha_{i-1} & c\theta_i c\alpha_{i-1} & -s\alpha_{i-1} & -s\alpha_{i-1}d_i \\ s\theta_i s\alpha_{i-1} & c\theta_i s\alpha_{i-1} & c\alpha_{i-1} & c\alpha_{i-1}d_i \\ 0 & 0 & 0 & 1 \end{bmatrix}$$

where $c\theta_i, s\theta_i, c\alpha_{i-1}$, $s\alpha_{i-1}$ denote $\cos\theta_i$, $\sin\theta_i$, $\cos\alpha_{i-1}$ and $\sin\alpha_{i-1}$ respectively.

Denoting this transformed matrix was written in the compact form $\dot{X} = J[\dot{\theta}]$

$$J = \begin{bmatrix} \frac{\partial \overline{x}_5}{\partial \theta_1} & \frac{\partial \overline{x}_5}{\partial \theta_2} & \cdots & \frac{\partial \overline{x}_5}{\partial P_{y12}} \\ \frac{\partial \overline{y}_5}{\partial \theta_1} & \ddots & & \vdots \\ \vdots & & \ddots & \frac{\partial \overline{x}_1}{\partial P_{y12}} \\ \frac{\partial \overline{y}_1}{\partial \theta_1} & \cdots & \frac{\partial \overline{y}_1}{\partial P_{x12}} & \frac{\partial \overline{y}_1}{\partial P_{y12}} \end{bmatrix}$$

. The Jacobian of the manipulator was derivated.

A1.2 FORMULA OF INVERSE KINEMATICS

The discrete form of the general solution provided by inverse kinematics is $\dot{\phi} = J^{+} \cdot \dot{S} + \left(I - J^{+} \cdot J\right)\left(-k \frac{\partial P}{\partial \phi}\right)^{T}$, where $\dot{\phi}$ is the unknown vector in the state variation space, of dimension n. $\dot{S}$ describes as a variation of end effector position in Cartesian space. J is the Jacobian matrix of the linear transformation representing the differential behaviour of the controlled system over the dimensions J^{+} is the unique pseudo-inverse of J providing the minimum norm solution, I is the identity matrix of the joint variation space $(n \times n), \dot{\phi}$ is not an exact solution because it is only a least-square solution. $\left\|\dot{S} - J\dot{\phi}\right\|$ becomes minimum. The solution is not unique because of the arbitrary term $-k \frac{\partial P}{\partial \phi}$, which is the redundancy of the system. When $\left\|\dot{S} - J\dot{\phi}\right\| = 0$, the solution is valid.

The pseudoinverse J^{+} is satisfy the following condition: $\begin{cases} J^{+}JJ^{+} = J^{+} \\ JJ^{+}J = J \\ \left(JJ^{+}\right)^{T} = JJ^{+} \\ \left(J^{+}J\right)^{T} = J^{+}J \end{cases}$

The kinematic problems can be treated linearly with the Jacobian matrix and the inverse kinematics problem can be resolved merely by computing an inverse of the Jacobian matrix. If an initial state is determined, the position and orientation of the end-effector in the Global reference frame can be obtained by optimization.

A1.3 OPTIMIZATION

For optimization problems, the general formulation for using redundancy to try problems.

$$\dot{\phi} = J^{+} \cdot \dot{x} + \left(I - J^{+} \cdot J\right)\left(-k\,\frac{\partial P}{\partial \phi}\right)^{T}$$

In Matlab code, we write the above expression as follows:

<local optimization with potential function>≡

```
function dTh = local_optim(J,K,X,dPhT)
    iJ=pinv(J);
    dTh=iJ*X+(eye-iJ*J)*K*(-dPhT);
endfunction
```

A1.4 MATHEMATICAL EQUATIONS FOR DETERMINATION OF THE INTERVERTEBRAL MOVEMENTS

We summarized the partial work of Lee (LEE, RYW and EVANS, J 1997) and same notations on the study of Takayangi (TAKAYANAGI, K, TAKAHASHI, K et al. 2001) for your reference.

A1.4.1 Treatment of data

Tracing of the vertebral body images was performed on the radiograph under Matlab. The local coordinate system of the motion segment which was used for computing the intervertebral movements is shown in Figure B. The local coordinate system of the L1/2 motion segment is shown for illustration. The origin of the system is located at the anterosuperior corner of the body of the inferior vertebra of the motion segment. The x-axis is directed posteriorly formed by the superior endplate of the inferior vertebra and the y-axis superiorly perpendicular to the x-axis. Position of each vertebra was represented by the four corner points A, B, C and D.

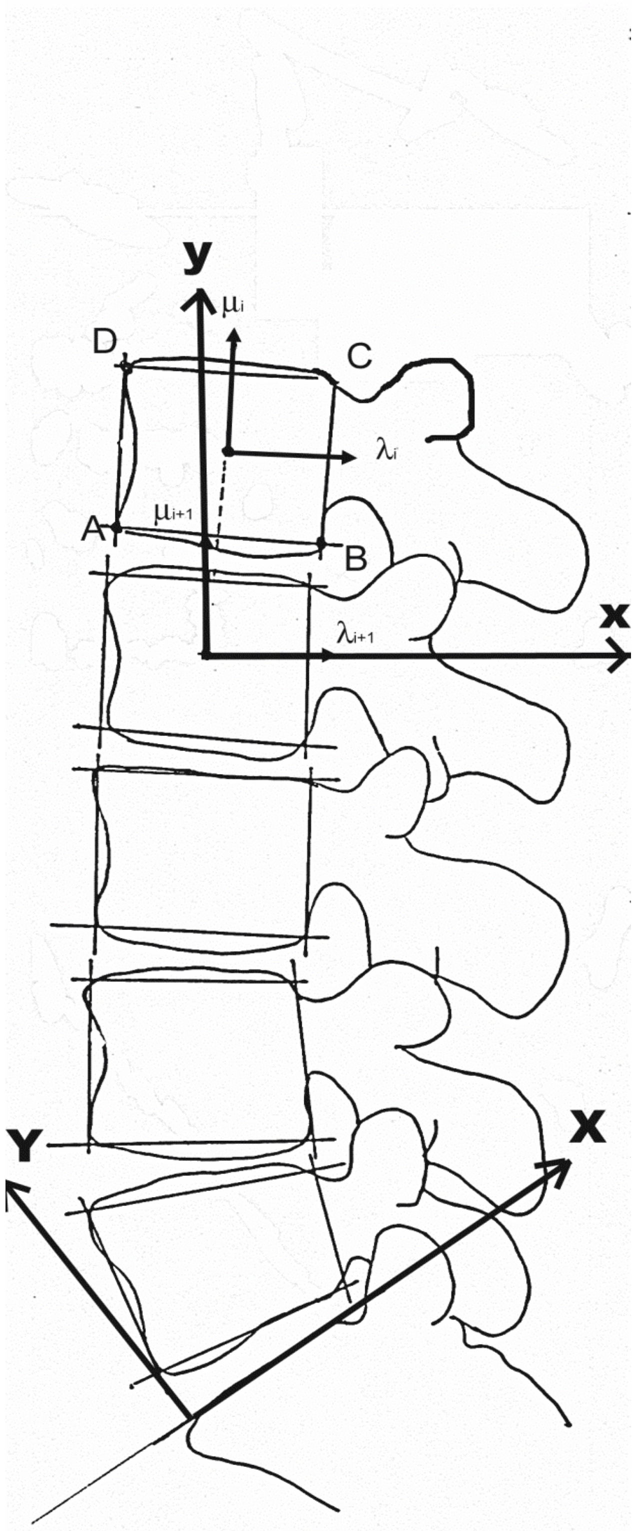

Fig.B Tracing of a typical radiograph.

Determination of vertebral displacement is divided into 3 steps:

The initial displacement between two adjacent vertebrae at initial posture.

(1) Incremental displacement of each vertebra between one posture and the next posture.

(2) Combine initial and incremental displacements to produce the exact vertebral displacement.

(1) Initial displacement at initial Posture

From the global coordinate, the coordinates of each vertebra is determined by 4 corner points (x_{i1},y_{i1}), (x_{i2},y_{i2}),(x_{i3},y_{i3}),(x_{i4},y_{i4}). The positions of the center, the most posterior part of the spinous process of the ith vertebra and the anterosuperior and posterosuperior corners of the sacrum are given by (x_i,y_i), (x_{ie},y_{ie}) , (x_{s1}, y_{s1}) and (x_{s2}, y_{s2}) respectively. The position of center of the vertebra is

$$\left(\overline{x}_i, \overline{y}_i\right)$$

$$\overline{x}_i = \frac{1}{4}\left(x_{i1} + x_{i2} + x_{i3} + x_{i4}\right)$$
$$\overline{y}_i = \frac{1}{4}\left(y_{i1} + y_{i2} + y_{i3} + y_{i4}\right)$$

Define that the displacement of the (i+1)-th vertebrae to i-th vertebrae,

$$d_i = \left(\overline{x}_i - \overline{x}_{i+1}, \overline{y}_i - \overline{y}_{i+1}\right)$$

There are unit vector parallel to anteriorposterior (a-p) direction of the ith vertebra λi and unit vector normal to anteriorposterior (a-p) direction of the ith vertebra μ_i .

$$x_{ia} = \frac{1}{2}\left(x_{i2} + x_{i3}\right), x_{ip} = \frac{1}{2}\left(x_{i1} + x_{i4}\right)$$
$$y_{ia} = \frac{1}{2}\left(y_{i2} + y_{i3}\right), y_{ip} = \frac{1}{2}\left(y_{i1} + y_{i4}\right)$$

The unit vectors λ_i and μ_i are given by the following:

$$\Delta x_{ipa} = x_{ia} - x_{ip}, \Delta y_{ipa} = y_{ia} - y_{ip}$$
$$d_{ipa} = \left(\Delta x_{ipa}^2 + \Delta y_{ipa}^2\right)^{\frac{1}{2}}$$

$$\lambda_i = \left(\frac{\Delta x_{ipa}}{d_{ipa}}, \frac{\Delta y_{ipa}}{d_{ipa}}\right), \mu_{i=} \left(-\frac{\Delta y_{ipa}}{d_{ipa}}, \frac{\Delta x_{ipa}}{d_{ipa}}\right)$$

Sagittal rotation of the two adjacent vertebrae was determined by relative θ_i

$$\cos\theta_i = \lambda_{i+1} \bullet \lambda_i$$

The x (posteroanterior) and y (superoinferior) translations at the centre of the ith vertebra were calculated with respect to the local coordinate system attached on the i-1th vertebra , as shown in Fig.B.

$$d_{i,t} = d_i \bullet \lambda_{i+1}, d_{i,n} = d_i \bullet \mu_{i+1}$$

(2) Incremental displacement between flexion and the extension posture

To know the change of relative position of ith vertebra to i+1th vertebra when the motion proceeded from flexion posture to the extension posture, positions of the two (ith and i+1th) vertebrae at the flexion posture are gotten supposing their rigid body motion so the (i+1)th vertebrae at extension fully coincides to (i+1)th vertebra of the flexion as shown in Fig. C. The incremental displacement can be resolved into two translations.

$$\Delta d_{i,t}^{f} = \Delta d_{i}^{f} \bullet \lambda_{i+1}^{n}, \Delta d_{i,t}^{f} = \Delta d_{i}^{f} \bullet \mu_{i+1}^{n}$$

The incremental sagittal angle is determined by $\Delta\theta_i^f$

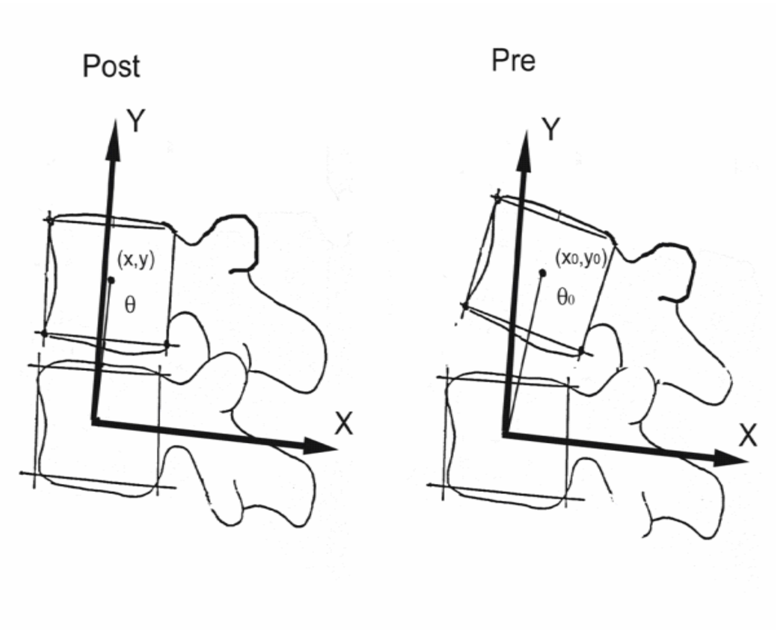

Fig.C Calculation of incremental displacement and relation angle between flexion and extension posture

After superimposed, a new coordinates were generated. Then the transformation between flexion and extension was determined. Afterward, the incremental rotation angle is found and the total displacement of each vertebra was calculated.

$$\begin{pmatrix} x' \\ y' \end{pmatrix} = \begin{pmatrix} \cos\Delta\theta_i^f & -\sin\Delta\theta_i^f \\ \sin\Delta\theta_i^f & \cos\Delta\theta_i^f \end{pmatrix} \bullet \begin{pmatrix} x \\ y \end{pmatrix}$$

$$x = \begin{pmatrix} x_1 & x_2 & x_3 & x_4 \end{pmatrix}, y = \begin{pmatrix} y_1 & y_2 & y_3 & y_4 \end{pmatrix}$$

$$x \bullet x' = \cos\Delta\theta_i^f x^2 - \sin\Delta\theta_i^f x \bullet y$$
$$y \bullet y' = \sin\Delta\theta_i^f x \bullet y + \cos\Delta\theta_i^f y^2$$

$$\cos\Delta\theta_i^f = \frac{(x \bullet x' + y \bullet y')}{x^2 + y^2}$$
$$\sin\Delta\theta_i^f = \frac{(x \bullet y' - x' \bullet y)}{x^2 + y^2}$$

$$d_{i,t}^f = d_{i,t} + \Delta d_{i,t}^f, d_{i,n}^f = d_{i,n} + \Delta d_{i,n}^f$$

A1.5 EULER ANGLE

Euler angle represents by α, β, γ. They are sequence dependent. c and s denote as cosine and sine function respectively.

$$R_{ZYX}(\alpha \quad \beta \quad \theta) = \begin{pmatrix} c\alpha c\beta & c\alpha s\beta s\gamma - s\alpha c\gamma & c\alpha s\beta c\gamma + s\alpha s\gamma \\ s\alpha c\beta & c\alpha c\gamma - s\alpha s\beta s\gamma & s\alpha s\beta c\gamma - c\gamma s\beta \\ -s\beta & c\beta c\gamma & c\beta c\gamma \end{pmatrix}$$

■ APPENDIX II KINEMATIC CHARACTERISTIC OF THE LUMBAR SPINE

A2 OBJECTIVES

This part summarizes the basic characteristics of the various structures of the lumbar spine and the interaction of these structures during normal spine function. It provides an understanding of some fundamental aspects of lumbar spine biomechanics.

A2.1 Flexion and Extension

Both disc height and the horizontal length of the vertebral end plate affect the range of motion attainable during sagittal plane movement of the lumbar spine. The first 50 to 60° of spine flexion occur in the lumbar spine, mainly in the lower motion segments (FARFAN, HF 1975). Tilting the pelvis forward allows further flexion. The thoracic spine contributes little to flexion of the total spine because of the oblique orientation of the facets and the limitation of motion imposed by the rib cage. The facets of the thoracic spine are oriented at a 60° angle to the transverse plane and at a 20° angle to the frontal plane. The abdominal muscles and the vertebral portion of the psoas muscle initiate flexion. The weight of the upper body produces further flexion, which is controlled by the gradually increasing activity of the erector spinae muscles as the forward-bending moment acting on the spine increases. The posterior hip muscles are active in controlling the forward tilting of the pelvis as the spine is flexed. In full flexion the erector spinae muscles become inactive and are fully stretched; in this position the forward bending moment may be counteracted passively by these muscles and also by the posterior ligaments, which are initially slack but become taut at this point because the spine has fully elongated (FARFAN, HF 1975). From full flexion to upright positioning of the trunk, a reverse sequence is observed. The pelvis tilts backward and the spine then extends. When the trunk is extended from the upright position, the extensor muscles are active during the initial phase. This initial burst of activity decreases during further extension, and the abdominal muscles become active to control and modify the motion. In extreme or forced extension, extensor activity is again required.

A2.2 Lateral Bending

When the lumbar spine is laterally flexed, the annular fibers toward the concavity of the curve are compressed and begin to bulge, while those on the convexity of the curve are stretched. The contralateral fibers of the outer annulus and the contralateral intertransverse ligaments help to resist extremes of motion (BOGDUK, N and TWOMEY, LT 1991). Lateral flexion and rotation occurs as coupled movements (NORRIS, CM 1998). In the neutral position, rotation of the upper four lumbar segments is accompanied by lateral flexion to the opposite side; rotation of the L5-S1 joint, however, occurs with lateral flexion to the same side. The nature of the coupling varies with the degree of flexion and extension. In the neutral position, rotation and lateral bending occur to the opposite side, called Type I movement (i.e., right rotation is coupled with left lateral bending). But when the lumbar spine is in flexion or extension, rotation and lateral flexion occur in the same direction, called Type II Movement (i.e., right rotation is coupled with right lateral flexion). In the concavity of lateral flexion, the inferior facet of the upper vertebra slides downward on the superior facet of the vertebrae below, reducing the area of the intervertebral foramen on that side. On the convexity of the laterally flexed spine, the inferior facet slides upwards on the superior facet of the vertebra below, increasing the diameter of the intervertebral foramen.

A2.3 Rotation

During rotation, torsional stiffness is provided by the outer layers of the annulus, by the orientation of the facet joints, and by the cortical bone shell of the vertebral bodies themselves. Moreover, the annular fibers of the disc are stretched as their orientation permits- since alternating layers of fibers are angled obliquely to each other, some fibers will be stretched while other relax. A maximum range of 3° of rotation can occur before the annular fibers will be microscopically damaged and a maximum of 12° before tissue failure (BOGDUK, N and TWOMEY, LT 1991). The spinous processes separate during rotation, stretching the supraspinous and interspinous ligaments. Impaction occurs between the opposing articular facets on one side, causing the articular cartilage to compress by 0.5mm for each 1° of rotation and providing a substantial buffer mechanism (BOGDUK, N and TWOMEY, LT 1991). If rotation continues beyond this point, the vertebra pivots around the impacted facet joint, causing posterior and lateral movement. The combination of movements and forces stress the impacted facet joint by the opposite facet joint by traction. The disc provides only 35 % of the total resistance (FARFAN, HF 1975).

■ APPENDIX III REFERENCE FORMS

A.3 Subject Information Sheet and Consent Form

DETERMINATION OF THE INTERVERTEBRAL MOVEMENTS OF THE LUMBAR SPINE

Subject Information Sheet

You are invited to take part in a research project that examines the intervertebral movements of the lumbar spine during forward bending motion. The study will enhance our understanding of the intervertebral motions of each individual joint of the lumbar spine and the segmental kinematics of the spine. The lead researcher of this study is Dr Raymond Lee, Associate Professor, The Hong Kong Polytechnic University. The co-investigators are Mr LW Sun, PhD student, The Hong Kong Polytechnic University, Dr William Lu, Associate Professor, and Professor K Luk, Department of Orthopedics and Traumatology of the University of Hong Kong. This study is the collaborative work of the Department of Rehabilitation Sciences of the Hong Kong Polytechnic University and the Department of Orthopaedics and Traumatology of the University of Hong Kong.

You should have no any signs of fracture or dislocation, spinal instability or any structural disorders of the lumbar spine. You have no any history surgical operations or serious injuries of the spine. You should not have any radiological examination in the past 12 months. You should notify your doctor if you do so. If you agree to participate in this study, you will be requested to answer a few questions. This is to ascertain that you are not currently suffering from any disorders that will exclude you from the study.

You do not receive any additional radiation because of participation in this research. We understand that you have been requested by your doctor to undergo radiological examination because of low back pain. This study involves obtaining data from radiograph taken during this examination on the orthopaedic clinic of Duchess of Kent. You were diagnosed with non-specific LBP with no pathologies. Sensors will be attached to the skin of your back. Lateral x-ray films of the lumosacral spine will be taken in the upright standing, flexion and extension position. Radiographs will be used by your doctor for clinical assessment. Our research team will also use the radiograph to measure intervertebral movements. In order to assess the duality of radiographic data, a motion tracking system will be used to measure of the movements of your back. You will be requested to expose your back, to which 6 sensors will be attached (L1 to S1) using double-sided adhesive tape. You will perform forward and backward bending. Each movement will be performed over a 10-second period and will be repeated three times. A minute warm-up exercise will do in all of the six different directions - forward, backward, side bending, axial rotation to the left and right before data collection.

The experimental procedure should not produce any pain or discomfort. There should be no increase in your back pain or any related symptoms. The radiological examination involves a small amount of radiation, but there have been no scientific data that suggest that there is any risk (e.g. cancer) at such low doses. You should not have radiological examination more in the coming 12 months.

There is also no known risk associated with the electromagnetic technology employed in the motion tracking procedure. Participation in this study is entirely voluntary. You are not obliged to participate, and if you do participate, you can withdraw at any time without penalty or prejudice.

All aspects of the study including the results will be strictly confidential and only the researchers named above will have access to information on participants. You will have the right to request access to your own personal data. A report of the study may be submitted for publication in international journals, but individual participants will not be identified in such a report.

The procedure will be explained clearly to you. If you have any questions or concerns at any stage in the study, please feel free to contact Dr Raymond Lee at 27664889. Complains related to the project should be directed to Mrs Michelle Leung, Secretary of the Departmental Research Committee, Department of Rehabilitation Sciences, The Hong Kong Polytechnic University, Yuk Choi Road, Hunghom, Hong Kong (Telephone: 27665397).

You can keep this information sheet. Thank you for your participation.

測量人體脊椎個別關節的椎間活動

研究內容資料

現誠意邀請你參與一項研究人體進行曲肢前傾及伸展活動時，測量腰部脊椎個別關節的椎間的活動。此項研究的目的是提高了解脊椎骨個別關節的椎間活動與脊椎體節的動力學。是項研究由香港理工大學康復治療科學系副教授李潤華博士、研究生辛來華先生、香港大學矯形外科及創傷學系副教授 Dr. William Lu、教授 Prof. K Luk 負責。此項研究是由香港理工大學康復治療科學系和香港大學矯形外科及創傷學系共同合作。

你應沒有骨折、位置、脊椎結構不正常等之徵狀，同時從未曾有嚴重脊骨受損和/或進行外科手術。你在過去六個月內沒有進行 X 光檢查。如有發生，請向你的醫生報告。如果你同意參與此項研究，你將會被問及一些問題,證明你並沒有下肢毛病或其他身體毛病所影響，以致你不能參與這項研研研究。

你將不會因參加本項研究而要求額外的放射檢查。我們知道你因下肢背痛被醫生要求作 X 光檢查，你被診斷爲沒有下肢背痛病狀。是次研究將收集你在根德公爵夫人骨科門診的診所內所拍攝的 X 光片。我們會將鋁的小片用雙面膠紙貼在腰部脊椎上（五節腰椎及尾龍骨）。 同時會爲你立正、向前伸展和向後彎的姿勢拍背部的 X 光片。X 光片將會作爲醫生的檢查及本研究之用。我們會採用運動軌跡追蹤系統來量度有關你背部的運動資料。在研究過程中，我們

會將六個感應器於於你的腰背上，然後會要求你做曲肢前傾及伸展的動作。每一個動作須維持進行十秒鐘、並重複三次。整個數據收集前，會要求你做三種動作，包括：1. 向前伸展和向後彎、2.向左右兩邊彎曲身體，和 3.向左右兩邊搖擺身體。

此項研究，並不會有任何危險及副作用。也不會感到痛楚或不舒服。是次研究中，你所接受的放射檢查，只含少量放射劑量。現時並沒有科學研究顯示，接受該等份量的放射會構成任何危險(例如癌症)。另外，運動軌跡追蹤系統所用的電微波運動科技也不會構成任何危險。

參與此項研究完全屬於自願性質，你沒有義務參與，即使已答應參與，你仍可隨時拒絕參與而不會受到任何懲罰和歧視。所有有關今次研究的資料，包括結果將會絕對保密，只有是次研究的研究員才可取得參與者的資料。你亦有權要求取得你的個人資料。此項研究報告可能會刊登在一些國際性論文報告作中，但參與者的名字不會被公開。

我們會向你解釋清楚每個步驟，如果你在任何時間有任何問題或諮詢，請聯絡李潤華博士，電話號碼是 27664889。如有任何投訴，請與康復學系研究委員會秘書梁有愛女士聯絡，電話號碼是 27665397，地址是九龍紅磡香港理工大學，康復學系研究委員會。此份資料是給予你作參考之用的。多謝你的參與。

測量人體脊椎個別關節的椎間活動

<u>同意書</u>

本人__________________以自願性質同意參與此項由香港理工大學康復治療學系副教授李潤華博士、研究生辛來華先生、香港大學矯形外科及創傷學系副教授Dr. William Lu、教授Prof. K Luk負責的研究。我明白所有有關此項研究的資料和結果是絕對保密的。如果他們把這個研究結果刊登在學術論文刊物上，我的個人私隱會被保留，即我個人資料將不會被公開。

所有列明在資料紙上的每個步驟已經被詳細解釋，我已明白此研究所帶來的得益及有可能產先的不良反應。我的參與是完全屬於自願性質的。

本人知道我有權提出問題或諮詢有關的步驟，我也有權隨時拒絕參與此項研究而不會受到任何懲罰或歧視。

本人已很了解所有步驟。

參與者姓名:________________________
地址:____
參與者簽名:________________________
研究者簽名:________________________
見證人姓名:________________________
見證人簽名:________________________
日期: ______________________________

DETERMINATION OF THE INTERVERTEBRAL MOVEMENTS

OF THE LUMBAR SPINE

Consent Form

I, ________________________________, voluntarily consent to participate in the above-mentioned research conducted by Dr Raymond Lee, Mr LW Sun, Dr William Lu, and Professor K Luk.

I understand that the information and results obtained from this research study are strictly confidential, and that if they are submitted for publication, my right to privacy will be retained, that is, my personal details will not be revealed.

The procedure as set out in the attached information sheet has been fully explained to me and I understand what is expected of me as well as any benefits and risks involved. My participation in the project is entirely voluntary.

I acknowledge I have the right to question or query any part of the procedure and can withdraw at any time without penalty or prejudice.

I have been familiarized with the procedure.

Name of Participant: ____
Of (Address: ____
Signature of Participant: ____
Signed (Researcher): ____
Name of Witness: ____
Signature of Witness: ____
Date: ____

■ REFERENCES

ADAMS MA, DOLAN P and HUTTON WC (1988) The lumbar spine in backward bending. Spine **13**: 1019-26.

AGUADO AS, NIXON MS and MONTIEL ME (1998) Parameterizing arbitrary shapes via Fourier Descriptors for Evidence-gathering Extraction. Comput Vis Image Understanding **69**: 202-21.

ALLARD P, STOKES IAF and BLANCHI J-P (1995) Three-dimensional analysis of human movement. Champaign, IL, Human Kinetics.

ALLBROOK D (1957) Movements of the lumbar spinal column. J Bone Joint Surg Br **39-B**(2): 339-45.

AMEVO B, WORTH D and BOGDUK N (1991) Instantaneous axes of rotation of the typical cervical motion segments. Clinical Biomechanics **6**: 111-7.

ANDERSON JA and SWEETMAN BJ (1975) A combined flexi-rule/hydrogoniometer for measurement of lumbar spine and its sagittal movement. Rheumatol Rehabil **14**(3): 173-9.

ANDERSSON GBJ (1991) The epidemiology of spinal disorders. In The Adult Spine: Principles and Practice. New York, Raven Press, Ltd.

BELL GD (1990) Skeletal application of videofluoroscopy. J Manip. and Physiol Ther **13**: 396-405.

BIFULCO P, CESARELLI M, ALLEN R and BRACALE M (1995) Automatic extraction of kinematic parameters from video-fluroroscopic sequence of the spine. Proceeding of Health Telematics, Naples, Italy: 147-8.

BLAKE A and ISARD M (1998) Active contours: the application of techniques from graphics, vision, control theory and statistics to visual tracking of shapes in motion. London; Hong Kong, Springer.

BOGDUK N and TWOMEY LT (1991) Clinical Anatomy of the lumbar spine. Churchhill Livingstone, 2nd ed. Edinburgh.

BOONE DC and AZEN SP (1979) Normal range of motion of joints in male subjects. J Bone Joint Surg Am **61**: 756-9.

BRYANT JT, REID JG, SMITH BL and STEVENSON JM (1989) Method for determining vertebral body positions in the sagittal plane using skin markers. Spine **14**(3): 258-65.

BURNETT AF, BARRETT CJ, MARSHALL RN, ELLIOTT BC and DAY RE (1998) Three-dimensional measurement of lumbar spine kinematics for fast bowlers in cricket. Clin Biomech (Bristol, Avon) **13**(8): 574-83.

CHAFFIN DB, ANDERSSON G and MARTIN BJ (1999) Occupational biomechanics. New York, Wiley.

CHAU CC (2001) Efficient generalized hough transform algorithms for modern applications. PhD thesis.The Hong Kong Polytechnic University,Hong Kong.

CHEN K, GIBLIN P and IRVING A (1999) Mathematical explorations with Matlab. New York. Cambridge University Press.

CHEN YL and LEE YH (1997) A non-invasive protocol for the determination of lumbosacral vertebral angle. Clin Biomech (Bristol, Avon) **12**(3): 185-89.

COOPER R, CARDAN C and ALLEN R (2001) Computer visualisation of the moving human lumbar spine. Comput Biol Med **31**(6): 451-69.

COOTES TF, HILL A, TAYLOR CJ and J. H (1994) The use of active shape models for locating structures in medical images. Image Vision Computing **12**(6): 355-366.

CRAIG JJ (1989) Introduction to robotics: mechanics and control. Reading, Mass., Addison-Wesley.

CUNNINGHAM BW, GORDON JD, DMITRIEV AE, HU N and MCAFEE PC (2003) Biomechanical evaluation of total disc replacement arthroplasty: an in vitro human cadaveric model. Spine **28**(20): S110-7.

DEYO RA and BASS JE (1989) Lifestyle and low-back pain: The influence of smoking and obesity. Spine **14**(5): 501-6.

DIMNET J (1980) The improvement in the results of kinematics of in vivo joints. J Biomech **13**: 653-61.

DOUGHERTY ER (1992) An Introduction to Morphological Image Processing. SPIE, Optical Engineering Press.

DVORAK J, PANJABI MM, CHANG DG, THEILER R and GROB D (1991) Functional radiographic diagnosis of the lumbar spine. Flexion-extension and lateral bending. Spine **16**(5): 562-71.

DVORAK J, PANJABI MM, NOVOTNY JE, CHANG DG and GROB D (1991) Clinical validation of functional flexion-extension roentgenograms of the lumbar spine. Spine **16**(8): 943-50.

ECABERT O and THIRAN JP (2004) Adaptive Hough Transform for the Detection of Natural Shape under Weak Affine Transformations. Pattern Recognition **25**: 1411-9.

FARFAN HF (1975) Muscular mechanism of the lumbar spine and the position of power and efficiency. Orthop. Clin. North Am **6**: 135-43.

FIELDING JW (1957) Cineroentogenography of the normal cervical spine. J Bone Joint Surg Br **39A**: 1280-8.

FROBIN W, BRINCKMANN P, BIGGEMANN M, TILLOTSON M and BURTON K (1997) Precision measurement of disc height, vertebral height and sagittal plane displacement from lateral radiographic views of the lumbar spine. Clin Biomech (Bristol, Avon) **12 Suppl 1**: S1-S63.

FROBIN W, BRINCKMANN P, LEIVSETH G, BIGGEMANN M and REIKERAS O (1996) Precision measurement of segmental motion from flexion-extension radiographs of the lumbar spine. Clin Biomech (Bristol, Avon) **11**(8): 457-65.

FRYMOYER JW (1988) Back pain and sciatica. N Engl J Med **318**: 291-300.

FUJIE H, MABUCHI K, WOO SL, LIVESAY GA, ARAI S and TSUKAMOTO Y (1993) The use of robotics technology to study human joint kinematics: a new methodology. J Biomech Eng **115**(3): 211-7.

GATTON ML and PEARCY MJ (1999) Kinematics and movement sequencing during flexion of the lumbar spine. Clin Biomech (Bristol, Avon) **14**(6): 376-83.

GILAD I and NISSAN M (1985) Sagittal evaluation of elemental geometrical dimensions of human vertebrae. J Anat **143**: 115-20.

GOLUB GH and VAN LOAN CF (1996) Matrix computations. Baltimore, Md., Johns Hopkins University Press.

HARADA M, ABUMI K, ITO M and KANEDA K (2000) Cineradiographic Motion Analysis of Normal Lumbar Spine During Forward and Backward Flexion. Spine **25**(15): 1932-7.

HARREBY MS, NYGAARD B, JESSEN TT, LARSEN E, STORR-PAULSEN A, LINDAHL A, FISKER I and LAEGAARD E (2001) [Risk factors for low back pain among 1.389 pupils in the 8th and 9th grade. An epidemiologic study]. Ugeskr Laeger **163**(3): 282-6.

HARVEY SB and HUKINS DWL (1997) Measurement of lumbar spinal flexion-extension kinematics from lateral radiographs. Journal of Back and Musculoskeletal Rehabilitation **9**: 43-6.

HARVEY SB and HUKINS DWL (1998) Measurement of lumbar spinal flexion-extension kinematics from lateral radiographs: simulation of the effects of out-of-plane movement and errors in reference point placement. Medical Engineering & Physics **20**(6): 403-9.

HILL A, COOTES TF, TAYLOR CJ and LINDLEY K (1994) Medical image interpretation: a generic approach using deformable templates. Med Inform (Lond) **19**(1): 47-59.

HOUGH PVC (1962) A Method and Means for Recognizing Complex Patterns. U.S. Patent 3069654.

ITO M, TADANO S and KANEDA K (1993) A biomechanical definition of spinal segmental instability taking personal and disc level differences into account. Spine **18**(15): 2295-304.

JOSEPHSON M, HAGBERG M and HJELM EW (1996) Self-reported physical exertion in geriatric care. A risk indicator for low back symptoms? Spine **21**(23): 2781-5.

JUNG ES, CHOE J and KIM SH (1994) Psychophysical cost function of joint movement for arm reach posture prediction. Proc 38th Annual Meeting Human Proc 38th Annual Meeting Human Factors and Ergonomics Society **1**: 636-640.

KAIGLE AM, POPE MH, FLEMING BC and HANSSON T (1992) A method for the intravital measurement of interspinous kinematics. J Biomech **25**(4): 451-6.

KANAYAMA M, ABUMI K, KANEDA K, TADANO S and UKAI T (1996) Phase lag of the intersegmental motion in flexion-extension of the lumbar and lumbosacral spine. An in vivo study. Spine **21**(12): 1416-22.

KARDUNA AR, MCCLURE PW, MICHENER LA and SENNETT B (2001) Dynamic measurements of three-dimensional scapular kinematics: a validation study. J Biomech Eng **123**(2): 184-90.

KIMME C, BALLARD D and SKLANSKY J (1975) Use of the Hough Transform to Detect Lines and Curvers in Pictures. Commun. ACM **15**(1): 120-2.

KO WH (1986) Solid-state physical transducers for biomechical research. IEEE Trans Biomed Eng **33**: 153-62.

LAHAD A, MALTER AD and BERG AO (1994) The effectiveness of four interventions for the prevention of low back pain. Journal of the American Medical Association **272** (16): 1286-91.

LAU EMC, EGGER P, COGGON D, COOPER C, VALENTI L and O'CONNELL D (1995) Low back pain in Hong Kong: prevalence and characteristics compared with Britain. Journal of Epidemiology and Community Health **49**: 492-4.

LEAVERS VF (1992) Shape detection in computer vision using the Hough transform. London; Hong Kong, Springer-Verlag.

LEAVERS VF (1993) Which Hough transform? CVGIP: Image Understanding **58**: 250-64.

LEE RY, LAPRADE J and FUNG EH (2003) A real-time gyroscopic system for three-dimensional measurement of lumbar spine motion. Med Eng Phys **25**(10): 817-24.

LEE RYW (1990) Biomechanics of spinal posteroanterior mobilisation. MPhil thesis.The Hong Kong Polytechnic University,Hong Kong.

LEE RYW (1995) The biomechanical basis of spinal manual therapy. PhD thesis.University of Strathclyde,Glasgow, UK.

LEE RYW (2001) Kinematics of rotational mobilisation of the lumbar spine. Clin Biomech (Bristol, Avon) **16**(6): 481-8.

LEE RYW and EVANS J (1997) An in vivo study of the intervertebral movements produced by posteroanterior mobilization. Clin Biomech (Bristol, Avon) **12**(6): 400-8.

LEE RYW and MUNN J (2000) Passive moment about the hip in straight leg raising. Clin Biomech (Bristol, Avon) **15**(5): 330-4.

LEE RYW and WONG TKT (2002) Relationship between the movements of the lumbar spine and hip. Human Movement Science(21): 481-494.

LEE YH, CHIOU WK, CHEN WJ, LEE MY and LIN YM (1995) Predictive model of intersegmental mobility of lumbar spine in the sagittal plane from skin markers. Clin Biomech (Bristol, Avon) **10**(8): 413-20.

LETTS M, QUANBURY A, GOUW G, KOLSUN W and LETTS E (1988) Computerized ultrasonic digitization in the measurement of spinal curvature. Spine **13**(10): 1106-10.

LOEBL WY (1967) Measurement of spinal posture and range of spinal movement. Annals of Physical Medicine **9**: 103-10.

LUINGE HJ, VELTINK PH and BATEN CTM (1999) Estimating orientation with gyroscopes and accelerometers. Technology and Health Care **7**: 455-9.

MACRAE IF and WRIGHT V (1969) Measurement of back movement. Annuals of the Rheumatic Diseases **28**: 584-9.

MARENA C, GERVINO D, PISTORIO A, AZZARETTI S, CHIESA P, LODOLA L and MARRACCINI P (1997) [Epidemiologic study on the prevalence of low back pain in health personnel exposed to manual handling tasks]. G Ital Med Lav Ergon **19**(3): 89-95.

MARRAS WS and WONGSAM PE (1986) Flexibility and velocity of the normal and impaired lumbar spine. Arch Phys Med Rehabil **67**: 213-7.

MCCARTHY JM (1990) An introduction to theoretical kinematics. Cambridge, Mass., MIT Press.

MCGILL S (2002) Low Back Disorders: Evidence-based prevention & Rehabilitation, McGill. Human Kinetics.

MCGILL SM and KIPPERS V (1994) Transfer of loads between lumbar tissues during the flexion-relaxation phenomenon. Spine **19**(19): 2190-6.

MCGILL SM and NORMAN RW (1986) Partitioning of the L4-L5 dynamic moment into disc, ligamentous, and muscular components during lifting. Spine **11**(7): 666-78.

MINNE HW, LEIDIG G, WUSTER C, SIROMACHKOSTOV L, BALDAUF G, BICKEL R, SAUER P, LOJEN M and ZIEGLER R (1988) A newly developed spine deformity index (SDI) to quantitate vertebral crush fractures in patients with osteoporosis. Bone Miner **3**(4): 335-49.

MUGGLETON JM and ALLEN R (1997) Automatic location of vertebrae in digitized videofluoroscopic images of the lumbar spine. Med Eng Phys **19**(1): 77-89.

NELSON JM, WALMSLEY RP and STEVENSON JM (1995) Relative lumbar and pelvic motion during loaded spinal flexion/extension. Spine **20**(2): 199-204.

NG JK, KIPPERS V, RICHARDSON CA and PARNIANPOUR M (2001) Range of motion and lordosis of the lumbar spine: reliability of measurement and normative values. Spine **26**(1): 53-60.

NORRIS CM (1998) Sports Injuries. Diagonsis and management. Butterworth Heinemann, 2nd Ed. Oxford.

OGSTON NG, KING GJ, GERTZBEIN SD, TILE M, KAPASOURI A and RUBENSTEIN JD (1986) Centrode patterns in the lumbar spine. Baseline studies in normal subjects. Spine **11**(6): 591-5.

PAGE WH, MONTEITH W and WHITEHEAD L (1993) Dynamic spinal analysis - fact or friction. chropractic Journal of Australia **23**(3): 82-8.

PANJABI M, CHANG D and DVORAK J (1992b) An analysis of errors in kinematic parameters associated with in vivo functional radiographs. Spine **17**(2): 200-5.

PANJABI MM (1979) Centers and angles of rotation of body joints: a study of errors and optimization. Journal of Biomechanics **12**: 911-20.

PANJABI MM, BOEL VK and TAKATA K (1982) Physiologic strains in the lumbar spinal ligaments. An in vitro biomechanical study. Spine **7**: 192-9.

PANJABI MM, GOEL V, OXLAND T, TAKATA K, DURANCEAU J, KRAG M and PRICE M (1992) Human lumbar vertebrae. Quantitative three-dimensional anatomy. Spine **17**(3): 299-306.

PEARCY M (1986) Measurement of back and spinal mobility. Clin Biomech **1**: 44-51.

PEARCY M, GILL JM, HINDLE RJ and JOHNSTON GR (1987) New method for the non-invasive three-dimensional measurement of human back movement in three dimensions by optoelectronic devices. Clin Biomech **2**: 199-204.

PEARCY M, PORTEK I and SHEPHERD J (1984) Three-dimensional x-ray analysis of normal movement in the lumbar spine. Spine **9**(3): 294-7.

PEARCY MJ (1985) Stereo radiography of lumbar spine motion. Acta Orthop Scand Suppl **212**: 1-45.

PEARCY MJ and BOGDUK N (1988) Instantaneous axes of rotation of the lumbar intervertebral joints. Spine **13**: 1033-41.

PEARCY MJ and HINDLE RJ (1989) New method for the non-invasive three-dimensional measurement of human back movement. Clin Biomech (Bristol, Avon) **1**: 73-9.

PITKANEN M, MANNINEN H and LINDGRER K (1997) Limited usefulness of traction-compression films in the radiolographic diagonsis of lumbar spinal instability: Comparison with flexion-extension films. Spine **22**: 193-7.

POPE MH and PANJABI M (1985) Biomechanical definitions of spinal instability. Spine **10**(3): 255-6.

PORTER RW, WICKS M and OTTEWELL D (1978) Measurement of the spinal canal by diagnostic ultrasound. J Bone Joint Surg Br **60-B**(4): 481-4.

ROGERS BP, HAUGHTON VM, ARFANAKIS K and MEYERAND ME (2002) Application of image registration to measurement of intervertebral rotation in the lumbar spine. Magn Reson Med **48**(6): 1072-5.

ROSEN M, BREEN A, HAMANN W, HARBER P, JAYSON MIV and KELLY E (1994) Management guidelines for back pain. Report of a clinical standards advisory group committee on back pain. Her Majesty's Stationery Office HMSO, London.

SAUR PM, ENSINK FB, FRESE K, SEEGER D and HILDEBRANDT J (1996) Lumbar range of motion: reliability and validity of the inclinometer technique in the clinical measurement of trunk flexibility. Spine **21**(11): 1332-8.

SCHOBER P (1937) Lendenwirbelasuale und krenzschemerzen. Muncherner Medizinische Wochenschr **84**: 226-8.

SELVIK G (1989) Roentgen stereophotogrammetry. A method for the study of the kinematics of the skeletal system. Acta Orthop Scand Suppl **232**: 1-51.

SELVIK G (1990) Roentgen stereophotogrammetric analysis. Acta Radiol **31**(2): 113-26.

SHABANA AA (1994) Computational Dynamics. New York, John Wiley & Sons.

SHAFFER WO, SPRATT KF, WEINSTEIN J, LEHMANN TR and GOEL V (1990) 1990 Volvo Award in clinical sciences. The consistency and accuracy of roentgenograms for measuring sagittal translation in the lumbar vertebral motion segment. An experimental model. Spine **15**(8): 741-50.

SHINOZUKA N, OIE Y, YAMAKOSHI Y and TAKETANI Y (1996) Transvaginal sonographic orientation detection system using ceramic gyroscopes. J Ultrasound Med **15**: 107-13.

SICARD C and GAGNON M (1993) A geometric model of the lumbar spine in the sagittal plane. Spine **18**(5): 646-58.

SIMONIS C, ALLEN R and CLOKE R (1993) Spatial analysis of the movement of the spine: Application of parallel computing in the field of spine biomechanics. Transputer Applications **1**: 35-8.

SIMONIS C, ALLEN R and CLOKE R (1994) Parallel calculation and analysis of spine kinematic parameters using videofluoroscopy and image processing. Ph.D thesis.University of Southampton,Sounthampton.

SKLANSKY J (1978) On the Hough technique for curve detection. IEEE Trans Comput. **C-27**: 923-6.

SMYTH PP, TAYLOR J and ADAMS E (1999) Automatic Measurement of Vertebral Shape Using Active Shape Models. RSNA scientific assembly, Radiology **211**: 571-8.

SOMMER HJ, 3RD and MILLER NR (1980) A technique for kinematic modeling of anatomical joints. J Biomech Eng **102**(4): 311-7.

STERNBACH RA (1986) Pain and 'hassles' in the United States: Findings of the Nuprin Pain Report. Pain **27**: 69-80.

STOKES IA, BEVINS TM and LUNN RA (1987) Back surface curvature and measurement of lumbar spinal motion. Spine **12**(4): 355-61.

STOKES IA, MEDLICOTT PA and WILDER DG (1980) Measurement of movement in painful intervertebral joints. Med Biol Eng Comput **18**(5): 694-700.

STOKES IA, WILDER DG, FRYMOYER JW and POPE MH (1981) 1980 Volvo award in clinical sciences. Assessment of patients with low-back pain by biplanar radiographic measurement of intervertebral motion. Spine **6**(3): 233-40.

STURESSON B, UDEN A and VLEEMING A (2000) A radiostereometric analysis of movements of the sacroiliac joints during the standing hip flexion test. Spine **25**(3): 364-8.

SUN LW and LEE RYW (2004) Development of a new motion analysis system using gyroscopic sensors. Proceedings of the XVth Congress of the International Society of Electrophysiology and Kinesiology: 251.

SUZUKI S, YAMAMURO T, SHIKATA J, SHIMIZU K and IIDA H (1989) Ultrasound measurement of vertebral rotation in idiopathic scoliosis. J Bone Joint Surg Br **71**(2): 252-5.

TAKAYANAGI K, TAKAHASHI K, YAMAGATA M, MORIYA H, KITAHARA H and TAMAKI T (2001) Using cineradiography for continuous dynamic-motion analysis of the lumbar spine. Spine **26**(17): 1858-65.

TENCER AF and MAYER TG (1983) Soft tissue strain and facet face interaction in the lumbar intervertebral joint--Part II: Calculated results and comparison with experimental data. J Biomech Eng **105**(3): 210-5.

TEZMOL A, SARI-SARRAF H, MITRA S, LONG R and GURURAJAN A (2002) Customized hough transform for robust segmentation of cervical vertebrae from x-ray images. 5th IEEE southwest symposium on image analysis and interpretation SSIAI'02: 100-2.

THE MATHWORKS INC (1994) Genetic Algorithm & Direct Search Toolbox. UK, Department of Automatic Control and Systems Engineering of the University of Sheffield.

TIBREWAL SB, PEARCY MJ, PORTEK I and SPIVEY J (1985) A prospective study of lumbar spinal movements before and after discectomy using biplanar radiography -correction of clinical and radiographic findings. Spine **10**: 455-60.

TILG B, FISCHER G, MODRE R, HANSER F, MESSNARZ B, SCHOCKE M, KREMSER C, BERGER T, HINTRINGER F and ROITHINGER FX (2002) Model-based imaging of cardiac electrical excitation in humans. IEEE Trans Med Imaging **21**(9): 1031-9.

TONG K and GRANAT MH (1999) A practical gait analysis system using gyroscopes. Med Eng Phys **21**: 87-94.

ULRICH M, STEGER C, BAUMGARTNER A and EBNER H (1996) Real-time object recognition using a modified generalized hough transform. 1-8.

VALLFORS B (1985) Acute, Subacute and Chronic Low Back Pain: Clinical Symptoms, Absenteeism and Working Environment. Sweden, Kompendietryckeriat-Kallered.

VAN DEN BOGERT AJ, SMITH GD and NIGG BM (1994) In vivo determination of the anatomical axes of the ankle joint complex: an optimization approach. J Biomech **27**(12): 1477-88.

VAN HERP G, ROWE P, SALTER P and PAUL JP (2000) Three-dimensional lumbar spinal kinematics: a study of range of movement in 100 healthy subjects aged 20 to 60+ years. Rheumatology (Oxford) **39**(12): 1337-40.

VISUAL AUTOMATION LIMITED C (1998) ASM Toolkit User Guide. Manchester, Stopford Building.

WALL MS and OPPENHEIM WL (1995) Measurement error of spondylolisthesis as a function of radiographic beam angle. J. Pediatr Orthop **15**: 193-8.

WANG X (1999) A behavior-based inverse kinematics algorithm to predict arm prehension postures for computer-aided ergonomic evaluation. J Biomech **32**(5): 453-60.

WEILER PJ, KING GJ and GERTZBEIN SD (1990) Analysis of sagittal plane instability of the lumbar spine in vivo. Spine **15**: 1300-6.

WHITE AA and PANJABI MM (1978) Clinical Biomechanics of the Spine. Philadelphia, J.B., Lippincott.

WHITE AA and PANJABI MM (1990) Clinical Biomechanics of the Spine. Philadelphia, J.B., Lippincott.

WILKE HJ, ROHLMANN A, NELLER S, GRAICHEN F, CLAES L and BERGMANN G (2003) ISSLS Prize Winner: A Novel Approach to Determine Trunk Muscle Forces During Flexion and Extension: A Comparison of Data From an In Vitro Experiment and In Vivo Measurements. Spine **28**(23): 2585-93.

WONG TKT and LEE RYW (2004) Effects of low back pain on the relationship between the movements of the lumbar spine and hip. Human Movement Science **23**(1): 21-34.

WRIGLEY W, HOLLISTER WM and DENHARD WG (1969) Gyroscopic theory, design and instrumentation. Cambridge, The MIT Press, Cambridge.

YAMAMOTO I, PANJABI MM, CRISCO JJ and OXLAND T (1989) Three-dimensional movements of the whole lumbar spine and lumbosacral joint. Spine **14**(11): 1256-60.

YOSHIOKA T, TSUJI H, HIRANO N and SAINOH S (1990) Motion characteristic of the normal lumbar spine in young adults: Instantaneous axis of rotation and vertebral center motion analyses. J Spinal Disord **3**: 103-13.

YOSHIOKA Y, IWATA H, OHSAWA R and NINOMIYA S (2004) Analysis of petal shape variation of Primula sieboldii by elliptic fourier descriptors and principal component analysis. Ann Bot (Lond) **94**(5): 657-64.

YOSHIOKA Y, IWATA H, OHSAWA R and NINOMIYA S (2005) Quantitative evaluation of the petal shape variation in Primula sieboldii caused by breeding process in the last 300 years. Heredity **94**(6): 657-63.

ZATSIORSKY VM (1998) Kinematics of human motion. Champaign, IL, Human Kinetics.

ZHANG X and CHAFFIN DB (1996) An optimisation-based differential inverse kinematics approach for modelling three-dimensional dynamic postures during seated reaching movements. Technical report TR96-15.Univ. of Michigan,MI.

ZHANG YM, VOOR MJ, WANG M and JOHNSON JR (1998) Intervertebral measurement of lumbar segmental motion with a new measuring device. Med Eng Phys **20**(2): 139-48.

ZHENG Y, NIXON MS and ALLEN R (2003) Lumbar spine visualisation based on kinematic analysis from videofluoroscopic imaging. Med Eng Phys **25**(3): 171-9.

ZHENG Y, NIXON MS and ALLEN R (2004) Automated segmentation of lumbar vertebrae in digital videofluoroscopic images. IEEE Trans Med Imaging **23**(1): 45-52.

ZHENG Y, NIXON S and ALLEN R (2000a) Automatic Lumbar Vertebrae Registration Using the Hough Transform in Digital Videofluoroscopy. Procs 7th Annual Scientific Conference of the Institute of Physics and Engineering in Medicine.

ZHENG Y, NIXON S and ALLEN R (2000b) Automatic Lumbar Vertebrae Segmentation in Fluoroscopic Images via Optimised Concurrent Hough Transform. Procs of 23rd Annual International Conference of the IEEE Engineering in Medicine and Biology Society **1**: 1-4.

ZHENG Y, NIXON S and ALLEN R (2000c) Finding Lumbar Vertebrae by Evidence Gathering. Procs 6th Annual Scientific Conference of the Institute of Physics & Engineering in Medicine **1**: 95-6.

ZHENG Y, NIXON S and ALLEN R (2001) Automatic Lumbar Vertebrae Segmentation in Fluoroscopic Images via Optimised Concurrent Hough Transform. Procs of 23rd Annual International Conference of the IEEE Engineering in Medicine and Biology Society **1**: 1-4.

ZHOU SH, MCCARTHY ID, MCGREGOR AH, COOMBS RR and HUGHES SP (2000) Geometrical dimensions of the lower lumbar vertebrae--analysis of data from digitised CT images. Eur Spine J **9**(3): 242-8.